Agricultural Monitoring System using Images through a LPWAN Network

William Fabián Chaparro Becerra
Department of Electronics Engineering
Pontificia Universidad Javeriana

Doctoral Advisors,
Ph.D. Manuel Ricardo Pérez Cerquera
Ph.D. Diego Méndez Chaves

Members of the Examining Committee,
Ph.D. Jose Ignacio Martinez
Ph.D. Cesar Dario Guerrero S.
Ph.D. Eduardo Castellanos

A thesis submitted for the degree of
Doctor of Philosophy

2022

Acknowledgment

I want to begin by thanking God and Our Lady, thanks a lot for your company, support and give effort in the difficult moments.

I'd like to express my gratitude to my wife for her unwavering support and never-ending encouragement over all of my years of study as well as during the process of gathering information and writing this thesis. All of this would not be possible without you. I am grateful that my daughter, who arrived in the middle of this process and gave me a special motivation to fight for this dream. I'm grateful. Juli and Sofí, this is for you, my loves.

I must convey my sincere gratitude to my family, specifically to my parents, my brother, my sister, and my wife's parents and sister.

I'd like to express my gratitude to my thesis advisors, Ph.D. Manuel Ricardo Pérez and Ph.D. Diego Méndez, for their time, encouragement, and ability to point me in the right path when I needed it.

Additionally, I'd like to express my gratitude to the researchers who contributed to this work: Ph.D. Andrea Abrardo of the Universitá degli Studi Siena in Italy, Ph.D. Jeison Marín of Colombia, and the Universidad Rey Juan Carlos in Móstoles-Madrid, Spain.

As readers of this thesis, I would also want to thank Ph.D. Jose Ignacio Martinez of the Universidad Rey Juan Carlos in Spain, Ph.D. Cesar Dario Guerrero S. of the Universidad Autónoma de Bucaramanga, and Ph.D. Eduardo Castellanos of the Pontificia Universidad Javeriana - Bogotá. I owe them a gratitude for their for the lecture of this thesis.

I want to thank Universidad Santo Tomás, my "alma mater" for all of their assistance and support throughout this process.

Finally. I would like to thank my friends from this process, including Freddy, Camilo, Guti, Javier, Julián, among others.

Contents

List of Figures

Dedication

This thesis is dedicated to God and Our Lady. To my family members who have supported me along the journey, especially my wife, daughter, parents, brother, and sister as well as my wife's parents and sister.

It is also dedicated to everyone who had faith in me, gave me the courage, and prayed for me to succeed.

Abbreviations

SDR	Software Defined Radio.
DL	Down Link
ISM	Industrial, Scientific and Medical.
NB-LTE	Narrow Band Long-Term Evolution
MAC	Medium Access Control
PHY	Physical
IoT	Internet of Things.
UL	Up Link.
RF	Radio Frequency
QoS	Quality of Service.
LPWAN	Low Power Wide Area Network.
LoRaWAN	LoRa modulation technique to Wide Area Network.
SF	Spreading Factor
BW	Bandwidth.
CSMA	Carrier Sense Multiple Access.
WSVN	Wireless Visual Sensor Network.
RGB	Red - Green - Blue components of color.
Cs	Compressive Sensing.
CR	Cognitive Radio.
ITU	International Telecommunication Union.
WPAN	Wireless Personal Area Network.
WLAN	Wireless Local Area Network.
WNAN	wireless Neighbor Area Network.
CDMA	Code Division Multiple Access.
SS	Spread Spectrum.
FDMA	Frequency Division Multiple Access.
TDMA	Time Division Multiple Access .
IETF	nternet Engineering Task Force.
6LowPAN	Six LoW Personal Area Network.
IPV6	Internet Protocol version 6 .
MTU	Maximum Transmission Unit .
ICT	Information and Communication Technologies .
DSSS	Direct Sequence Spread Spectrum .
OFDMA	Orthogonal Frequency Division Multiple Access ISI . Inter Symbol Interference
ICI	Inter Carrier Interference .
RPMA	Random Phase Multiple Access .
CSS	Chirp Spread Spectrum .
UNB	Ultra Narro Band .
	.

Abstract

Internet of things (IoT) has turned into an opportunity to connect millions of devices through communication networks in digital environments. Inside IoT and mainly in the technologies of communication networks, it is possible to find Low Power Wide Area Networks (LPWAN). Within these technologies, there are service platforms in unlicensed frequency bands such as the LoRa Wide Area Network (LoRaWAN). It has features such as low power consumption, long-distance operation between gateway and node, and low data transport capacity. LPWAN networks are not commonly used to transport high data rates as in the case of agricultural images. The main goal of this research is to present a methodology to transport images through LPWAN networks using LoRa modulation. The methodology presented in this thesis is composed of three stages mainly.

The first one is image processing and classification process. This stage allows preparing the image in order to give the information to the classifier and separate the normal and abnormal images; i.e. to classify the images under the normal conditions of its representation in contrast with the images that can represent some sick or affectation with the consequent presence of a particular pathology. For this activity. it was used some techniques were used classifiers such as Support Vector Machine SVM, K-means clustering, neuronal networks, deep learning and convolutional neuronal networks. The last one offered the best results in classifying the samples of the images.

The second stage consists in a compression technique and reconstruction algorithms. In this stage, a method is developed to process the image and entails the reduction of the high amount of information that an image has in its normal features with the goal to transport the lowest amount of information. For this purpose, a technique will be presented for the representation of the information of an image in a common base that improves the reduction process of the information. For this activity, the evaluated components were Wavelet, DCT-2D and Kronecker algorithms. The best results were obtained by Wavelet Transform. On the other hand, the compression process entails a series of iterations in the vector information, therefore, each iteration is a possibility to reduce that vector until a value with a minimum PSNR (peak signal to noise ratio) that allows rebuilding the original vector. In the reconstruction process, Iterative Hard Thresholding (IHT), Ortogonal MAtching Pursuit (OMP), Gradient Projection for Sparse Reconstruction (GPSR)and Step Iterative Shrinage/Thresholding (Twist) algorithms were evaluated. Twist showed the best performance in the results.

Finally, in the third stage, LoRa modulation is implemented through the creation of LoRa symbols in Matlab with the compressed information. The symbols were delivered for transmission to Software Defined Radio (SDR). In the receptor, a SDR device receives the signal, which is converted into symbols that are in turn converted in an information vector. Then, the reconstruction process is carried out following the description in the last part of stage 2 - compression technique and reconstruction algorithms, which is described in more detailed in chapter 3, section 3.2. Finally, the image reconstructed is presented. The original image and the result image were compared in order to find the differences. This comparison used Peak Signal-to-Noise Ratio (PSNR) feature in order to get the fidelity of the reconstructed image with respect of the original image. In the receptor node, it is possible to observe the pathology of the leaf. The methodology is particularly applied for monitoring abnormal leaves samples in potato crops.

This work allows finding a methodology to communicate images through LPWAN using the LoRa modulation technique. In this work, a framework was used to classify the images, then, to process them in order to reduce the amount of data, to establish communication between a transmitter and a receiver through a wireless communication system and finally, in the receptor, to obtain a picture that shows the particularity of the pathology in an agricultural crop.

1. Introduction

1.1. Agricultural monitoring system with images in Colombia

Colombia has a broad spectrum of possibilities in agricultural crops, due to its diverse geographical zone that allows the production of a huge number of fruits and vegetables for the human consumption [1]. The agricultural sector needs the implementation of smart techniques, that allow improvement and efficiency in the quality of the processes and make it possible the early prevention of pests and diseases in order to avoid losses in the chain of production and achieve the effective marketing of the products. In Colombia, potatoes are one of the main agricultural products, particularly in the region of Boyacá due to its tradition. Potato crops are present among 2500 and 3200 meters above sea level, which makes it difficult to undergo many process around the planting, production and harvesting stages. In the production stage, there are different known phases: the selection, classification and planting of the seed, and the crop growth, in which, the production is expected to strengthen with a reduction in pest or diseases risk. An opportune and appropriate monitoring will reduce the negative effects of pest or diseases with an acceptable level of quality [1].

The easiest way to detect abnormalities in the crops is through a visual method, that aims to distinguish between normal crops or those with the presence of a particular pathogen [2, 3]. A pathology can be associated with the pigmentation of the leaves of the plant. There are several types of pathology that can be represented by brown, black or yellow colors. These colors that differ from the traditional green show some abnormalities such as Phythophthora infestans or Alternaria Solani, mainly. Figure **1-1** shows the normal or abnormal features in the leaves of potato crops [3, 4].

Figure **1-1**.: Normal or abnormal leaves of potato

The diagnosis of diseases in plants is considered an art which involves the experience of the farmers. In general, agriculture techniques entail monitoring with the use of variable control, such as temperature, humidity, nutrients, light conditions, among others, in order to set up the control of these features. However, the traditional methods used by the farmers involve the function of looking at behavioral patterns and, to a lesser degree, technological support that could improve the early and accurate detection of abnormalities in the crops. The digital analysis and processing of images offer an advantage in the early detection of diseases through pattern extraction, features and attributes that allow farmers to define whether the plant belongs to a normal or abnormal class [5,6]. In addition, different works have reported that capturing images of agricultural monitoring with image processing in outdoor environments entails particular problems related to illumination and image capturing [7, 8]. Therefore, in order to avoid those problems, we proposed a controlled environment for image capturing where the main focus is to present an entire methodology framework combining image classification

and compression, wireless communication through a LPWAN network and image reconstruction. The controlled environment allows taking every leaf sample with a white background for image processing and transmission. The proposed methodology framework presented several challenges, for example, in the processing stage, the reconstruction of the image at the receiver node with an acceptable resolution level after the application of the compression techniques which reduces the information even under the Shannon-Nyquist theorem [9]. Another challenge was to implement a complete Tx-Rx communication setup of LoRa in its physical layer in order to adapt the image transmission over narrow-band frequency channels for the proposed methodology framework.

1.2. Research problem and solution strategy

When real time data or high amount of information need to be transported through wireless sensor networks, some critical points should be considered such as low computational complexity, memory limitations, narrow bandwidth and low energy consumption. The work in [10] presents how to reduce the energy consumption of a sensor network during image transmission with an energy efficient scheme, using image compression techniques based on the compression standard JPEG2000. In [11], the results of images and voice transmission using LoRa are presented, image and voice compression is set to a JPEG2000 standard and the A-law method, respectively. In [12], a platform of video sensor network architecture is presented, with a proposed solution to deliver high quality video over IEEE 802.11 networks. The compression method used is differential JPEG. In [13], a framework is proposed and developed for streaming video flows through wireless multimedia sensor networks. For the above, three main blocks were designed: an encoder to compress information, a congestion control mechanism to avoid loss of information, and a selective priority automatic request mechanism at the MAC layer.

LPWAN technologies are gaining incredible interest due to their efficient integration inside IoT, which represents a union of data and communication systems that allows sensor data to transport through wireless environments with some special features such as long range coverage, low power consumption and the possibility of using non-licensed spectrum (Industrial-Scientific-Medical, ISM bands). This feature entails an additional advantage such as less operational cost. However, LPWAN has disadvantages such as limited bandwidth, spectrum access duty cycling and low data payload. Capacity restriction for high data rates is a challenge for applications where images and video should be transmitted through a LPWAN as in the case of Wireless Visual Sensor Networks (WVSN) [14], wireless camera sensors [15, 16] and image sensors [17–19].

LoRaWAN is a LPWAN solution that uses Chip Spread Spectrum (CSS) modulation, known as LoRa PHY. The modulation system is a subcategory of the Direct Sequence Spread Spectrum (DSSS) that takes advantage of the controlled frequency diversity in order to recover data from weak signals, even near to the noise level. It works with a continuous phase between different symbols called “chirp”. The main technical features of LoRa modulation are Bandwidth (BW) and the Spreading Factor (SF), commonly set from 7 to 12. The SF is the number of bits in a LoRa symbol. It is possible to transmit from 2^0 to 2^{SF} data codes, called chips, in one symbol time, thus, the value of the coded chip will be the value of the phase change of the signal within a symbol time. With each increase of SF, the data rate is reduced, while the transmission and the symbol time is increased. As a result, large coverage and high energy consumption is achieved at the end device. Theoretical references about LPWAN networks and LoRaWAN technology will be addressed in detail in follow chapters.

In order to better understand the research problem of transmitting images through a LoRaWAN network, Table 1 presents the data rate limitation of this technology. With the relation between SF, bit rate, BW, symbol time T_s and the time on air (T_s multiply by packet number) for a packet of 255 bytes, which is the maximum payload of LoRaWAN.

Table 1 - Main features of LoRa technology

SF	BW (kHz)	Ts	Bit rate (kbit/s)	Time on Air 255 bytes (ms)
7	125	1.024 ms	6.836	389.38
8	125	2.048 ms	3.906	686.59
9	125	4.096 ms	2.197	1,229.82
10	125	8.192 ms	1.220	2,213.89
11	125	16.384 ms	0.671	4,837.38
12	125	32.768 ms	0.366	8,855.55
7	250	512 μs	13.672	194.69
8	250	1.024 ms	7.812	343.30
9	250	2.048 ms	4.395	614.91
10	250	4.096 ms	2.441	1,106.94
11	250	8.192 ms	1.342	2,009.09
12	250	16.384 ms	0.732	3,772.42
7	500	256 μs	27.343	97.34
8	500	512 μs	15.625	171.65
9	500	1.024 ms	8.789	307.46
10	500	2.048 ms	4.882	553.47
11	500	4.096 ms	2.685	1,004.54
12	500	8.192 ms	1.464	1,886.21

In this research, we took images of 16384 (128 x 128) pixels of information, which allow detecting normal or abnormal features of leaves with the aim to find possible diseases. With that image size, each pixel is represented by one byte (8-bits), then, 16384 bytes must be transmitted with the wireless network. Besides that, as mentioned above, LoRaWAN has the capacity to transport 255 bytes of information per packet. This creates the need to use around 68 packets (including headers) to transport the complete image in the process, which will take around 5 hours considering the spectrum access time restrictions of the ISM bands. This duration is possible to observe in 1.2, the best performance scenario with the use of a BW=500 kHz and a SF=7, the duration of each packet in the air will be of 97.34 ms. For this reason around 176.8 seconds are need to transmit the image without any spectrum regulation policy. However, since ISM bands policies are used in most of the LPWAN works, as in the case of LoRa and Sigfox [20,21], there has been a duty cycle establishment which uses 1% (ETSI EN 300 220-1) [22] of the real time to transmit an image of that size, which will be around 5 hours. Now, with the same conditions of SF and BW, but doing frequency hopping between 915 MHz to 928 MHz. (which must be implemented between channels with no contiguity [22]), the time will be around 3 minutes without considering saturation, collisions and other problems related to the use of shared spectrum. In both cases, image transmissions in applications of agriculture monitoring is a challenge and it is a general problem addressed in the literature for LPWAN networks when high data rates are needed in IoT services with low-power consumption and long communication range requirements. [14,23].

In the literature, few works have tackled the problem of image transmission over LPWAN network because an image has high amount of bits and consumes more energy in the transmission process. In [23], a method was proposed for a monitoring application using an image sensor working over the LoRa physical layer. The work in [18] presents a low cost, low power, and long range image sensor through a Teensy 3.2 board as the micro controller host to drive the CMOS uCamII camera capable of providing a JPEG bit stream. The sensor integrates LoRa long radio module inAir 9 from Modtronix, which is built upon Semtech SX1276 chip. In [19], two control mechanisms are presented to enable the deployment of image sensor devices through LoRa technology. The first mechanism is the Carrier Sense Multiple Access (CSMA) adapted to avoid packet collision. The second one is the sharing time in order to mitigate the limit of duty cycling. Authors in [14] describes a theoretical proposal of low power wide area network protocol, which combines LoRa modulation technique with

embedded microprocessor technology. The proposed network is composed of three LoRa modules that provide three physical channels, thus providing a diversity gain scheme.

A SDR is a device formed by a radio communication system that uses a software for the modulation and demodulation of radio signals. It can make transmission and reception of data from several standards of communication protocols at a time, which provides a flexibility and limitless platform [24]. SDR has been used in the implementation of the physical layer of LoRa technology.

In [25], a LoRa signal is decoded through *gr-lora*, an open source software defined as an implementation of the LoRa PHY, which defines blocks through Python for implementing LoRa. The authors guide its investigation according to Josh Blum [25] and a *gr-lora* out of a tree module written in GitHub. It implements a receiver in Python that uses a modified FM demodulation process, however, the author has not successfully decoded messages with it. The authors in [26] give an overview into the technologies to support LoRa, and describe the outdoor setup with the SX127x family of Semtech and the importance of transceiver generation that arrives with a SDR. It allows reaching significant benefits for range, robust performance and battery lifetime. In [27], it is possible to identify a description of the LoRa PHY layer, where the document shows a methodology for detecting and decoding LoRa frames with the use of SDR (USRP B210, HackRF and RTL-SDR). In order to transmit, it used commercial platforms (RN2483, HopeRF RFM96 and Semtech SX1272, mainly).

The aforementioned works will be described in more detail in Chapter 3. Nevertheless, it is worth mentioning that some of them only reached a theoretical analysis without implementation, besides, there is lack of information about the implementation process. To the best of our knowledge, there are no proposals or studies in the literature that involve a general framework methodology for image transmission considering compression, classification and adaptation to an LPWAN technology through the implementation of the physical layer of LoRaWAN on a SDR.

To increase the amount of information to transmit with LPWAN network, it is necessary to work with licensed technology (to avoid duty cycle) or increase the capacity per node to tackle the duty cycle problem (Multiple In multiple Out- MIMO). Nevertheless, to transport a high amount of information with one node, it is necessary to implement a method to increase the transmission data, thus improving the use of the transmission channel that is limited. From the above, it is necessary to find the form to exploit the use of a channel within maximum usable time (400 ms) [22], then, hopping to other available channel until all the information is transmitted. In theory, there are diverse techniques to improve the efficiency of the transmission and increase the amount of information, thus some methods such as space, time or frequency diversity can be applied. The main goal of these methods is to protect the information and avoid losses of the frame. In our context, we need to increase the amount of information to transmit an image through a LPWAN network. To make this happen, the solution can be divided into two scenarios: (i) implementing a form of diversity with the aim to increase the transmitted data and attack the limit with the use of ISM bands under consideration of the duty cycling or (ii) reducing the amount of information in order to optimize the data transmission process. Therefore, in the present research these options were considered, to determine that with the second option it is possible to transmit images with the use of the LPWAN network within LoRa symbols creation through a high level of compression rates to reduce the amount of information by employing compressive sensing and source coding methods.

The solution strategy contemplates the use of image processing techniques with the aim of classifying normal or abnormal leaves samples of a potato plant to transport only the abnormal samples through the LPWAN network. Besides a compression form of the captured image, it is necessary to reduce the high amount of information to transmit with the aim of reaching a reduction rate of about 95% of information. Thereby, the transmission time will be reduced to 2,51 seconds with only one frequency channel or 0,74 seconds employing frequency hopping. Additionally, implementation through the use of SDR in the receiver and transmitter involves the creation of LoRa symbols and setting up the features to adapt the symbols to the LoRa transmission.

1.3. Organization of the document

The organization of the document is briefly described as follows. Chapter 2 presents the dissertation proposal through the discussion of the research question, objectives, and hypothesis, followed by the description of the methodology framework, which is the core of the dissertation. Finally, the contributions of this work will be highlighted.

Chapter 3 provides an overview of the system and methodology proposed in this work. First, image processing techniques which allowed the classification of the leave samples into normal or abnormal are described. Second, the compression techniques that allowed the reduction of the amount of data of abnormal samples in order to deliver it to the LPWAN network are presented with the subsequent transmission and reception process between nodes, transmitter and receiver, respectively. Third, the main LPWAN networks references and in particular LoRaWAN technology are described in order to justify its use in the present work. Finally, the works that described the use of LPWAN networks for image monitoring systems will be detailed. Chapter 4, the evaluation of the system will be outlined in order to propose agricultural monitoring systems with the use of images through LPWAN network. Finally, in Chapter 5, the conclusions of this work will outlined.
—

2. Dissertation proposal: Agricultural monitoring system using images through a LPWAN network

In this chapter, the thesis proposal will be described, therefore, we present the research question, the objectives and the hypothesis in Sections 2.1, 2.2 and 2.3, respectively. Section 2.4 shows the framework used for developing a prototype of an agricultural monitoring system with images in a LPWAN network. In addition, the contributions of this work are presented in Section 2.5.

2.1. Research question

The research question that guides the investigation is:

How can a method that allows to structure an agricultural monitoring system be implemented with the use of images through a LPWAN network?

2.2. Research objectives

The general research objective is divided into six specific objectives.

General Objective:

To implement a methodology that allows structuring an agricultural monitoring system with the use of images through LPWAN network supported by image processing, samples classification, compression-reconstruction of information, and use of LoRa modulation implemented on SDRs to transport information between transmitter and receiver nodes.

Specific Objectives:

- To implement an image processing and classification technique for identifying normal or diseased-affected leaf samples in agricultural crops.

- To evaluate the implemented image processing and classification technique for identifying normal or diseased-affected leaf samples in agricultural crops.

- To implement a compression technique for images of agricultural crops in order to reduce the amount of information to transport on a LPWAN network.

- To implement and evaluate a reconstruction algorithm for testing the implemented compression technique through the comparison of the reconstructed and original images.

- To evaluate a technique that allows an improvement in the data transmission in a LoRaWAN network through LoRa modulation.

- To integrate and validate the proposed system for agricultural monitoring.

2.3. Research hypothesis

The research hypothesis that guides the investigation is:

It is possible to implement a methodology in an agricultural monitoring system with the use of images through a LPWAN network supported by image processing, compression and reconstruction, and the use of LoRa modulation technology implemented on SDR transport information between network end-devices.

2.4. Proposal framework

First, we briefly recall the research problem. Second, the problem is considered by proposing a framework. Finally, it matches each stage of the framework, which will be presented in this document with the aim to give an overview of the approach of this proposal research.

LPWAN has disadvantages such as limited bandwidth, the use of duty cycle and low payload to transport information. The capacity restriction to transport a high amount of information is a problem and a challenge that needs solutions where necessary, to be able to use applications that transport images such as wireless visual sensor networks (WVSN), wireless camera sensors and an image sensors, mainly.

Figure **2-1** shows the node – gateway communication in order to develop the proposal of an agricultural monitoring system using images on a LPWAN network. The system is composed of the process of data acquisition implemented through a normal camera with 12MP and a sensor of f/1.8 that takes images of leaves in agricultural crops of potato, which are sent to the transmitter (Tx) node. In the transmitter node, image processing must be implemented, and the image data represented in an information matrix of its features. This matrix will be sent, either to the classification process or to the compression process, if the sample has non-normal features.

The classification process will generate a response indicating a normal or abnormal sample in the image, and the response will be sent to the functional block of information grouping. If the sample is abnormal, the functional block responsible for sending decisions allows the abnormal image vector to be delivered to the functional block of compression, which is entrusted with reducing the amount of information and delivering a response to the information grouping block. The classification response and the compressed information in the information grouping functional block will be sent to the radio transmission interface.

The functional radio transmitter block is composed of a software defined radio architecture (SDR), which implements the proposed technique in order to use LoRa modulation that will allow information to be transmitted toward the radio receptor (Rx). The functional receptor block will receive the transmited signal and perform the necessary LoRa modulation process. The functional receptor radio block will send the information to the Rx node through the functional block responsible for visualizing the received image. The data received provide the possibility of understanding the response of the classification and developing the reconstruction process of the compressed samples in order to view the images with abnormal features.

Figure **2-1** shows four stages. In stage I, processing techniques will be implemented to classify samples into normal or abnormal. Each leaf is captured in a control scenario with a white background with the aim to facilitate the classification process. Abnormal samples will be used in stage II, during compression technique, in order to reduce the image information, thus making data transportation easier through the LPWAN network. During stage III, transmission process between TX and Rx will be used in order to improve the transport of

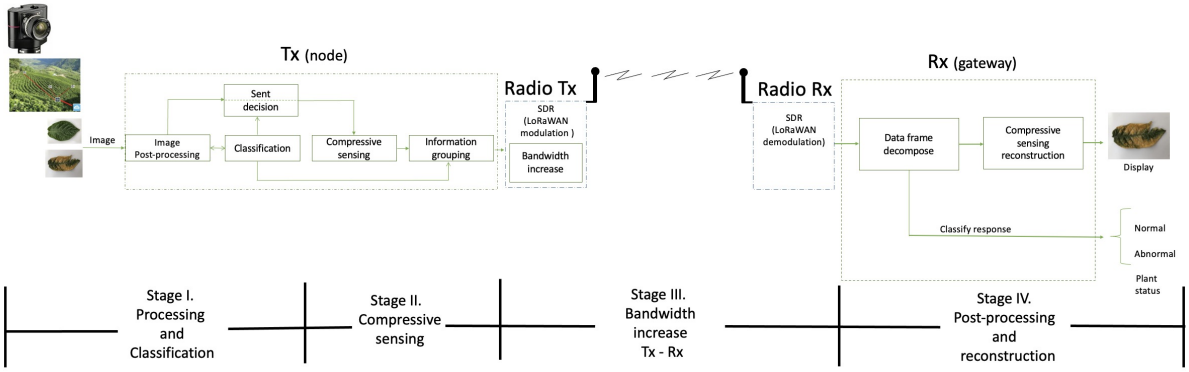

Figure **2-1**.: Framework proposal

information in the LoRa modulation. Finally, in stage IV, post processing and reconstruction, the received data will be processed and the data frame analyzed in order to inform the condition of the plant and execute the reconstruction process of the abnormal images for their display.

In order to complete stage I, the proposal uses image-processing techniques for performing the classification. The capture of images in exterior environments entails problems, due to variables such as sunlight intensity, shadows, angle of capture and more, which can cause problems inherent to image processing, such as high probability of noise or un-real data. For this reason, the captures presented in this work correspond to a controlled capture, where these problems were avoided. Figure **2-2** shows stage I, processing and classification, which represents the image process used to classify it. Initially, the image data will be received in the Tx node, then, the extraction process will be executed to obtain the features that will be used in the classifier. Next, the classification will be made and the output will indicate whether the sample is normal or abnormal. This stage aims to find general information of the plant in terms of whether its growth is normal or affected by the presence of a disease or attacked by a pest. The response in stage I is a binary solution (normal or abnormal sample), nevertheless, the provision of specific details or levels of abnormality with quantitative indexes are limited in the classification process. For this reason, further stages will be implemented to allow the transportation of images that indicate abnormal conditions toward the Rx node with the use of a LPWAN network under LoRa modulation.

A literature review on image processing and classification methods that can be applied in the context of agricultural monitoring reveals that there is progress towards a process of image acquisition in order to identify normal and abnormal samples. Then, the review and evaluation of image-processing methods allow the construction of inbound data for the classifier. For this purpose, a review of image-processing techniques was carried out to gather the representative samples and filter the data information that includes errors in the classification process. The next step was to elaborate a features matrix with the output data from image processing. From this matrix, the process of data labelling was performed to identify which images were normal and which were abnormal, then, the matrix of data and its labels were divided into training and test sets. Those sets were used to evaluate the chosen classification process and calculate its precision under application with images. Finally, the evaluation process of the classifiers was performed at several different moments with different samples in order to validate the results. The outcomes allow establishing a strong criterion to choose the best tool to classify and justify its use in this research.
In stage II, compression technique, this proposal uses a technique that allows reduction in the amount of information of the images with abnormal features in order to transport this information vector on the LPWAN network. Figure **2-3** presents a scheme that allows understanding the process for reducing image size through a compression technique. In the transmission node, compression algorithms will be applied to the output data of the image vector (with abnormal features) obtained during capture, acquisition and processing. Then, it is sent to the reception node through a LPWAN network, where a reconstruction algorithm will be used in order

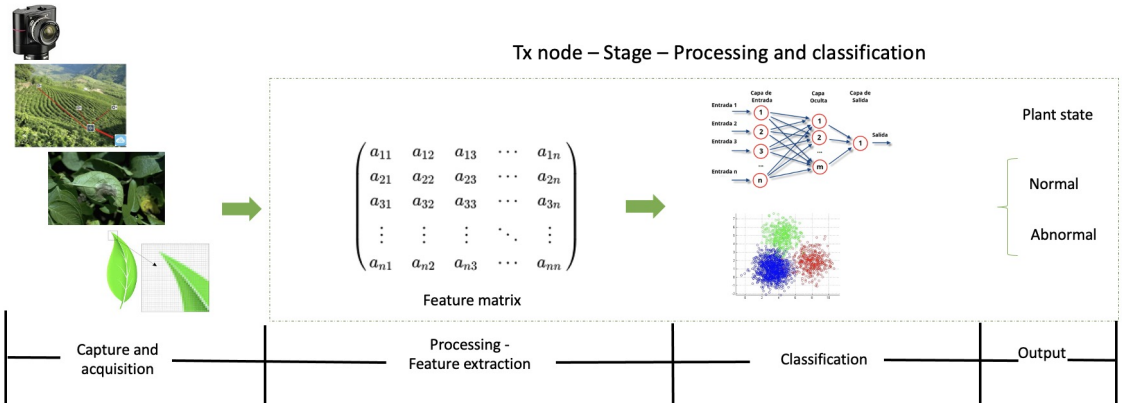

Figure **2-2**.: Stage I, Processing and classification

to recover the image and allow its display.

A literature review of compression techniques and reconstruction algorithms with image application was performed in order to evaluate this process. The images taken of a crop must be processed in order to find the data vector that represents an image. As a predisposition to high dispersion, which exists in the vector data, transformation methods that reduce the dispersion should be evaluated in order to find which of them provides a better transformation base, thereby obtaining less information to be processed. Then, a compression technique is applied for reducing the data and asses the reconstruction algorithms in order to establish the best result through a comparison of the original vector from the reconstruction, before making the inverse transformation to rebuild the image and compare it with the original.

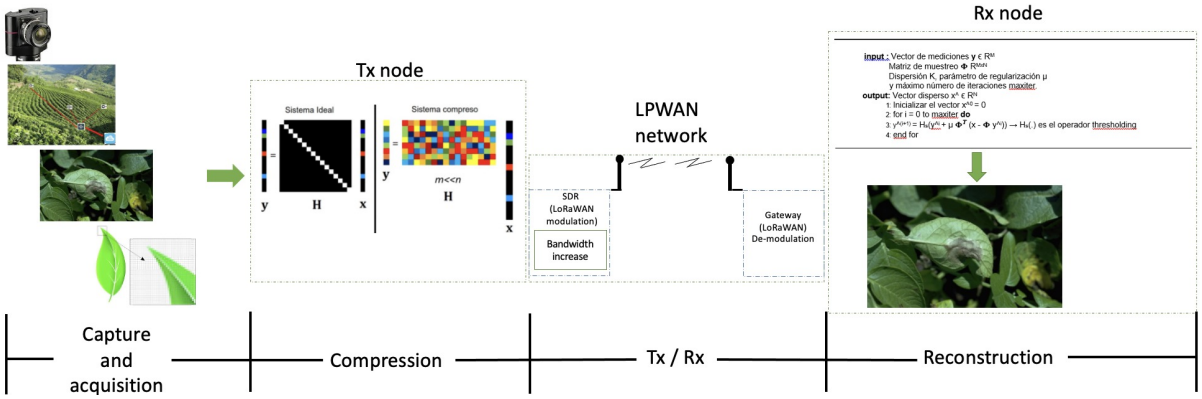

Figure **2-3**.: Stage II, Compression technique

Stage III is named transmission process between TX and Rx. This proposal implements changes within transmission and reception SDRs in order to transmit data through the LoRa modulation with the application of a technique that implements LoRa symbols and modulation. Figure **2-4** shows a diagram of stage III, which represents input data, coding (Tx), decoding (Rx), modulation (Tx), and demodulation (Rx) with LoRa technology. With this proposal, it is possible to send a major amount of information through each transmitter, thereby, it obtains efficiency in features such as energy consumption by reducing the transmission time.

A literature review in LPWAN networks is carried out to define the efficient and applicable methods to achieve

images through communication in a wireless LPWAN network. LoRa modulation is the technology choosen to work by due to its capacity inside LPWAN technologies. The technical features can be consulted in the next chapter of this document. For the transmission of images, it was necessary to evaluate its implementation in SDR platforms between transmitter and receiver, as well as evaluating techniques that allow the convertion of data in LoRa symbols and communicating them to a receiver with LoRa modulation. The use of SDR allows understanding the LoRa modulation features, thus obtaining a better perspective of the technology in its operation. Another technique susceptible of evaluation was the diversity in LPWAN, which is a possible solution to increase the number of sent packets, which means there can be another way that allows the transmission of images with the use of LPWAN networks.

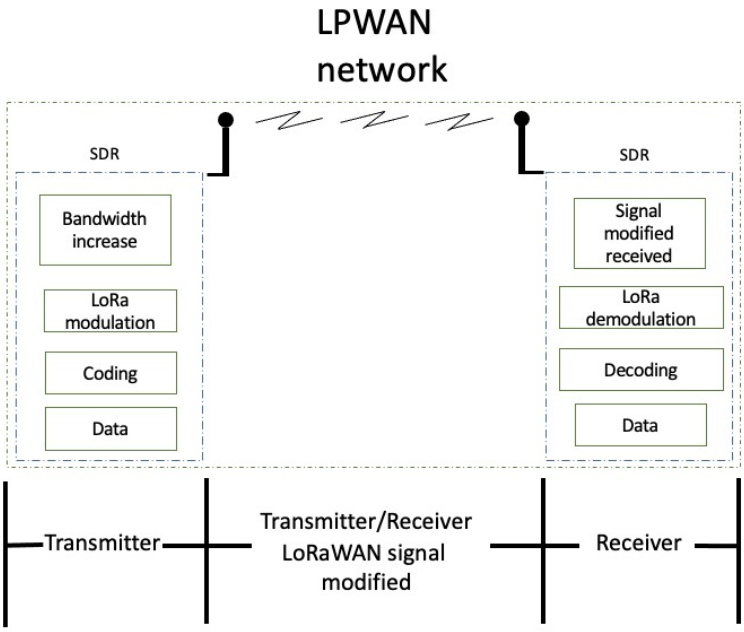

Figure **2-4**.: Stage III, Tx and Rx stage

To improve the capacity of data transport and consider the possibility of working only with the system of modulation called LoRa, it has been proposed to analyze a diversity method in order to evaluate if the transmission time is enhanced. Based on the above and consequently with the main feature such as duty cycle and others, LoRa works with operating frequency, bandwidth and SF, mainly.

Stage IV, post-processing and reconstruction is represented in figure **2-5**. In this stage, the reception node receives the data sent by the radio transmitter. These data is processed through the decomposition of the data frame in order to organize and deliver the classification information, as well as the reconstruction of the images. The reception node will display the result of the classification and the reconstructed images.

Finally, the connection and evaluation of the methodology of an agricultural monitoring system with use of images through LPWAN network is included. The processes presented at each stage were evaluated independently in order to determine their effectiveness. Therefore, stages of classification, compression technique, image reconstruction and use of LoRa modulation to transport data between transmitter and receiver nodes through the creation of LoRa symbols were evaluated.

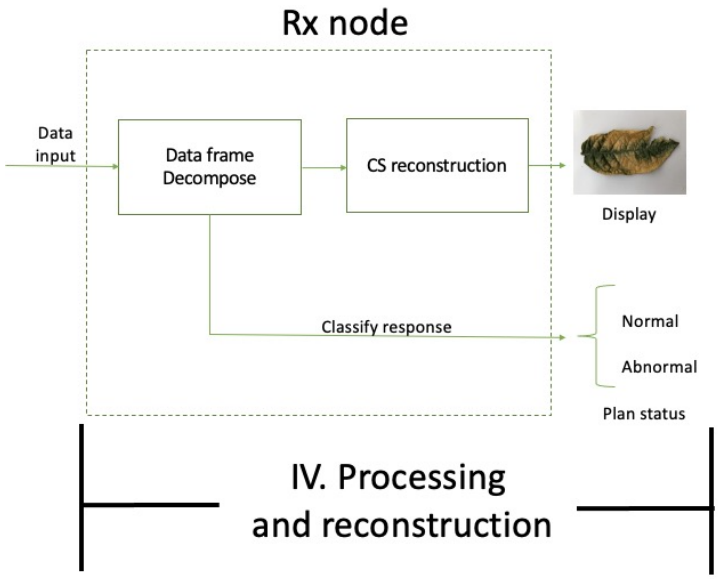

Figure **2-5**.: Stage IV, Post-processing and reconstruction

2.5. Contributions

The main contribution in this thesis is a methodology in order to transmit images of agricultural crops showing disease features through LPWAN networks with the use of LoRa modulation. Only images with abnormal visual features will be transmitted, which entails an optimization process that allows reducing the amount of information to transport since to the best of our knowledge it is not necessary to load a limited resource through the transmission of normal samples, where it has integrated features such as energy consumption and use of spectrum, specifically. All the above is consequent with the follow stages:

First, the classification method is used in order to represent the normal or abnormal status of the sample (in our case, in a leaf of a plant).[Chapter 3-16]

Second, the use of a compression technique is used in order to reduce information, thus saving time and processing resources, among other features. [Chapter 3-23]

Third, the deployment of a LPWAN network with LoRa modulation is used to transport short information over large distances with minimum energy consumption. [Chapter 3-30]

Finally, the goal to implement LoRa modulation in SDRs is to know the features of the modulation technique and thus understand its potential to enhance it, particularly, in a method that allows improving its capacity of data transport. [Chapter 3-55]

Based on the above, this research has produced two papers, which are currently in submission process:

1. Coverage and Energy-Efficiency Experimental Test Performance for a Comparative Evaluation of Unlicensed LPWAN: LoRaWAN and SigFox in IEEE Access - https://doi.org/10.1109/ACCESS.2022.3206030 .

2. A Communication Framework for Image Transmission through LPWAN Technology in Electronics (MDPI) - https://doi.org/10.3390/electronics11111764.

Systems of agricultural monitoring use communication networks such as mobile cellular networks inside IoT technologies. Their use may imply unattractive factors, for example access restriction in the modification of network operations, monthly fees with capacity limitation, high-energy consumption and limitations based on coverage availability. Other solutions involve high costs for variables such as energy consumption, installation, operation, management and maintenance. LPWAN networks present appealing features for monitoring processes in remote areas, as in agricultural monitoring processes. Nevertheless, current processes in which it is necessary to transmit a high amount of information, such as images, are limited. Consequently with the above, this proposal seeks to contribute to the implementation of a methodology for an agricultural monitoring system with the transmission images through LoRa modulation. —

3. Overview - Agricultural Monitoring System using Images through LPWAN network

This chapter presents an insight into the framework and explains its concepts and state of the art of each stage shown in Figure **2-1**. For this purpose, previous works are presented, compared and analyzed regarding the problems to transport images through LPWAN networks. In summary, this chapter gives the reader an overview of numerous techniques that partially tackle the research problem.

3.1. Image processing and classification

In this part is presented the main features, theory of image processing and classification features, the purpose is to make an overview of the fundamental concepts which are useful in understanding the main contributions of this thesis.

Recognition is the scientific discipline whose goal is the classification of objects into a number of categories or classes. Depending on the application, these objects can be images or signal wave-forms or any type of measurements that need to be classified [28]. In some cases, the objects use the generic term patterns. Pattern recognition is an integral part in most machine intelligence systems built for decision making. Machine vision is an area in which pattern recognition is important to capture images via hardware as a camera and analyzing them. To make classification, it is necessary to create feature vector of the images.This features allows training a classifier method and then evaluating and testing the classifier. In practice, the features correspond to statistical data (mean, mode, standard deviation and more...). The number of the features to use is very important since a larger number of feature candidates is better. To design the classifier, it is common to use a linear or non linear classifier and the performance is evaluated through the classification error rate. In addition, there are supervised versus unsupervised pattern recognition. When a set of training data is available and a classifier was designed by exploiting this a priory know information, this is known as supervised method to recognition. Nevertheless, this is not always the case, there is another type of pattern recognition tasks for which training data of known class labels are not available, therefore, a set of feature vector information is provided and the goal is to find the similarities, which is known as unsupervised pattern recognition [28–30].

In a classification task of M classes, $\omega_1, \omega_2, ..., \omega_m$ and an unknown pattern represented by a feature vector x, it is possible to form the M conditional probabilities $P(\omega_i|x), i = 1, 2, ..., M$. Sometimes, these probabilities are also refered to as subsequent probabilities, since, each of them represents the probability that the unknown pattern belongs to the respective class ω_i, given that the corresponding feature vector takes the value $\mathbf{x}$ [28]. Bayes decision theory could initially focus on the two class case ω_1, ω_2 to which pattern belongs. It is possible to assume subsequent probabilities $P(w_1), P(w_2)$, which are known. It is a reasonable assumption, because even if they are not known, they can be estimated from the available training feature vectors. Indeed, if N is the total number of available training patterns, and N_1, N_2 of them belong to ω_1 and ω_2, respectively, then $P(w_1) \approx N_1/N$ and $P(w_2) \approx N_2/N$ [28].

In any classification process the goal is to minimize the risk of the error probability, which is equivalent to partitioning the feature space into M regions, for a task with M classes. If regions R_i, R_j happen to be contiguous, then, they are separated by a decision surface in the multidimensional feature space. For the minimum error probability case, this is described by $P(w_i|x) - P(w_j|x) = 0$. From one side of the surface, this difference is

positive and from the other it is negative. The approach of classification problem via Bayesian probabilistic arguments is to minimize the classification error probability. However, not all problems are well suited to Bayesian probabilistic arguments. In many cases, the problems are too complicated and their estimation is not an easy task. In such cases, it may be preferable to compute decision by linear classifiers, such as Linear Discriminant Functions and decision hyper planes, the Perceptron algorithm, Mean Square Error Estimation, stochastic approximation, sum of error squares estimation, Support Vector Machines, among others, and non linear classifiers, such as Multi layer Perceptron, back propagation algorithm, polynomial classifiers, Support Vector Machines to nonlinear cases, and decision trees, among others [28–30].

A hyper plane in R^d is composed of $X \in R^d$ that satisfy $w^T X + w_0 = 0$ where $w \in R^d$ and $w_0 \in R$. In 1-Dimension $w_1 x_1 + w_0 = 0$ in 2-D $w_1 x_1 + w_2 x_2 + w_0 = 0$ and in 3-D $w_1 x_1 + w_2 x_2 + w_3 x_3 + w_0 = 0$. If $w_0 = 0$, then, the hyper plane passes through the origin. If $\langle w, x \rangle > 0$ in one site of the hyper plane - one class and $\langle w, x \rangle < 0$ in the other site of the hyper plane, two class.

3.1.1. Linear classifier

This subsection describes the main features and the main tools used to classify with linear method for two classes. The classification is done through the use of a hyper plane that allows separating one class of the other. For this purpose a lineal combination of the features is used. A hyper plane is composed of $X \in R^d$. The hyper plane $\{w, w_0\}$ divides R^d into two regions, thus, if $X \in R^d$,

$$w^T X + w_0 > 0, \text{ then, x can be found it in one site of the plane.}$$

$$w^T X + w_0 < 0, \text{ then, x can be found in the other site of the plane.}$$

The hypothesis H of the lineal classification can be defined as:

$$H(x) = +/- \left(w^T x + w_0\right) = \begin{cases} 1 & if \quad x \in class \quad A \\ -1 & if \quad x \in class \quad B \end{cases}$$

Consequently, a set of data is linearly separable if there is a separator hyper plane that could classify it.

Some tools of linear classifiers are:

- Least mean square (LMS) algorithm is an iterative noisy gradient descent algorithm that approximates the sample from the training example.

- Perceptron algorithm is a binary classifiers represented by a vector of numbers that belongs to some specific class and its prediction is based on a linear function with a set of weights with the feature vector.

- Fisher linear discriminant finds the projection to a line or a plane from different classes that are well separated.

- Support vector machine is a discriminate classifier defined by a separating hyper-plane.

In the two-dimensional space, the hyper plane is a line that divides a plane into two parts (class A or Class B). Now, if in a conventional plane (x,y), it is not possible to separate the two classes, it is necessary to apply a transformation that generates another dimension that allows separating the samples to classify [28–30].

3.1.2. Non-linear classifier

When it is not possible to classify through linear methods, it is common to use Kernels that make linear models work in nonlinear settings. To do this, it is possible to do mapping (changing the feature representation) of data to high dimensions where it exhibits linear patterns. Then, the linear model is applied in the new input space and thus, the data now is linearly separable in the new representation. The following are the most popular kernels for real-value vector inputs:

- Linear (trivial) Kernel:

$$(x, z) = x^T z \tag{3-1}$$

- Quadratic Kernel

$$k(x, z) = (x^T z)^2 \quad or \quad (1 + x^T z)^2 \tag{3-2}$$

- Polynomial Kernel (of degree d)

$$k(x, z) = (x^T z)^d \quad or \quad (1 + x^T z)^d \tag{3-3}$$

- Radial basis function (RBF) kernel $k(x, z) = exp\left[-\Upsilon||x - z||^2\right]$, where Υ is a hyper-parameter also called the kernel bandwidth - The RBF kernel corresponds to an infinite dimensional feature space.

It is worth noting that kernel hyper-parameters are chosen via cross validation. Kernels give a modular way to learn nonlinear patterns using linear models, therefore, it is necessary to replace the inner products with the kernel.

The cluster analysis allows finding similarities between data according to features underlying the data and grouping similar data objects into a cluster. The method used is an unsupervised learning where there are no predefined classes for a training data set and the goals are to identify the natural clustering number and properly group objects into sensible clusters. The typical applications are:

- As a stand alone tool to gain an insight into data distribution, and

- As a pre-processing step of other algorithms in intelligent systems.

The distance measures used are Manhattan, Euclidean distance, Mahalanobis and Cosine measure. The major clustering methodologies are partitioning, hierarchical, model-based and spectral clustering. [28–30].

The partitioning clustering approach has a typical clustering analysis via an iterative training dataset to learn a partition of the given data space produce several non-empty clusters and search and optimal partition achieved by minimizing the sum of squared distance in each cluster through a measure of distance. In K-means, each cluster is represented by the centre of the cluster and the algorithm converges to stable centroids of clusters. K-means algorithm is the simplest partitioning method for clustering analysis and widely used in data applications. Given the cluster number k, then, the k-means algorithm is carried out in three steps after initialization. First, each object is assigned to the cluster of the nearest seed point measured with a specific distance metric. Second, new seed points are computed as the centroids of the cluster of the current partition where the centroid is the centre as a mean point, for example, of the cluster. Third, it is necessary to return to the first point and stop when a new assignment is not presented. It is possible to say that K-means algorithm is a simple and popular

method for clustering analysis where its performance is determined by initialization and appropriate distance measure.

K-Nearest Neighbor has features such as: all instances correspond to points in a n-dimensional Euclidean space, and the classification is done through the comparison of feature vectors of the different points. For the samples, weights are assigned to the neighbors based on their distance from the query point and the target function for a whole space, which may be described as a combination of less complex local approximations.

Neuronal networks are a type of model for machine learning used for image recognition, natural language processing and more. The great potential is its high speed processing that offers thanks to a massive parallel implementation. It is also used for approximation in numerical paradigms because it has excellent properties of self-learning, adaptive tolerance to fouls, and non-linear processes. The literature review says that neuronal network can perform similarly to the human brain. The human brain has neurons working together to solve specific problems on daily basis. A Neuronal network has layers that are independent of one another, and a specific layer can have different numbers of nodes, called bias nodes. A bias value enables to move the activation function either to the right or the left, which can be analytical for training success. When a neuronal network is used as a classifier, the input and the output nodes will match input features and output classes [31].

Deep Learning refers to artificial neuronal networks with complex multi-layers. The distinction between deep learning and neuronal networks like feed-forward and feed backward neuronal networks is in their features. Besides, Deep Learning has more complex ways of connecting layers, more neurons count than previous networks to express complex models, more computing power to train and automatic extraction of the features. In the same way, deep learning is defined as a neuronal network with a broad of variables and layers with a single basic network architecture of un-supervised pre-trained networks [32].

The innovation with deep learning in image identification, object detection, image classification, among other tasks has great success. The major concept of deep learning is learning data representations by increasing the quality of handling ideas rather than event levels [31].

3.1.3. Survey on image processing and classification

Table 2 presents a summary of the state of the art about image processing and classification methods. Some data are not presented because they were not found in the works.

In [33] the authors present the management of a crop for early detection of diseases, the Red/Green/Blue (RGB) components are obtained and pre-processed for color balance. The image is then transformed and clustered to detect the cluster image of interest. After masking green pixels, the image is converted from RGB to HSV (Hue-Saturation-Value) color space for computation of textual features. These selective features are the input to the neuronal networks program, which can detect the disease.

In [34], high resolution multi-spectral and hyper-spectral remote sensing data has been used to detect and analyze a fungal sugar beet disease. A high-resolution satellite image was chosen to produce the results for the multi-spectral part of the study. To indicate the difference between healthy and unhealthy plants, image classification was made and evaluated. The authors conclude that the red and near infra-red parts of the reflectance spectrum are important for agricultural applications. The significant difference of the reflectance at the red portions of the spectrum compared with the near infra-red ones can be used to predict vegetation conditions.

The work in [35] studies a gray leaf spot disease. A component was chosen to segment disease spots and reduce the disturbance of illumination changes and the vein. Then, disease spot regions were segmented by using Sobel operator to examine disease spot edges. Finally, plant diseases are graded by calculating the quotient of the

Table 2. State of the art . Image Processing and Classification

Reference	Classification method	Image processing method	Authors	Year	Accuracy (%)
[33]	Neuronal networks	RGB components HSV color	S. K. Pilli Nallathambi, S.J.	2015	88
[34]		Hyperspectral and multispectral resolution, red / infrared components	R. Laudien, G. Bareth	2004	
[35]	Statistical	Segmentation, total area, sick area, RGB components, HSI color	S. Weizheng, W. Yachun	2008	
[36]	Neuronal networks	Edge and values	M.S.P. Babu B.S. Rao	2007	
[6]	Statistical	RGB components, H color I3a, I3b	A. Camargo J.S. Smith	2009	80
[3]	K-means Neuronal networks	RGB components, HSV color, texture and area	G. Athanikar M.P. Badar	2016	92
[37]	Deep Learning	area	S. P. Mohanty D.P. Hughes	2016	99-train 31-test
[8]	Software Color Pro		J.K. Sainis, R. Rastogi	1998	
[38]	K-means	RGB components, texture	M.B. and S.B. Dheeb Al Bashis	2011	93
[2]	K-means	Segmentation, green mask pixels, RGB	H. Al Hiary S. Bani Ahmad	2011	94
[5]	Neuronal networks	Spectral component	X. Wang, M. Zhang	2008	
[39]		Serological, molecular, hyperspectral data, infra-red fluorescence	C.D. Sindhuja Sankaran, Ashis Mishra	2010	
[40]	SVM	Spectral index	U. S. Rumpf K Mahlein	2010	97 binary solution 80 sick
[41]	SVM	Hyperspectral index	L.P. Jan Behmann Jorg Steinrucken	2014	70
[42]	Nearest Neighbors	Gray levels	A.S. Jagadeesh D. Pujari, Rajesh Yakkundimath	2015	90
[42]	PCA + Mahalanobs distance	Wavelet Discret Transform	A.S. Jagadeesh D. Pujari, Rajesh Yakkundimath	2015	83
[42]	Neuronal network		A.S. Jagadeesh D. Pujari, Rajesh Yakkundimath	2015	86
[42]	K-means + SVM	Color, shape and texture	A.S. Jagadeesh D. Pujari, Rajesh Yakkundimath	2015	85

disease spot and leaf areas. Researchers indicate that this method to grade plant leaf spot diseases is fast and accurate.

In [36], a software model is developed for remedial measures for pest or disease management in agricultural crops. This software can scan an infected leaf to identify its species, pest or disease incidence on it and possible solutions for its control. The software is divided into modules, namely leaves processing, network training, leaf recognition and expert advice. Recognition and classification were done in a feed-forward back propagation neuronal network. The inputs for this neuronal network are the individual samples of a leaf image.

The authors in [6] describe an image processing-based method that identifies the visual symptoms of plant diseases from an analysis of colored images. The processing algorithm developed starts by converting the RGB image of the diseased plant or leaf into H, I3a and I3b color transformations. I3a and I3b were developed from a modification of the original intensity of RGB components to meet the requirements of the plant disease dataset. The transformed image is then segmented by analyzing the distribution of intensities in a histogram. The set of local maximums is located and the threshold cut-off value is determined according to its position in the histogram. This technique is particularly useful when the target in the image dataset has a large distribution of intensities. Results showed that the developed algorithm was able to identify a diseased region even when it was represented by a wide range of intensities.

Deep Learning was used in [37] with a public dataset of images of diseased and healthy plant leaves collected under controlled conditions. The authors trained a deep convolutional neuronal network to identify 14 crops species and 26 diseases. The trained model achieves an accuracy of 99.35% on a held-out test set. When testing the model on a set of images from trusted online sources under conditions different from those for training, the model achieves an accuracy of 31.4%, then, more a diverse set of training data is needed to improve the general accuracy.

Image processing is performed in [8] using a ColorPro software developed in computer vision. The system was used in color image analysis for estimation of leaf area, infected leaf area and chlorophyll. Attacks on plants result in degradation of chlorophyll pigments in leaves. The infected leaves have patches of green and yellow color, mainly. The software can perform area measurements on green and non-green sectors of the leaf, thus the extent of infection can be quantified without high effort. In addition, the software can be used for quantitative estimation of chlorophyll in situ and measuring the intensity of color in the leaves.

In [38], an image processing based software was designed, implemented and evaluated for detection and classification of plant leaf diseases. Human vision observation to detect and classify diseases can be expensive, for this reason, a methodology of the proposed solution is described with image processing based on color transformation structure for RGB leaf image. The images are segmented using k-means clustering technique, then its texture features are calculated for the segmented infected objects and data are processed through a pre-trained neuronal network. The results indicate that the proposal can support an accurate and automatic detection and recognition of leaf diseases.

The authors in [2] proposed a software solution for automatic detection and classification of plant leaf diseases. First, a phase of segmentation was implemented, then, the mostly green colored pixels was identified. These pixels are masked based on specific threshold values that are computed using Otsu‘s method. Additionally, the pixels with zeros, red, green and blue values and the pixels on the boundaries of the infected cluster were removed. This process allows finding a form for detection of plant leaves diseases with a precision from 83% to 94% and can achieve 20% higher speed than approach proposed in other techniques referenced in the paper.

In [5], a development for spectral predicting of late blight infections on tomatoes was proposed based on artificial neuronal network (ANN). It was designed as a back propagation neuronal network that used gradient descendent learning algorithm to train the ANN to predict healthy and diseased tomato canopies with various infection

stages for any given spectral wavelength intervals. The results provide a highly accurate classification of healthy and diseased tomato plants.

The authors in [39] describe the currently used technologies that can be used for developing a ground based sensor system to assist in monitoring health and diseases in plants under field conditions. The technologies include spectroscopic and imaging based, and volatile profiling-based plant disease detection methods. Two categories for non invasive monitoring of plant diseases are: (i) spectroscopic and imaging techniques that include fluorescence spectroscopy, visible InfraRed spectroscopic, fluorescence and hyperspectral imaging, and (ii) volatile organic compounds (VOC) that involve the use of nose-based metabolite analysis.

In [40], a procedure is presented for the early detection and differentiation of sugar beet diseases based on Support Vector Machines (SVM) and spectral vegetation indices. The objectives were to discriminate diseased from non-diseased sugar beet leaves, to differentiate between the diseases Cercospora leaf spot, leaf rust and powdery mildew, and to identify diseases even before specific symptoms became visible. The discrimination between healthy sugar beet leaves and diseased leaves resulted in classification accuracies up to 97%. The multiple classification between healthy leaves and leaves with symptoms of three diseases still achieved an accuracy higher than 86%. Depending on the type and stage of disease, the classification accuracy was from 65% to 90%.

In [41] the proposed approach combines unsupervised and supervised methods in order to identify several stages of progressive stress development from series of hyper-spectral images. Stress of an entire plant was detected by stress response levels at pixel scale. Unsupervised learning was used to separate hyperspectral signatures into clusters related to different stages of stress response and progressive senescence. SVM was used to quantify and visualize the distribution of progressive stages and to separate well-watered from drought stressed plants.

3.2. Compression techniques and reconstruction algorithms

This section presents the main features of the theory of compression techniques and reconstruction process, to give an overview of the fundamental concepts useful for understanding the main contributions of this thesis.

3.2.1. Compression technique

In order to compress data, this document emphasizes two concepts: Compressive sensing (CS) and Source Coding (SC). CS works with high dimensional source data without loss, which allows compression into a lower dimensional measurement data and it can be ultimately reconstructed. In contrast, SC compression technique removes redundancy from the data sequence, and stores the data on a storage device or transmit them over a communication channel.

An image is a rectangular array of dots, distributed into m rows and n columns. The expression $m \times n$ is called resolution of the image and the dots are commonly called pixels. The term resolution is sometimes also used to indicate the number of pixels per unit length of the image. There are some types of images, for example: a monochromatic image (also called bi-level) has pixels with one out of two values $0, 1$ that correspond to black or white colors and it is considered the simplest type of image. In a gray scale image, a pixel can have one out of the n values 0 through n-1 indicating one of 2^n, where n could be $4, 8, 12, 16, ...$ A continuous-tone image can have many similar colors (or gray-scales) and it is hard for the eye to distinguish their colors. A discrete tone image is normally an artificial image that may have a few or a many colors, but it does not have the noise and blurring of a natural image. A cartoon image has a color image that consists of uniform areas, where each area has a uniform color but adjacent areas may have very different colors. It is clear that each type of image may has feature redundancy, but they are redundant in different ways. This is why any given compression method may not perform well for all images and different methods are needed to compress the different image types [43].

Modern hardware can display many colors, which is why it is common to have a pixel represented as a 24-bit number (R-G-B components, where each one occupies 8 bits), Therefore, a 24-bit pixel can specify 1 to 2^{24} million colors, thus an image of a resolution of 512 x 512 pixels occupies 786432 bytes (262144 in each component), and resolution of 1024 x 1024 occupies 3145728 bytes. Then, image compression is highly important. In general, the information can be compressed if it is redundant, however, there is a concept called "remove irrelevancy" where an image can be compressed with loss through the removal of irrelevant information even if the image has no redundancy [43]. The principle of image compression uses spatial redundancy; for this reason, if we select a random pixel in an image, then it is possible that its neighbors have the same or similar colors, thus the neighboring pixels are highly correlated. With this information, it is possible to rebuild the original data with high values of efficiency.

Within compression methods, it is possible to find CS that performs acquisition and compression simultaneously. CS offers a framework for simultaneous signal acquisition and compression, which is based on linear dimensionality reduction. It guarantees accurate source reconstruction from far fewer number of measurements (rather than high dimensional raw measurements), under the condition that the source signals can be illustrated in spars forms. Nevertheless, the information of an image needs to be digitized and coded when it must be transported through a communication network, thus it uses quantizers for compression, transmission and storage, for example, in order to satisfy the delay constraints of modern network services. The prototype of classical coding and communication techniques needs to be reconsidered. Therefore, it is important to re-design quantization and coding techniques to meet performance features of recent network data systems. For this purpose, it is important to design and analyze source and channel coding schemes, based on quantization and real time transmission under CS [9].

CS has gained attention in the last years, since it is a technique to create and retrieve sparse signals with low noise in a known basis, with far fewer samples those needed through the Shannon-Nyquist sampling theorem. CS allows working with a high dimensional signal to be accurately retrieved from relatively fewer measurements

through a non-linear optimization procedure. For the above, the documents present in [44] [45] used a program that represents the original signal in a sparse signal through an adequate sparse representation. The original signal can be represented in a vector with an Nx1 size, where N is equal to:

$$n \times n \quad [rows] \times [columns]$$

which belongs to the matrix of original information or signal.

In the literature, some papers have implemented CS as a tool for several applications, for example, the work in [46] describes a framework location accuracy of sparse transmitters in a wireless environment. Authors in [47] introduce a algorithm to solve CS problems. The works in [48] [49] use CS in spectrum cartography to discover spectrum holes in the space. CS for multi-target sparse localization algorithm is used in [50] with cross correlation of the signal readings at several access points. In [51], CS stands out as digital image processing, wireless channel estimation, radar imaging and cognitive radio (CR) communications. The paper is a survey that focused on CR, which is used in radio spectrum allocation and occupancy measurements through sparse signal in multiple domains such as time, frequency and space, because these are mechanisms that allow improving the future generation on wireless networks where CS is highlighted as a theory that help to retrieve any signal from fewer samples with a wide margin than traditional methods.

CS is a method for building a sparse signal, since it is a vector with a few samples of the original signal that allow the reconstruction algorithms methods to rebuild the original signal with higher precision and fewer losses. For improving CS, the original signal is transformed into a representation base as Wavelet Transform, Discrete Cosine Transform, Fourier Transform and Kronecker Transform, mainly. This allows the samples to be in a common domain and reduce the variability of the original data.

CS techniques helps to reduce a information signal with a samples lower than Shannon-Nyquist theorem [45,52], all the above with sparsity technique and original signal processing, mainly. Sparsity uses information signal as *"s"*, which is equal in discretely form as a vector $S \quad \in \quad R^n$. The term s has a spreading factor k and s elements different from zero of the original signal (the most representative). The signals with low dispersion (high k factor) can to convert to a signal with a greater dispersion through lineal transformation f by $f = s$ and $f \in R^{nxn}$, which represents data of Wavelet Transform, DCT Transform or Kronecker Transform, mainly.

A k-disperse signal $f \in R^n$ is sampled with CS to obtain a $g \in R^m$ signal, where $m << n$. The sampling can be represented in matrix form as $g = f \quad y \quad \in \quad R^{mxn}$, called system sampling matrix. If f is unknown, it is possible to find an indeterminate system of linear equations (infinite solutions). This problem can be solved with an optimization problem converted to a complex mathematical problem that is not convex. Another solution is to employ g and the sense matrix with algorithms such as "IterativeHardThresholding" (IHT), "OrthogonalMatchingPursuit" (OMP), "GradientP rojectionforSparseReconstruction" (GPSR) o "Two − stepIterativeShrinkage/Thresholding" (Twist). [45, 53–55].

CS allows representing a signal with a few samples of the original signal. If a signal or its transformation basis can be represented as a sparse signal, then, it is possible to use these techniques to represent a vector of information with fewer samples and recover with high values of the original signal. This provides advantages in wireless communications, particularly in energy consumption and bandwidth.

For the aforementioned reasons, the process of CS help to reduce data payload, process time and energy consumption, mainly. Particularly, an image can be represented by a vector. For example, some components RGB or Gray components of image have components or spectral bands R, G, B, gray. Spectral bands have a large number of pixels, but why is it important to work with a high number of data? It is important because this entails more precision, quality and reliability of process information, nevertheless, this mean a problem for the computational process such as high energy consumption, delays in process and more. Consequently, it is necessary to reduce the data numbers to represent a image. In recent years, methods have appeared to acquire least data through CS that reduces the data redundancy and manage the data with minor dispersion through

base transforms. The main bases were listed above, and are well suited for the compression methods used in JPEG 2000, MPEG and MP3 standards, mainly.

On the other hand, Source Coding (SC) is a compression technique that removes redundancy from the data sequence, SC works in order to store the data on a storage device or transmit it over a communication channel. The source or the measurements have to be mapped in a good digital format. For the above, SC techniques are typically classified into two categories: lossless and lossy SC.

The aim of lossless SC is to digitally represent the source, so that it can be perfectly reconstructed. On the other hand, the objective of lossy source coding is to reconstruct the source from arbitrary source coded information within a small amount of distortion. In applications where there is not much concern about a small amount of source information such as compressing multimedia, audio, image and CS measurements, lossy SC provides more flexibility compared with lossless coding, where the source coding rate is not restricted. Some examples of lossy SC are MP2, MP3 and JPEG [9, 56].

Peak Signal To Noise Ratio - PSNR

PSNR is a parameter that is typically used to assess the quality of an image transmitted over a network. As image quality is assessed quantitatively, it is based on the difference between the pixels of the image reconstructed following transmission and the original image [23]. The PSNR of a transmitted image can be calculated as 3-4:

$$PSNR = 10log\left(\frac{S^2}{MSE}\right) \tag{3-4}$$

For an image of 8-bits, s is 255 and MSE is the mean squared error, which is the average of the squared difference in the intensity pixels in the original and the output images. MSE is calculated as in 3-5

$$MSE = \frac{1}{mn}\sum_{i=0}^{m-1}\sum_{j=1}^{n-1}[I(i,j) - K(i,j)]^2 \tag{3-5}$$

where m and n are the respective length and width of the image in pixels, and $I(i,j)$ and $K(i,j)$ are functions describing the intensity of individual pixels in the transmitted and received image, respectively [23, 43].

3.2.2. Reconstruction Algorithms

Reconstruction techniques are tools that allow the signal to be constructed using few samples of its original signal. These samples are a resultant vector of the compression technique process. Several tools are available from the scientific literature, such as Iterative Hard Thresholding (IHT), Orthogonal Matching Pursuit (OMP), Gradient Projection for Sparse Reconstruction (GPSR) or Two Step Iterative Shrinkage/Thresholding (Twist). These tools were evaluated and compared with the aim to find the best solution. Their main features are presented bellow:

- IHT: If we have y[0]=0 and use the iteration:

$$y^{[n+1]} = H_s * [y^n + \phi^T * (X - \phi * y^n)] \tag{3-6}$$

where $H_s(a)$ is a non-linear operator that configures the values of s-smaller in magnitude than a vector in zero. The convergence of this algorithm was described under condition $\| \phi \|_2 < 1$. In this case, the algorithm converges to a local minimum in the optimization problem. IHT involves the operation of ϕ and ϕ^T once in each iteration, as well as the addition of two vectors. The H_s involves a partial order of the elements in magnitude and requires a storage of X and the storage of a vector with length N [57–59].

$$a^{[n]} = (y^{[n]} + \phi^T * (X - \phi * y^{[n]})) \tag{3-7}$$

The IHT algorithm is referred to as:

Input: measurement vector $y \in R^M$
sample matrix $\phi \in R^{MxN}$
K dispersion, regularization parameter μ and maxiter (maximum number of iterations)
Output: disperse vector $X^\Lambda \in R^N$
1: vector start $X^{\Lambda 0=0}$
2: for i=0 to maxiter do
3: $y^{\wedge(i+1)} = H_s(y^{\wedge i} + \mu * (\phi^T * (X - \phi * y^{\wedge i})) \rightarrow H_s(.)$ thresholding operator
end for

OMP: If s is an arbitrary m-sparse signal in R^d and $X_1, ..., X_N$ is a representation of measurements vectors N where a matrix ϕ on $N \times d$ is formed, whose lines are the measurement vectors, N is the measurements of the signal grouped into a N-dimensional data vector $v = \phi * s$ which is a combination of the m columns of ϕ. In terms of sparse approximation, v has a representation of term m on the ϕ dictionary. The sparse representation algorithm can be used for sparse signal recovery. To identify the ideal s signal, the column of ϕ that participates in the measurement of vector v is determined. The goal of the OMP algorithm is to choose the column of ϕ where data belongs. In each iteration, the column of ϕ with the highest correlation with v is chosen, afterward, the contribution is extracted an the next iteration is carried out with the residuet. After m-iterations, it is expected that the algorithm can correctly identify the original vector-column with a minimum error [17, 57–60].

The OMP algorithm is referred as:

Input: measurement vector $y \in R^M$
sample matrix $\phi \in R^{MxN}$
K dispersion
Output: disperse vector $X^\Lambda \in R^N$
1: Initialize vectors $X^{\Lambda 0=0}$
$X^{\Lambda 0=0}$,r^0, and $\Lambda 0 = 0$
2: for i=1 to K do
3: proj = $\phi^T r^{i-1}$
4: λi=λ_{i-1} U $supp(H_1(proj))$
5: $X_{\lambda i}^{\lambda i}$=$\phi_{\lambda i}^{+}$ and, $X_{\lambda i}^{\lambda i} = 0$
6: $r^i = y - \phi X^{\lambda i}$
end for

Algorithms of GPSR and Twist correspond to developments where they have a limit in the capacity to structure a working logic. Nevertheless, with prior implementation of IHT and OMP algorithms, it is possible to understand the configuration to adapt the implementation and run them based on literature features [57, 61].

3.2.3. Survey on compression techniques and reconstruction algorithms

The following lines present works in compression technique and reconstruction algorithms. This information is presented with the aim to reduce information for agricultural crop images. The image information is compressed in order to transmit it through a LPWAN wireless infrastructure and the remote server recovers the images with the use of reconstruction algorithms almost equal to the original. The following works show compression techniques to use and reconstruction algorithms techniques.

Table 3 presents a summary of the state of art in compression techniques and reconstruction algorithms, mainly. Some data are not presented, because they were not submitted in the papers.

The work in [57] shows CS method to reduce information below Shannon-Nyquist theorem and also describes CS to energy preserve, efficiency in data transmission and optimal reconstruction of the signals. Analytic method is presented in [62] in order to implement CS with a signal (digital image). If a result $\boldsymbol{x}$ is a unknown vector in R^m, a linear function "n" is used for rebuilding the original signal. If $\boldsymbol{x}$ is known, then, a code is used for rebuilding the signal; in both cases $m << n$. An adaptative group sparse representation is proposed in [63] for image CS recovery. A framework based on alternating direction method of multipliers is presented, where the adaptative singular value thresholding is introduced to solve the group sparse representation problem. The threshold adaptively decreases during iterations, in contrast to the traditional methods where it is independent of the iteration number. The results reveal a good convergence performance and improve the CS recovery.

Authors in [58] describe a method for monostatic ultra wideband microwave imaging of breast cancer using CS. Instead of using all of the conventional radar returned signals, a few received signals, by randomly choosing the antenna, are sufficient for obtaining reliable images even at high noise levels. The simulations show that sparse images are obtained comparing the delay and sum beam forming technique and using only a few received signals. The work in [59] describes the features and advantages of CS for images (CSI) and develops a mechanism to carry information of images in an unsure channel. It uses only a few data given by CSI. By using only a few samples, security is improved.

Compression and reconstruction techniques for images with CS are described in [64] and several tools are evaluated with Gaussian model and sensing matrix for reconstruction. In [60] the authors obtained information

Table 3. State of the art . Compression techniques and reconstruction algorithms

Reference	**Compression technique application**	**Reconstruction algorithm**	**Authors**	**Year**
[57]	Efficiency in data transmission	IHT	R. G. Baraniuk	2007
[62]	Image compression	Basis pursuit OMP	D. L. Donoho	2006
[63]	Image compression	DWT, CT, TV, MH, CoS, sgsr, AGSR	T.Geng, G. Sun Y. Xu, B. Zheng	2018
[58]	Medicine Image compression		N.Z. Naghsh, A. Ghorbani H. Amindavar	2018
[59]	Channel security through image compression		C. Ruland	2018
[64]	Image compression	Gaussian, abolghasemi and sense matrix method	M. K. B. Suhani Salan	2008
[60]	Spectral image compression	AG-JSM1 FG-JSM-1 S-s-CS JSM2	L. Deng, Y. Zheng P. Jia, S. Lu, J. Yang	2017
[17]	Image encryption	DCRE DPRE	Q. Wang, J. Wang Q. Wang	2018
[61]	Image compression for radar application	IHT PKS	W. Zei, L. Yang Z. Wang, B. Zhang, Y. Lin, Y. Wu	2018
[65]	Image compression for magnetic resonance	Basis Pursuit OMP	S. Ramdani	2018
[17]	Medical image compression	Basis Pursuit OMP	L. Wang, L. Li, J. Li B. Gupta, X. Liu	2018
[66]	Test GPRS reconstruction algorithm	GPRS	M. figuiredo, R. Nowak, S.J. Wright	2007
[67]	Test reconstruction algorithm	Quadratic problem L1 Lagrange, multiplier, Twist, Lasso	J.N. Tehrani, C. Jin A. McEwan A. Van Schaik	2010
[68]	Test IHT reconstruction algorithm	IHT	N. Koep R. Mathar	2017
[69]	Test OMP reconstruction algorithm	Basis pursuit OMP	X. Cai, Z. Zhou Y. Yang, Y. Wang	2018

about hyper-spectral images and evaluated the data information through sparsity models and adaptative clustering techniques AG-JSM1, FG-JSM-1, S-s-CS and JSM2. A encryption method of images is developed in [17] with the use of CS techniques called DCRE and DPRE. CS for compression of images in magnetic resonance is described in [61] using a reconstruction technique called Basis Pursuit OMP. In [65] and [17], the authors use CS in images compression for magnetic resonance and a reconstruction technique called OMP. In the following references, it is possible to find the evaluation of algorithms reconstruction to use in CS: GPRS [66], L1 norm, lagrange multiplier, Twist and Lasso [67] IHT [68] and OMP [69].

3.3. IoT-LPWAN networks

This part of the document introduces the main and most important features of LPWAN networks, its uses and main technologies in licensed and non-licensed frequency bands. The purpose is to give an overview of the fundamental concepts useful for understanding the main contributions of this thesis.

IoT wireless networks designates a new digital time to facilitate data transport information. It is considered to be the third wave of information technology after the Internet and mobile communications. IoT concept was formally proposed in 2005 by ITU [70,71]. The technologies inside IoT are used in wireless networks sensors for service control in telemetry applications, smart cities, health or precision agriculture. Nevertheless, it can be used in other scenarios where the main objective is data transport with low amount of information. [21,72–75].

IoT grows with the relation of Internet in 5 stages: (1.) one to one communications, known as the stage of pre-Internet; (2.) "www" communications or content Internet; (3.) the WEB 2.0 services-Internet; (4.) the Social WEB, people-Internet and (5.) stage M2M (Machine to Machine) Internet of Things [20,76–82]. IoT facilitates the local and remote process control with connectivity of information networks, especially in Internet [83]. IoT is a concept that allows gathering technologies for specific uses, for example, low consumption battery, large range or low data transport [84–87]. In [88], it is possible to observe IoT elements for understanding it. Categories have an identification: sensing, communication, computation, service, and semantics, that serve to deliver the functionality of IoT. One of the objectives of IoT is to collect wireless communication technologies with common goals for connecting heterogeneous objects to deliver specific smart services. Typically, the IoT nodes should operate with low power lossy and noisy communication links.

The main IoT tools from range and coverage are: Wireless Personal Area Network (WPAN), where it is possible to find technologies such as Bluetooth, Zig-bee and Wireless Hart with coverage among 10 - 100 meters; Wireless Local Area Network (WLAN), where it is possible to find technologies within IEEE 802.11a/b/g/n/ac/ah with coverage among 100 - 1000 meters, Wireless Neighborhood Area Network (WNAN) with technologies such as Wireless Smart Utility Network (WI-SUN), a precursor of WPAN networks with IPV6, whose coverage is among 3 - 10 kilometers; Wireless Wide Area Network (WWAN), including technologies such as mobile networks (2G/3G/4G) and LPWAN (Low Power Wide Area Networks) where it is possible to find technologies such as 4G mobile, particularly, the Release 12 and 13 of Third Generation Partnership Project (3GPP) with Long Term Evolution for Machines (LTE-M) and Narrow Band IoT (NB-IoT) in the private spectrum, and Sigfox, LoRaWAN, Weightless, Ingenu and others in the free spectrum. Private and free spectrum technologies have medium coverage among 10 - 50 kilometers, approximately [21,89–91].

Many companies develop new applications and services under IoT with low power consumption, high coverage and low data transport and are interesting for standardization bodies like 3GPP or IEEE Standard Committee [92]. For example, NB-IoT and IEEE 802.11 try to develop common technologies that can be used in a vast range of scenarios. On the other hand, there are technologies like Sigfox, LoRa and Ingenu that are proprietary technologies. Here, it is important to highlight Semtech (developer of LoRa), which published a LoRa Specification for opening the door to independent performance evaluation [91,93,94].

3.3.1. LPWAN communication technologies

This part shows the general access techniques employed in wireless networks, particularly in LPWAN, as well as presents the main features of IoT and LPWAN wireless networks such as specifications, protocols, and main technologies.
The next lines present the main features of IoT and LPWAN wireless networks such as specifications, protocols, and technologies. Wireless networks technologies give a support of development of the IoT environment. Some references are (i) devices working in a small range of coverage, for example, Near Field Communication (NFC); (ii) Radio Frequency Identification (RFID); (iii) Technologies such as 6LowPAN and Zig-bee, under IEEE 802.15.4; (iv) systems such as Bluetooth and Bluetooth Low Energy (BLE); (v) private technologies such

as Z-WaveTM, CSRMeshTM, Nwave (Weightless -N), M2COMM (Weightless –P), Acellus, Telensa, Dart, Wavelot, Qowisio, Wifi Halow (IEEE 802.11ah) and Ingenu (On-Ramp), and (vi) systems in IEEE 802.11/WIFI-TM [91, 91, 95–110].

In the ERC 70-03 recommendation of the Electronic Communication Committee (ECC), it is possible to find information about Short Range Devices (SRD-devices). The main goal is to do radio transmissions in uni-directional or bidirectional ways with low interference capacity to others devices. In the recommendation, it is possible to find the relation and coexistence of frequency bands, power maximum levels, channel spacing, modulation, wide of band and duty cycle. With that recommendation, the developers in the IoT industry give the parameters for frequencies use.

In wireless systems, modulation techniques have been developed for supporting communications where multiple users are present among other advantages. There are some techniques that facilitate the communication process, such as Code Division Multiple Access (CDMA) and spread spectrum (SS) that employ pseudo-random number sequences to modulate a signal. Multiple transmitters use the same signal with orthogonal codes (called Walsh codes), to separate communication channels [111, 112]. Frequency Division Multiple Access (FDMA) allows different users with various carrier frequencies [113] and, Time Division Multiple Access (TDMA) uses time slots to coordinate multiple transmitters. The users transmit in fast sequence, one after the other, and each one uses its own time slot. It allows multiple stations to share the same transmission medium while they are using the available bandwidth. [114–116].

LPWAN networks used in IoT communications have special features, such as limited packet size (for example 127 bytes for IEEE 802.15.4), length address variable and low bandwidth [88, 117]. The Internet Engineering Task Force (IETF) and Six Low Wide Wide Pan Access Networks (6LoWPAN) groups were working on the development of the standard since 2007, where the mapping of services is required for Internet Protocol version 6 (IPv6) over LPWAN networks for maintaining the IPv6 protocol. The standard provides header compression to reduce the transmission overhead, fragmentation to set the IPv6 Maximum Transmission Unit (MTU) [83, 117].

Figure **3-1** presents the relation between information transport capacity and coverage of wireless technologies. LPWAN gathers broad coverage, lower capacity information and low battery consumption, mainly [118].

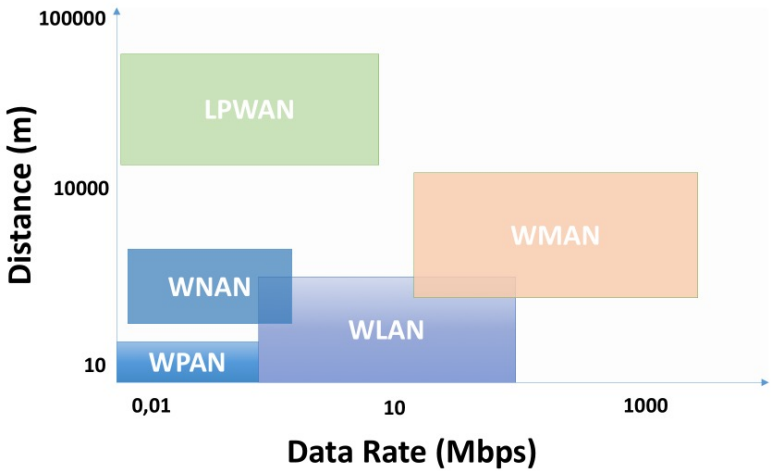

Figure **3-1**.: Data rate vs. Reach. Characteristic wireless of information transport capacity (Mbps) and coverage (meters).

Some applications of LPWAN networks are automation process, events control, smart illumination, smart parking, pets tracing, garbage collection, precision agriculture, monitoring in the mountains (fire, seismology), health, and others. LPWAN opens a broad possibility for development in the social environment inside Internet Communications Technologies (ICT's) projects [85, 95].

LPWAN works inside IEEE 802.15.4 for unlicensed frequency bands with Instrumental, Scientific, and Medical (ISM) free bands such as 2.4GHz, 868/915/433/169 MHz, in agreement with the operation area and in LTE-M / NB-IoT works in LTE bands for licensed bands. The main settings are tracing, control, capacity, payload, coverage, range and operation frequency. [90, 119–121]. Figure **3-2** presents the relation between IoT scenarios connectivity among licensed and unlicensed frequency bands.

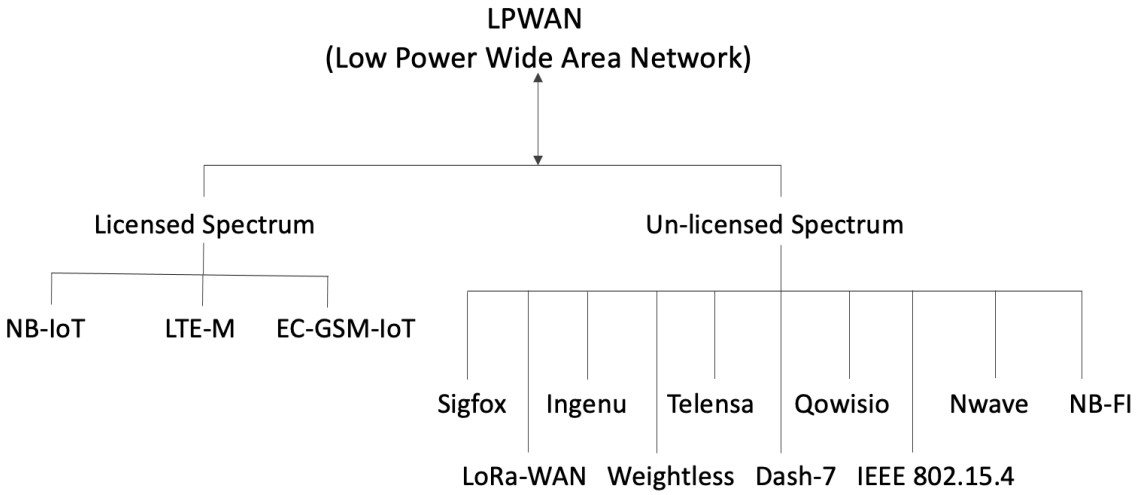

Figure **3-2**.: Scenarios for LPWAN networks with licensed and unlicensed bands frequency operation.

3.3.2. LPWAN technologies

This subsection describes the main technologies that work inside IoT LPWAN technologies. Developers of solutions LPWAN for Europe and America affirm that their devices work with a nominal sensitivity in Rx of approximately -150dBm- It is a feature that allows data transport with a broad reach. This aim contrasts with the low capacity data transport, delays and information losses. [21, 73, 122]. A section of this research presents the main licensed and non-licensed bands technologies by LPWAN services. The aim is to show a global vision of some technologies. Usually, academic papers are focused on the needs of special solutions, therefore, it is worth mentioning that in the references, no technology solution is more than other; therefore, the discussion is open.

LPWAN works in star topology among gateway and end-devices(motes). The network is used in many applications where it is possible to concentrate in communicating peripherals, machines, and devices with communication Machine to Machine (M2M). The main advantages are: data transport information with a high coverage, long time life of battery, low cost and free-spectrum use in some technologies. The disadvantages are a low duty cycle of co-existence in shared spectrum to reduce the functionally of the spectrum for regulation, low data rate and licensed spectrum for technologies around 3GPP group (LTE), mainly [86, 123].

Licensed Technologies

In technologies that use licensed frequency, it is possible to find 2G, 3G and 4G generations of mobile phone networks, with Quality of Service (QoS), low latency, and licensed frequency operation (high cost).

At the beginning, for LPWAN the goal is to adapt 2G and 3G for the developments in IoT; nevertheless, multiple medium access problems were found when sharing the system radio resources (time, frequency and space), among users in the same cell (intra-cell), and interference with other cells with same features that entails inter/co-cell interference.

2G generation phone network has technical limitations by the granularity offered that can not serve high values of devices. The system is not energetically efficient and the signaling is over-sized for small packets. In 2G, each cell uses a single frequency channel that was not used by its neighbors. This ensures low interference but miss a frequency re/use that complicates the growth of nodes number [73, 124].

3G uses all bandwidths and uses CDMA. For each transmitter, a single code is assigned the receptor takes all signals and only process those of interest. 3G uses Direct Sequence Spread Spectrum (DSSS) for carrier modulation, which increases the bandwidth and reduces the spectral efficiency. The output is similar, such as noise, therefore, it will only be processed by the interested source. 3G has disadvantages for IoT such as power control that needs high signalling values (overhead), its down-link interference from neighbor sources which reduce transmission capacity. The main problem of 3G for IoT is energy consumption, management overhead, power control and energy consumption, which involve disadvantages for IoT devices [73].

4G obtains the best of 2G and 3G: it keeps the transmissions orthogonality in each cell and allows frequency re-use. It uses Orthogonal Frequency Division Multiple Access (OFDMA), which allows reducing the Inter Symbol Interference (ISI) and Inter Channel Interference (ICI). The carriers are allocated among users of the same cell separated for diversity, thus reducing intra-cell interference and carrier change every OFDM symbol. Some topics should change, such as energy consumption and coverage; nevertheless, the most important challenge was to adapt the medium access protocol by massive access. Specifically, the Random Access Channel (RACH) would be overloaded by massive devices (nodes) that could affect the efficiency for e-nodes and mobile users. Finally, among different proposal solutions in the literature, the most convincing one is to give separate channels for IoT devices [125–128].

Third Generation Partnership Project (3GPP) presents LTE Rel-12 for low cost devices and in Rel-13-15. The features enhanced Machine Type Communication (eMTC) and Narrow Band (NB) - IoT were presented. eMTC introduces coverage enhancement, which was extended to NB-IoT. It can be used in three modes: (i). stand-alone, such as a dedicated carrier; (ii) in band with occupied bandwidth of a wideband LTE carrier, and (iii). with a guard band of an existing LTE carrier. NB-IoT has the same goals of LPWAN networks. It uses narrow band (similar to Sigfox) designed for IoT applications. It uses a 200 kHz in one channel GSM, while for in-band and guard band modes, it will use one physical resource block (PRB) LTE of 180 kHz [129]. NB-IoT includes low cost devices, high coverage (20 dB) [129–131], long battery life and massive capacity services. The bandwidth in LTE/GSM with licensed bands has similar values of spectral efficiency, latency and throughput to LPWAN in unlicensed bands (LoRa, Sigfox...). In the next versions, it intends to reduce latency, develop vehicular communications systems and reach the goals of 5G generation [132,133]. NB-IoT was designed in LTE infrastructure, re-using the same hardware and share spectrum without issues. For most LTE radio stations, NB-IoT can be supported via software upgrade, however, in some cases a hardware upgrade is necessary. Some of the main features of NB-IoT are:

- Improved indoor coverage for achieving extended coverage compared with GPRS devices. It corresponds to achieving around 164dB of link budget.

- Support of massive number of nodes: it supports around 52000 devices within a cell site sector.

- Reduced complexity devices to support IoT applications.

- Latency on 10 seconds or less for maximum number of devices.

- Improved power efficiency to provide around ten years of autonomy.

NB-IoT is part of 5G generation mobile networks where companies such as Nokia and Huawei have spent efforts in it standardization. Nevertheless, NB-IoT systems need to be performed in two dimensions: the modulation and coding scheme (MCS), with a selection level as in traditional LTE systems, and the repetition number determination. The reasons are: different MCS levels influence throughput of the system directly, and low MCS and high power will improve transmit reliability and enhance coverage, but it reduces the system throughput and repeat transmission and control data signals that have been selected as a promising approach to enhance coverage of NB-IoT systems, wherein more repetition number will enhance the reliability, but cause spectral efficiency loss [133]. More information on technical data of NB-IoT can be found on [132, 134]

In summary, 4G-LTE to NB-IoT has been adapted and it is in constant evolution. 2G and 3G can be modified but the solutions are not completely good in values of scalability, coverage and energy consumption.

Non-Licensed Technologies

This subsection describes the main technologies that work in unlicensed frequency bands for IoT LPWAN applications.

i. Sigfox

Sigfox is a method of information transport with LPWAN wireless characteristics: In 2004, Hal R. Walker proposes for the first time the use of Very Minimum Shift Keying (VMSK) for compressing data transmission in a narrow band frequency. In practice, this modulation technique gives steps for advancing in LPWAN networks, but did not reach the expected results for occupying the name of the ultra narrow band. The French company, called Sigfox, successfully reached the development and patent of Ultra Narrow Band (UNB) technology [21, 84, 135].

Modulation, Bandwidth and Frequency Bands

Sigfox works with a broadcast of binary data with BPSK modulation and low data rate "R_b", approximately 100 bps. Its transmitted signal has a frequency band *"B"* of 100 Hz. The novelty of Sigfox consists in multiple transmissions with bandwidth *"B"* in a bigger band and uses approximately 192 kHz in ISM bands (868/915) MHz. These bands could suffer a flat fading or frequency hopping, inside band of operation *"B"*, which supports diversity and hence improvement of the reliability [118].
An important factor in the Sigfox system is the precision of the oscillator, which induces an offset between the average frequency at the exact time and operation frequency. A low signal of bandwidth in UNB needs a high sensitivity of oscillator precision [75].

Access Method

The associated MAC to UNB is Random Frequency and Time Division Multiple Access (RFTDMA). The end-device access is random in the wireless environment in the time-frequency domain. This corresponds to Aloha access protocol without previously reviewing the channel occupancy. In contrast with classics Aloha transmissions, the carrier frequency was chosen inside *"B"* with a continuous interval in contrast to a discrete configuration pre-defined [77, 118].

The work in [21] shows an example where signals of 100 end-devices are generated and results of receiver monitoring appears in features as time and frequency. The benefits of using RFTDMA are:

- There is no energy consumption for channel review

- No network synchronization is needed. The message posting package could be eliminated.

- here is no restriction in oscillator precision. Any frequency can be chosen inside every operation band and any oscillator can be used without service degradation. It is important to consider that a medium access without control produces interference or packages collision.

An optimum demodulation process carries an efficient algorithm Software Design Radio (SDR), where the process allows analyzing the frequency band, transmitted signals detection and information recovery [90]. In Sigfox, we can find a signal processing that relates a Fourier Fast Transform (FFT), which is applied to the received signal and then used in an adaptive detector that allows identifying the transmitted signal in the spectrum [84]. For each detected transmission, the frequency band was filtered through Binary Phase Shift Keying(BPSK) demodulator.

Payload

To improve reliability, each message can be sent up to 3 times in different frequencies. Each station responds in the same frequency, thus allowing to maintain the reception in the end-device and avoiding the frequency band analysis. In the transmitted package, we can find 12 bytes that change to around 25 bytes when it is necessary to add network management information and the data payload has full information. With the information found about Sigfox literature, a frame of Sigfox technology was constructed and will be presented in figure **3-3**."

Preamble- A header of 4 bytes.

Synchronization frame (Syn) of 2 bytes.

Device identification (D.I.) of 4 bytes.

Duty payload of 12 bytes.

Code Hash (C.H.) of authentication in Sigfox network with variable length.

Cycling redundancy check (CRC) of 2 bytes for error detection and security.

Figure **3-3**.: Sigfox Packet, The structure of a frame of Sigfox wireless technology.

Capacity

Sigfox offers capacity based on devices number and transmitted messages numbers per day [71]. Its capacities are shown in Table **3-1**.

Table **3-1**.: Models Sigfox

Name	Messages number	Downlink number
Platinum	101 - 140	4
Gold	51 - 100	2
Siver	3 - 50	1
One	1 - 2	0

A typical frame duration is around 2 seconds [136].

Coverage

When we have a data link with line of sight (LoS) and without interference, it is important to consider the coverage and the noise level in 3-8

$$N_{dBm} = -174 + NF + 10 * log_{10}(BW) \tag{3-8}$$

where:

NF is the noise figure of the receiver.

BW is the bandwidth.

For UNB systems, the noise floor is (-154+NF) dBm.

On free space conditions and if antenna gain has a balance with noise factor losses, the signal to noise relation (SNR) is shown in 3-9.

$$SNR = P_r - N = PT_x + 132 - 20 * log(r/\lambda) \tag{3-9}$$

where:

P_r is the receiver power.

PT_x is the transmitter power.

r is the range.

λ is the wavelength.

With an SNR limit equal to 9 dB and a link margin of 5 dB, the reception power required in the receptor must be $P_r \geq -142$ dBm with maximum power among [14 - 27 dBm] according to regulations (Europe and Americas, respectively). The above ensures coverage in LPWAN networks [21].

The sensitivity to interference is important when transmission happens simultaneously. The interference situation is characterized by peaks on the average. When we have two transmitters in a multiple access channel, the signal in the receptor is shown in 3-10.

$$r(t) = \sum_{i=1}^{2} S_i(t).g(f_i, t) \otimes h_i(t) + n(t) \tag{3-10}$$

where:

$S_i(t), \forall_i \in 1, 2$ are the BPSK symbols sent by active user.

i; $g(f_i, t)$ is the impulse response of the emission Finite Impulse Response (FIR) filter in f_i (tensor products of the vectors).

$h_i(t)$ is the path loss of the link, and

$n(t)$ is the Additive Gaussian White Noise (AGWN) with zero mean and variance.

Energy Consumption

The energy consumption in a normal emission varies between 20 mA - 70 mA. This feature depends on the message size. It is worth mentioning that energy consumption can be kept very low for extending battery in IoT applications.

Unfortunately, the public information about Sigfox technology is very limited because it is a private development. The information presented in this document was extracted from [21], mainly.

ii. Ingenu

Ingenu is a method of information transport with LPWAN wireless features that uses On-Ramp (RPMA) access method.

Modulation and Access Method

In some texts it is also known as Random Phase Multiple Access (RPMA) based on DSSS or On-Ramp Wireless. The transmissions are made in 2.4 GHz ISM band and the signal is Differential Binary Phase Shift Keying (D-BPSK), modulated before spreading by a "Gold Code". Additional blocks (encoded, modulate, Gold Code, randomly delay before transmission) ensure time and frequency synchronization between the gateway and the end-devices.

RPMA Scenarios

In the literature, there is scarce information available about Ingenu technology. For this reason, we conducted a search of RPMA Access, which allows understanding Access Method that employs Ingenu for its operation. In the search, scenarios were found for the use of RPMA Access [137]. Also, document [21] was a useful to understand this technology.

The interface can connect with systems and devices using SS methods. The random selection of a chirp (or timing) offsets as a multiple access scheme and allows non-coordinated data transmission without the need to be assigned a unique code. All users transmitted use the same Pseudo Noise (PN) code such that a PN array de-spreader at the access point can be used. If two (2) signals are received at the access point at the same PN offset, then collision could occur and it would not be possible to demodulate these signals. The random of timing offsets in each time avoid more collisions that could happen during that frame. A re-transmission scheme and a new value of random offset is used to get through in the next attempt [137].

A scenario includes a transmitter at the end-device with a gateway. Each end-device includes its own transmitter which transmits information in frames. A frame can be formed from information provided on a channel with a fixed data rate. Data can be spread using the same PN (Pseudo-Noise) code and can have a randomly selected chip offset. The transmitter also applies frequency rotation and sample clock correction to match the reference oscillator of the access point. Any end-device is associated with a single gateway to form the network and each end-device transmits information using the same PN code with a randomly selected chip offset. The phase is randomly selected in each frame over a large number of chips [137].

A scenario includes a transmitter (end-device), a gateway and a method for transmitting signals from the gateway to end-devices. However, when transmitted the gateway uses a unique PN code for each end-device, which is communicated. Different PN codes for each end-device give warranty of security and allows ignoring

unwished signals. The frames transmitted by the gateway also include a preamble of approximately 9 symbols to allow a fast connection with end-devices [137].

A scenario includes a demodulator at the end-device and a method for demodulating a received signal by the end-device. An automatic frequency control (AFC) de-rotator is employed. Multiplication is applied to signals received at the end-device. The AFC de-rotator multiplication is a 1-bit complex operation with a 1-bit complex output such that gate count is improved. The end-device uses a PN array de-spreader that takes advantage of big computational saving in the 1-bit data path [137].

Another scenario includes a demodulator at the gateway and a method for demodulating signals received at the gateway. The gateway demodulator has capacity to simultaneously demodulate several thousands or more links received from end-devices. To demodulate such a large number of links, the gateway demodulator includes a PN array despreader [137] .

In the case of a scenario that includes synchronization of the end-device with a master timing of the gateway, the gateway can transmit in some moments a broadcast frame. During the free time acquisition, the end-device uses a PN de-spreader to analyze the broadcast frames and identify the master timing of the gateway. A free time acquisition is expected to occur one time when the end-device is first introduced into the system. After the free initial acquisition, the end-device can perform a "warm" timing acquisition each time the end-device wakes up to transmit or receive a signal. The warm timing acquisition uses less power than the free time acquisition. Each end-device separately generates a PN code. A gold code is an example of a PN code that is parameterizable such that each user has it is own. Therefore, only data sent to a particular user is visible to it: when using unique PN codes, an end-device does not process data that are not it is own [137].

A method for communicating through a multiple access communication interface includes receiving a first signal from a first end-device, where the first signal is spread using a predetermined PN code and where the first signal includes first payload data, a second signal is received. From a second end-device, the second signal is spread using the predetermined PN code and includes second payload data. The first payload data from the first signal is identified in part by a PN array despreader. The same situation happens with a second payload from the second signal [137].

The SF of the Gold Codes is 2^k with k among (2 - 13) each time the SF doubles process gain, which is +3dB. This allows adapting the data rate to the propagation conditions. For the uplink or downlink broadcast transmission, the Gold Code is unique and used for Unicast downlink transmission, the Gold code is built with each end-device. With this, any other end-device is able to decode the data. Uplink/Downlink are in a half-duplex way, with a downlink interval of two seconds followed by an uplink interval of two seconds too. This allows dynamically adapting the SF to the channel conditions in function of the received power. Smaller SF can be used in downlink compared with uplink, as the gateway is not energy constrained and can transmit at a higher power level [21].

When an end-device is included at a transmitter with a method for transmitting signals to a gateway, each end-device includes its own transmitter, which transmits information in the form of frames. A frame can be formed by information provided in a channel, then, the data can be spread [21].

RPMA is performed by delaying the signal to transmit at each end-device. The slot is first divided into N_s subslots, so that $N_s = \frac{8192}{2^k}$ with 2^k the used SF. The transmitter selects one subslot called access slot for $k \leq 13$. Within the sub-slot, a transmission is delayed by a random number $d \in [0; 2^k - 1]$. Ingenu estimates that up to 1000 uplink users can be served in each slot [21]. The approximate communication range corresponds in theory to 200 Km in free space with minimal received power in -145 dBm, but in practice the range estimated is 10 Km with Okumura-Hata model [21]. For interference characteristic sensitivity, the random delay allows changing the time of arrival of the different signals and gold codes have low auto-correlation, therefore, the probability of interference is reduced. [21].

A gateway for use in a multiple access communication system includes a processor in the receiver and the transmitter. The receiver (gateway) can be configured to receive a first signal from a first end-device, wherein the first signal includes first payload data spread with a predetermined PN code. The receiver is also configured to receive a second signal from a second end-device, where the second signal includes second payload data spread with predetermined PN code for different signals from different end-devices when changing a signal of one end-device that previously used the PN code change [21].

iii. LoRaWAN

This subsection presents LoRaWAN LPWAN technology. LoRa is a modulation technique for a broad coverage, low energy consumption, and low data rate. The technology LoRa was developed in North America by Semtech, IBM, Actility and Microchip. LoRaWAN network uses a star topology between e-nodes or motes and the gateway, which connects the messages of the end-devices with an information server through IP standard connection.

Modulation, Classes and Coverage

The Shannon-hartley theorem states that an increase of the transmission channel bandwidth is a way to overcome a poor Signal to Noise Ratio (SNR). This theorem support different spread spectrum techniques such as Direct-sequence spread spectrum (DSSS), which multiplies the wanted data signal by a spreading code at a much faster rate than the data signal with the spreading of original data bandwidth over a larger resulting bandwidth [136]. LoRa uses a concept of Chip Spread Spectrum (CSS) modulation, which is a subcategory of DSSS that takes advantage of the controlled frequency diversity to recover data from weak signals, even near the noise level. CSS modulation was used in military communications due to the relatively low transmission power requirements, robustness to channel degradation, multi-path, fading, doppler effect and jamming interference [21].

LoRaWAN is a solution of LPWAN networks, since it has a robust physic layer for medium access "CSS", it works with a continuous phase between different symbols "chirp", which allows knowing different nodes in the preamble of the package to physics layer level and contributes to frequencies synchronization in the gateway LoRa. [21, 77, 123]. In [26], authors describe spread spectrum techniques that lead to an increased link budget and better immunity to interference. LoRa works in three forms known as A, B and C [138, 138, 139, 139].

Class A allows bidirectional communications, since every end-device enables uplink transmission and then opens two (2) windows of reception. The transmission time is pre-programmed with the need to communicate with a short variation based on a random time for avoiding collisions (ALOHA Protocol). Class A is for systems with low consumption power, small down-link data and efficient uplink operation. For more downlink communications, it has to wait for the next programmed time slots.
Class B works with bidirectional communication, and it allows programming reception times. The device can be programmed with extra times to receive across synchronization of beacons in the gateway, which allows the server to know when the end-device is present in the reception window.
Class C works with continuous reception window, except when the device is in transmission mode. In this class, the device uses more energy and gives low latency in the communication process.

Spreading Factor (SF)

SF is a number of transmitted bits in a symbol, when we take the references of the number of symbols in chips of 2^{SF} and SF=12, then $2^{12} = 4096$ chips/symbol. Each increase of SF reduces data rate of payload and it is necessary to increase the transmission time. This increase grows the energy consumption and process delays; however, LoRa is flexible with the use of spectrum through the same frequency with different SFs that allow to implement the orthogonality frequency for the transport of multiple links at the same time. A channel can be divided into sub-channels, which gives concurrence and avoids errors in the transmissions.

SF is compared with CDMA. It uses chip code DSSS, and the code is known between transmitter and receptor. Each chip is a rectangular pulse with amplitude (+1, -1). These pulses are multiplied with the data sequence and the answer takes the form of the wave to be transmitted. In the coding process, it takes a captured signal and multiplied it with spreading code. The chip rate (code SF) is translated into a number of pulses by time unit. The information symbol is represented by multiple chips [140]. The SF is showed in 3-11

$$SF = \frac{chirp\ rate}{symbol\ rate} \tag{3-11}$$

In [21], LoRa defines the SF in 3-12

$$2^{SF} = \frac{B}{R_s} = B.T \tag{3-12}$$

Where:

B is the spread bandwidth.

R_s is the symbol rate, and

$T = \frac{1}{R_s}$ is the chirp duration.

The basic element of CSS modulation is the chirp and its waveform is written in 3-13.

$$c(t) = \begin{cases} e^{j\phi(t)}, & \text{if } -\frac{T}{2} \leq t \leq \frac{T}{2} \\ 0, & otherwise \end{cases} \tag{3-13}$$

where, $\phi(t)$ is a chirp phase

In [21], the instantaneous frequency 3-14 is presented and the linear chirps are described as used by LoRa in 3-15

$$f(t) = \frac{1}{2\pi}.\frac{d(\phi(t)}{dt} \tag{3-14}$$

$$f_{1c}(t) = f_c + \mu.\frac{B}{T}.t \tag{3-15}$$

Where f_c is the carrier frequency, and, μ is the level of the chirp $(+1, -1) = (up, down)$.

The authors in [21] showed a representation of a chirp, a frequency form in the chirp, the instantaneous phase, the period varying in phase and quadrature and the output of the filter. In the receiver, we can find the multiplication of an up-chirp with an up-chirp and a down-chirp with down-chirp, which leads to an up-chirp or down-chirp, respectively. Then, instantaneous frequencies are added. The multiplication of an up-chirp with a down-chirp, also called conjugate chirp, leads to a narrow peak at twice the carrier frequency [21]. It is worth mentioning that the basis of CSS modulation allows sending one bit per chirp.

CSS used in LoRa is an evolution, and it was a development for LPWAN services. The chirp may code up to $SF = 12$ bits, during a chirp period. A specific frequency is defined by each 2^{SF} symbols and achieved by a frequency shifting ramp based on the symbol value. As a result, each chirp code is obtained by a cyclic shift of the chirp reference [21].

For LoRa, the instantaneous frequency is 3-16:

$$f_{cc}(t) = \begin{cases} f_c + \mu.\frac{B}{T}.(t - \frac{k}{B} + B), & \text{if } -\frac{T}{2} \leq t \leq \frac{k}{B} \\ f_c + \mu.\frac{B}{T}.(t - \frac{k}{B}), & \text{if } \frac{k}{B} \leq t \leq \frac{T}{2} \end{cases} \tag{3-16}$$

where k is the number of shifted chips. The images that help to understand the concepts are in [21] and some of them will be shown in Chapter 4 inside the results. At the receiver, the multiplication of the received signal with the raw conjugate-chirp allows finding a carrier frequency f_d and a instantaneous frequency through 3-17 [21].

$$f_p(t) = \begin{cases} f_c + f_d - \mu.\frac{k}{T} + B, & \text{if } -\frac{T}{2} \leq t \leq \frac{k}{B} \\ f_c + f_d - \mu.\frac{k}{T}, & \text{if } \frac{k}{B} \leq t \leq \frac{T}{2} \end{cases} \tag{3-17}$$

In equation 3-17,it is possible to find two periods, where each one has a constant frequency and the transition occurs at a given time at a chirp code. These features can be observed in [21]. It is important to consider that the phase of the transmitted signal must be continuous from the beginning until the end of the symbol. Also $f_c + f_d$ allows obtaining the base-band signal. The shown scenario has an ideal time and synchronization frequency between transmitter and receiver.

In the modulation process of LoRa, a preamble is sent for the offset estimation intrinsic and the information (bits) is divided into words of SF bits, where there are 2^{SF} code words. There are free spaces for reducing the Bit Error Rate (BER) and it is possible to set bandwidth values, frequency bands and SF. The chirp duration can be modified with SF values among[7-12]. A high SF corresponds to a long chirp, where the raw data rate can be calculated in 3-18.

$$R_b = SF.\frac{BW}{2^{SF}} \tag{3-18}$$

A high SF value is for far devices from the gateway and a low SF value for devices that are near to the gateway. Usually, a high amount of data for transmitting works with frequency hopping patterns are known by the Transmitter (Tx) and Receiver (Rx).

An end-device LoRa, known as slave, is guided by a master if the Adaptative Data Rate (ADR) is enabled. In this case, the Medium Access Control (MAC) has the ability to control the SF, the bandwidth and the radio frequency (RF) for controlling the output power of each node and maximizing battery life in the node and the network capacity. This helps in the flexibility of the data rate, which reduce times [Tx-Rx] and switching nodes with a high data rate in the cell. When a node wants to transmit, it chooses an available channel. Afterward, it uses a Listen Before Talk (LBT) protocol for finding a free channel. When it can use a channel, it transmits with SF by default and BW values. If a node needs to check its connection on the network, a short frame is sent first at SF=8, then to SF=10 and SF= 12. With this, the end-device obtains a feedback of the received frame.

Industrial Scientifical and Medical bands (ISM-bands) have a limitation by duty cycle or channel occupation. For this reason, we can express in 3-19 [141] that:

$$Ts = Ta * \left(\frac{1}{d} - 1\right) \tag{3-19}$$

Where:

Ts = Time period in which the channel is not available for the device.

Ta = Transmission time, also called Time on air (ToA), is a time of link adaptation between transmitter and receiver, and depends on the coupling loss.

d = Duty Cycle.

If d= 1%, the maximum transmission time is 36sec/h for each channel sub-band in each device. The duty cycle limitations are translated into delays between the successive frames sent by one device. With a 1% of duty cycle, the device will have to wait 100 times before sending again in the same channel. For this case, the maximum package number is shown in 3-20.

$$M = \left(\frac{3600}{Ta + Ts}\right)[package * hour * node] \tag{3-20}$$

The receiver package number by second is derivated from the expression 3-21.

$$s = \sum_{i \in F} i\lambda_i e^{\frac{-2p_i N Ta_i \lambda_i}{n}}) \tag{3-21}$$

where:

N = Devices number.

n = Channels number.

SF= Spreading factor.

Pi = Probability that a node uses an specific SF_i.

λ_i = Package rate of user with SF_i.

Ta = Transmission time on the air, a function of SF.

The time of transmission is expressed as [139, 142]:

$$ToA = Ta = T_{preamble} + T_{packet} = T_{symbol}(L_{preamble} + L_{PHDR} + L_{PHDR\_CRC} + L_{PHY\_payload} + L_{PHY\_CRC})$$

$$= \left\{\frac{2^{SF}}{BW}\left[NP + 4.25 + \left[SW + max\left(ceil\left[\frac{8PL - 4SF + 28 + 16CRC - 20IH}{4(SF - 2DE)}\right](CR + 4)\right)\right]\right]\right\} \tag{3-22}$$

where:

$T_{preamble}$ is the time of the symbols of the header to synchronize.

T_{packet} is the time of the symbols of information.

T_{symbol} is the symbol time.

$L_{preamble}$ is the load of preamble.

L_{PHDR} is the load of the physical header.

L_{PHDR_CRC} is the load of the physical header to cyclic redundancy check.

$L_{PHY\_payload}$ is the load of the physical payload.

L_{PHY_CRC} is the load of the physical payload with cyclic redundancy check.

NP, is the number of preamble symbols. It is common to use 10 of preamble and 2 of synchronization.

SW is the length of synchronization word.

PL is the number of PHY payload bytes (1-255).

IH specifiesthe presence of PHY (IH=0 when PHY header is enabled and IH=1 when no header is present).

DE indicates the use of data rate optimization, which adds a small overhead to increase robustness to reference frequency variations over the timescale of the LoRa frame. It is enabled when the symbol time is larger than 16mS.

Frequency bands, bandwidth and data rate

In America, LoRa uses frequency bands of 169/433/915 MHz, while in Europe it uses 868 MHz, all under 1GHz and ISM free bands. [73].

The BW has repercussions in the quantity of information that can carry a communication channel [141]. A higher BW represents a low time of transmission and a low energy consumption, otherwise a low BW obtains higher energy consumption and low data rate. LoRa has flexibility with BW of (500, 250 and 125) kHz in high frequencies and ISM bands (868 y 915 MHz). In low frequencies, it works in (7.8, 10.4, 15.6, 20.8, 31.2, 41.7 y 62.5) kHz for (160 and 480 MHz) [141]. LoRa has data rate consistent with SF and the BW of 0.3Kbps (BW = 7.8kHz y SF = 12) to 27 Kbps(BW = 500 kHz y SF = 7). The hopping frequency is used in each transmission for mitigating the extern interference [21, 141].

For maximizing the battery life and the network capacity in each end-device, the network administrator can configure the data rate and RF output to each end-device under Adaptive Data Rate (ADR) schematic. The end-device can transmit in any available channel at any time. For this purpose, it uses the data rate available with restriction to implement a pseudo-random hop channel for each transmitter and accomplish the maximum transmission of a duty cycle. The management in the gateway supports 10^4 end-devices, with a gain of $>$ 20dBm. LoRa implements Forward Error Correction (FEC) to fix errors. The data rate is a factor between coverage and message duration ToA. The sensitivity of a radio receiver [143] is given in 3-23.

$$S = -174dBm + 10log_{10}(BW) + NF + SNR \tag{3-23}$$

Table 4. Relation among features in LoRa technology

SF	**BW (kHz)**	**Symbol Time**	**Bit rate (kbit/s)**	**Time on Air 255 bytes (ms)**	**Receiver sensitivity (dBm)**
7	125	1.024 ms	6.836	389.38	-126.5
8	125	2.048 ms	3.906	686.59	-127.25
9	125	4.096 ms	2.197	1,229.82	-131.25
10	125	8.192 ms	1.220	2,213.89	-132.75
11	125	16.384 ms	0.671	4,837.38	-134.5
12	125	32.768 ms	0.366	8,855.55	-133.25
7	250	512 μs	13.672	194.69	-124.5
8	250	1.024 ms	7.812	343.30	-126.75
9	250	2.048 ms	4.395	614.91	-128.25
10	250	4.096 ms	2.441	1,106.94	-130.25
11	250	8.192 ms	1.342	2,009.09	-132.75
12	250	16.384 ms	0.732	3,772.42	-132.25
7	500	256 μs	27.343	97.34	-120.75
8	500	512 μs	15.625	171.65	-124
9	500	1.024 ms	8.789	307.46	-127.5
10	500	2.048 ms	4.882	553.47	-128.75
11	500	4.096 ms	2.685	1,004.54	-128.75
12	500	8.192 ms	1.464	1,886.21	-132.25

In Table **4**, it is possible to find the relation between a bit rate, sensitivity, SF, symbol time and BW values according to the values presented in [94, 143].

Packet structure: LoRa packet structure is presented in figure **3-4**. It has some features of control and real data (payload). The packet structure is composed of:

Preamble: It synchronizes the receptor with input data and typically has 8 symbols, but it is programmable from 6 to 65535 symbols.

Header: It is optional, it describes a length and FEC rate of the payload. It indicates the presence of optional 16-bit CRC for the payload. It is always be transmitted with a 4/8 FEC rate. In operation, it has two (2) work modes:

1. Explicit operation (default): The header field gives information about bytes number and the encoding rate FEC.

2. Implicit operation: It is used when payload and rate code are fixed. In this mode, the header is removed from the package, for this reason, it has a reduction in transmission time.

Payload: Transmitter data among (51-222) bytes according to SF.

Payload CRC: It is present at the end of the payload and it has 16 bit of CRC that may be included [21].

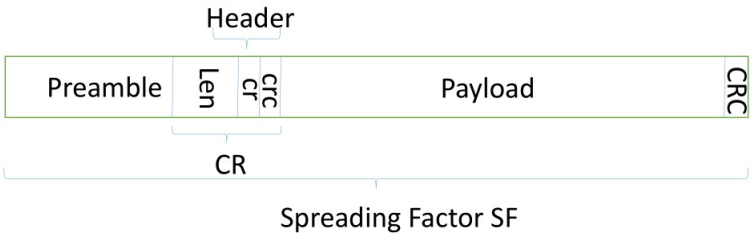

Figure **3-4**.: LoRa packet, The structure of a frame of LoRaWAN wireless technology

Other parameters: Code Rate, Duty Cycle, SNR and Energy Consumption.

The work in [89]shows a comparison between LoRa and Zig-bee. Zig-bee has a reach of 20 meters with 84.5μJ of energy consumption and LoRa has a reach of 150 meters with 86.5μJ. The first conclusion might be that a higher reach follows a higher energy consumption, but, it is worth mentioning that it is not the unique parameter to evaluate a technology. LoRa uses a battery that can reach 20 years in some operation modes. Settings such as carrier frequency, SF, modulation, BW, and code rate establish the energy consumption, transmission coverage, and noise. When SF, SNR array and reception sensitivity increase, the coverage area and transmission time increase too.

The code rate (CR) called FEC is used to protect against interference. Higher values of CR carry higher information protection but also increment the data transmission time on the air (ToA). It is important to know that inside features of the LoRa flexibility, the possibility to transmit information can be found with equal parameters of a carrier frequency, SF, BW and different CR.

The work in [141] states that the performance of LoRa network depends on duty cycle. According to the regulations, it can use a channel where the intrinsic collisions could appear by the use of Aloha Access method. Another important variable is ToA, which depends on the SF. A high time of transmission could carry overlaps on multiple transmissions and it shows a test with a uniform distribution of nodes in an area where a network gateway is found. The path loss is estimated with Okumura-Hata model for urban cells and the probability of using a node with specific SF $p_{12} = 0.28$, $p_{11} = 0.20$, $p_{10} = 0.14$, $p_9 = 0.10$, $p_8 = 0.08$ y $p_7 = 0.19$. This test is for estimating if the sensitivity should be variable for different SF_s.
If the transmitter node uses the high data rate and considers the duty cycle, then, the number of successfully received packages decreases with a high number of nodes. This is done by the probability of collisions in the Aloha Access method. The work in [141] shows a scenario of three channels $0 \leq N \leq 10000$, where N is the number of nodes of the network. The work describes three packages to transmit with three payloads (10, 30 and 50 bytes), a CR of 4/5 and a BW of 125 kHz. The document states that for low transmission rate values, the efficiency of the system is limited by collisions, and for high values, the duty cycle avoids the increase of the data rate and the system stability. The background shows for low quantity of nodes in a network that the probability of transmission is successful, but if it is increased in a number of nodes-carriers, the probability of successful transmission decreases. The capacity of the network LoRa is reduced in the transmission frame acknowledgment (ACK), in order to optimize the reliability and the dead time of these packages in ToA.

It is recommendable in the design of the network, and when the applications run, to reduce the frame numbers ACK for avoiding problems in the network capacity. After these appreciations, it is important to question if LoRa is viable under service condition with high reliability in dense networks.

The work in [141] affirms that in the future the development of LoRa networks could be inefficient. Specifically the model of LoRa network has been developed as a cellular network, where operators provide a network service and the gateways are base stations that cover large areas. When LoRa network grows, the operator coverage zone where applications or services that share the same infrastructure coexist, it will need new methods to

coordinate them and avoid collisions. Some network operators require technology for ensuring a balance when the spectrum is shared among different applications.

Wireless networks entail technical limitations such as latency, shadowing, multi-path, Fresnel zones. These and others negative factors need appropriate designs to avoid problems in the throughput of the network.
The noise level is 3-24:

$$N_{dBm} = -174 + NF + 10log_{10}(B) \tag{3-24}$$

where

NF = Noise Figure in the receptor.

For $125kHz \leq B \leq 500kHz$ in 900 MHz band and link budget in free-space,

$$SNR = PT_x + 132 - 20log(\frac{r}{\lambda}) + CG \tag{3-25}$$

where:

r = distance(Tx-Rx),

λ = wave-lenght, and

CG is a coding gain due to the spreading, estimated by 2.5SF

The theoretical maximum range was evaluated in a coverage of 22 Km. [21, 122]

In terms of interference, we can mention two sources: (i) no LoRa signals where a single signal less than 5 dB is not a problem and (ii) LoRa signals, where we could work with end-devices with different SF because the Fast Fourier Transform (FFT) would cause two unwanted peaks and receiver would not identify which end-device is talking. In [21] there is a report table with co-channel rejection when couples are presented with the same SF. An end-device can transmit without problems with different SFs, but the rejection coefficient increases with the SFs. The energy consumption is around 20 mA, however, it depends on the end-device state [21, 122].
LoRa uses two layers of security: (i) network and (ii) application. The network layer (i) ensures the authenticity of the node in the network. The application layer (ii) ensures that the network operator has no access to the end-user data. AES encryption is used with IEEE EUI64 identifier [123]. This security scheme is sufficient for most IoT applications.

Comparison among LPWAN main technologies

The following lines compare the LPWAN technologies that were detailed in this section, especially LoRa and Sigfox technologies, because it was possible to find more information on these tools. A table is presented where it is possible to find a perspective of these technologies and NB-IoT in technical values.

In unlicensed spectrum, IoT applications and its devices use more uplink than downlink transmissions, end-devices transmit data at intervals, while actuators are controlled irregulary. Uplink studies show that UNB sites with 10000 users (short messages) in a day need around 200 non-adjacent channels of 100 Hz. In this scenario,

a frequency band of 40 kHz would be enough [21]. In a study performed by real wireless environment, UNB LPWAN technology estimates that a 200 kHz channel should be able to provide an uplink throughput of 50 kb/s, for 500 simultaneous users using channels of 100 Hz at 100 bits/s. On the other hand with LoRa technology, the trade-off takes the form of different modulation types. It should ideally transmit at the modulation level, which includes the least error correction, but it can still get the message across. The most efficient modulation level is known as SF = 7 and the level with the highest level of error has SF = 12.

LoRa modulation improves practical sensitivity by around (6-10)dB versus FSK for the same bit rate. When a larger SF is used, the bit rate decreases, while sensitivity becomes equivalent or even better than UNB when using D-BPSK. Approximately, LoRa uses -137dBm with 300bps, while UNB uses -136dBm with 100bps [136].

LoRa uses more bandwidth than Sigfox (UNB) for transmitting low data rate. In LoRa, it is possible to transmit simultaneously 64 transmissions with various SFs and with optimum ADR. LoRa does not need a good alignment between Tx and Rx, it has a tolerable deviation, while UNB needs a crystal to do it. For LoRa, this lowers the cost and power consumption of the end point. CSS modulation exhibits good immunity to multipath fading and Doppler effect [136].

In licensed spectrum, LTE-M is primarily an evolutionary addition to the LTE techonology stack currently deployed by operators. An operator can modify the attributes of application with a software update to their base stations. LTE-M can be deployed in any LTE band under legal conditions of each region/country and devices capability. The first version LTE-M 1 worked with 1.4 MHZ of spectrum band, while the subsequent works with 200 kHz(NB-IoT), similar to UNB technologies. Licensed technologies estimates provide connection among 200.000 and 100.000 devices per cell. Simulations by ZTE technology manages to give support to 50.000 devices with 50.000 messages per hour in a 200 kHz channel without degradation (average message, among 100 - 280 bytes). These values are similar to the throughput in LoRa, since it has an effective uplink throughput around 21.1kbps in both cases. LTE is able to exert better power control, suffers less interference, and has permanent availability of use spectrum versus a 1% of the time for the unlicensed bands (duty cycle). Licensed technologies provide more capacity for acknowledgements and reduces the need to send the same message many times to increase the efficient reception [144]. Table **5** shows a comparison among the main LPWAN technologies used in this document.

The multiple medium access refers to multiple transmitters of a single application that want to use the same portion of spectrum. In order to prevent interference a form of access control is implemented. In licensed spectrum (as NB-IoT), only a single operator is allowed to use specific resources and it enables to allocate efficiently spectrum resources between users and avoid interference. In unlicensed spectrum (as Sigfox, LoRa...), multiple access for users is an issue. Different applications do not coordinate multiple access with each other, for this reason, regulations demand that transmitters use relatively low transmit power and limit their duty cycle. In some cases, even additional requirements are implemented such as Listen Before Talking. Each LPWAN technology deals with different requirements in order to facilitate multiple access for their own users and its coexistence with other services [144].

In order to reduce the effects of a collision, Sigfox transmits each message four times in a different channel, therefore, it decreases the efficiency of the spectrum usage but increases the possibility of reading the message in the receptor. In [144], the simulated performance of Sigfox is presented: it is resilient to errors resulting from collision, and when the number of collisions increases, the number of messages that are not received stays low. Real wireless networks find that the number of simultaneous users in a spread spectrum (such as LoRa) is around 70 per base station. Above this number of users, the base station noise rises quickly above usable levels, it assumes perfect power control in order to avoid losses. In multiple access, Sigfox is better technology under static conditions, UNB distributes their traffic over all channels equally and reduces the chance of a collision. The downside of this is that a message takes a long time to be transmited and if the signal fluctuates while transmitting, it decreases the chance of appropriate reception. LoRa can modify its parameters and the device may choose to increase the transmit power or use a better modulation-SF. Otherwise, the duty cycle regulations

Table 5. A comparative among the main LPWAN technologies

Feature	LoRaWAN	Sigfox	NB-IoT
Modulation	CSS/FSK	UNB/GFSK(downlinl) BPSK(uplink)	QPSK(downlink)/BPSK(uplink) OFDMA SC-FDMA
Bandwidth	500Hz - 500 kHz	400 x 100 Hz	200 kHz
Capacity	-	140 mss/day	Undefined
Data Rate	290bps - 50Kbps	100bit/sec(uplink) 500bit/sec(downlink)	226.7kbps uplink 20 kbps downlink\end{tabular}
Link Budget	154dB	151dB	164 dB
Messages/day	-	140	Undefined
Payload/size	2-255 bytes	12 bytes	4 x (128 - 256) bytes
Protocol Overhead	12 bytes	26 bytes	29 bytes
End-devices x´ Gateway	1000/Gateway	$1 * 10^6$	-
Coverage	(15-22)km rural and (3-8)km urban	(30-50)Km rural and (3-10)Km urban	15 Km rural and 4 Km urban
Sensitivity	-137 dBm	-129 dBm	$\sim$ -120 dBm
Transmission Power	{4:1:20}dBm	14dBm	20 / 23 dBm
Rx consumption	10.5mA	10mA	46 mA
Tx consumption	28mA	45 mA	74 - 220 mA
Carrier frequency	[137-1020]MHz	[868/915]MHz	LTE in-band LTE guardband standalone
Coding rate	4/5 4/6 4/7 4/8	N/A	-
Uplink	Data	Data	Data + ACK
Downlink	Data + ACK	ACK	Data + ACK
Encryption	AES-128	AES-128	LTE protocol
Open Standard	Yes	No	No
Duty cycle	1%	N/A	N/A
Spreading Factor	7-12	N/A	N/A
Frequency	868/920 MHz	868/920 MHz	800 MHz

apply to LoRaWAN gateways (base stations), therefore, the time that these base stations have to regulate the parameters is very limited and may be a limit for power control.

In [118], the authors establish technical differences between LoRa and Sigfox in the physical layer. Simulation results show that UNB has a larger coverage, while CSS is less sensitive to interference. In the document, it is possible to observe that it depends on the network load, size and distance. A LoRa network can send until six times more packets to the base station. In conclusion, it is possible to understand that the choice between LoRa or Sigfox depends mainly on the application.Thus, UNB has better long range communications where the amount of data is small and the number of devices is high. LoRa network is well-suited for applications for higher data transport.

The work in [102] makes a review between NB-IoT and LoRa LPWAN. The authors give an advantage to LoRa (Unlicensed) in terms of battery lifetime, capacity and cost, while NB-IoT (licensed - version light of LTE 5G) offers benefits as QoS (Quality of service), latency and reliability. Each application has its specific requirements, that allows choosing the best and both have their place in the IoT market. LoRa is a low-cost application, while NB-IoT is used in applications that require a high QoS and low latency.

Interference

If multiple access fails or different service providers do not coordinate spectrum usage, the presence of inter-

ference is possible situation where radio transmitters try a communication, but either or all transmissions may fail due to spectrum usage overlaps in time, space and frequency, which can affect quality of services. In [144], the authors showed a study of different scenarios of interference for LPWAN networks, in unlicensed spectrum where it is more possible that interference occurs. They show the results of interference analysis between UNB and CSS systems and they found four different scenarios: (i) own network UNB, (ii) another network UNB, (iii) own network CSS, and (iv) another network CSS. The results suggest that CSS systems are more likely to be a bad neighbour to other users of unlicensed spectrum. In the document, it is possible to found more information about interference between LPWAN IoT networks and existing users. The document gives some technical features such as measurements of power level signals, cyclic signals, duty cycle, interference from some source signals such as cordless microphones and telephones and interference from RFID, mainly.

Diversity

Communication channels present problems caused by multi-path and fading, mainly. Its effects could affect the throughput of the system. For the above, diversity techniques could be the way to avoid these problems. These techniques could be implemented in different ways in transmission and reception. In wireless networks, it is possible to find constructive and destructive interference. The signal power can be significantly diminished and the performance on a system in terms of probability of error can be severely degraded. Diversity techniques can also be used to improve system performance. Instead of transmitting or receiving the desired signal through one channel, it is possible to use different channels with the goal to avoid losses and obtain enough energy, which allows choosing the correct decision on the transmitted symbol. There are different systems of diversity that depend on the feature of interest, as follows:

- Depending on the place where it is implemented, it can be transmission or reception diversity.

- Depending on the physical medium with the goal to reach replica of the signal, it is possible to find in space or also called of antenna, in frequency, in time or in polarization.

- Depending on the use of the different signal replicas, it is possible to find: by selection, by feedback, by combination and by gain.

For the purpose of this thesis, space, frequency and time classes of diversity will be described with the goal to optimize the use of a channel in a communication system; it is clear that diversity techniques are used to avoid mistakes and interference effects that are made by multiple replicas of the signal, but in the present document they will be used with the goal to increase data transmission.

Frequency diversity: The aim is to modulate the information signal through multiple carriers where each carrier should be separated from the others by at least the coherence bandwith, the amount of frequency band that is taken by a channel to change significantly, therefore, it is possible to avoid fading. The coherence bandwith is necessary to multiple channels that have no relation among them.

Time diversity: The aim is to transmit the desired signal in different periods of time, thus, each symbol is transmitted multiples times. The intervals between the same symbol should be at least the coherence time, i.e. time taken by the channel to change significantly; it is common to take among 10 to 100 symbols time. Different copies of the same symbol will have independent fading.

Space diversity: The aim is to use multiple antennas to receive multiple copies of the transmitted signal. The antenna should be spaced far enough with the goal that the different received copies of the signal have independent fading. The space among antenna depends of local dispersion of the environment and the carrier frequency. The space diversity can be in the transmitter known as multiple input single output (MISO), in the receptor called single input multiple output (SIMO) and both, in the receiver and in the transmitter, known as multiple input multiple output (MIMO).
The information taken to present diversity techniques was taken mainly from [124, 145–147].

3.3.3. Survey on IoT-LPWAN networks

In the following lines, some works are presented about IoT applications and about the use of LPWAN communications technologies. First, this section presents works with general features about these technologies, second, it summarizes works with particular scenarios of its use; third, the selected works had as main objective the transport of a considerable amount of information through the use of LPWAN networks, and finally, there are some scenarios in order to transport images with the use of LPWAN networks.

In [10], authors simulate how to reduce the energy consumption of the sensor network during image transmission with an energy efficient image compression scheme . The compression scheme works with compression standard JPEG2000. The features were achieved using Discrete Wavelet Transform (DWT), and Embedded Block Coding with Optimized Truncation (EBCOT). The image compression scheme is studied with image quality and energy consumption.

In [72], the use of IoT hubs is presented to aggregate things using web protocols and suggest a staged approach to interoperability in the context of a UK government project that involve 8 IoT sub-projects to address cross-domain IoT interoperability. It introduces the Hypercat IoT catalogue specification, then, describes the tools and techniques to adapt an existing data portal and an IoT platform to this specification and provides an IoT hub focused on the highways industry, called Smart Streets. The main contribution of the paper is the effort in order to create an inter operable global IoT ecosystem.

The authors in [26] give an overview into the technologies to support LoRa, and describes the outdoor setup with the SX127x family of Semtech and the importance of transceiver generation that arrives with SDRs promising significant benefits for range, robust performance and battery lifetime.

In [121], a proposal is described in order to tune IEEE 802.15.4 MAC parameters and the sampling frequency of deployed sensor nodes with information about temperature, humidity and salinity for the control, due to the variability in crops. Data acquisition and transmission are generally achieved with wireless sensor networks, however, sensor nodes have limited resources, thus it is necessary to adapt the increase in sampling frequency for different crops, under application constrains such as reliability, packet delay and lifetime duration. The paper presents an analytical model of the network used to tune these trade-off parameters.

In [148], a solution is proposed for long range communications technologies through a tool that combines easily of use of the peripheral system with the long range LoRa network to develop the first true plug and play solution for a long range up to 3.5 kilometers in ad-hoc suburban deployments and multi-year battery lifetime. A similar work is presented in [149], where the main objective was to create a scenario in order to test LoRaWAN technology.

The work in [150] gives a perspective about the problem of energy consumption in mobile networks and proposes a new and original wake-up mechanism for base stations based on LPWAN networks. The proposal aims to carry out a complete shutdown of base stations during low traffic periods in order to reduce the radio access network energy consumption. The wake-up process is managed by the core network through LPWAN for Internet of Things applications.

In [25], a LoRa signal is decoded through the introduction of *gr-lora*, an open source software for the defined implementation of the LoRa PHY, which establishes blocks through Python for implementing LoRa. The authors guide their investigation thanks to Josh Blum [25] and a *gr-lora* out of tree module written in github user rpp0 [27]. It implements a receiver in Python that uses a modified FM demodulation process, however, the author has not been able to succesfully decode messages with it.

In [151], a methodology is presented in order to transport images with Zigbee tecnhnology. It is composed of 4 stages. The first is the Zigbee data transmission, then, it goes to the ARM data transmission stage where the configuration and communication of the information by serial port and its processing are carried out to guarantee the integrity and security of data as well as precision in the transmission of information. The third stage is data processing and, in the last stage, the image is saved and displayed. The image to be transmitted is in standard jpg format, since it has a high compression ratio and high quality. During the image compression process, the image is initially segmented into 8x8 pixel segments, then, the discrete cosine transform is applied, a two-dimensionality AC and DC is produced and finally the AC is encoded with a code modulation of differential pulse and length encoding is used to encode DC.

Authors in [152] study LoRa technology for IoT, providing an overview of LoRa and an analysis of its functional components. The physical and data link layer performance is evaluated by field test and simulations. The study in [153] focuses on transmission performance of LoRa technology and attempts to apply LoRa technology to a sailing monitoring system. The experiments involve spreading factor and bandwidth parameters, mainly to establish its influences on data transmission time and coverage. The measurements were conducted to analyze the performance of coverage and packet loss rate in sea area. The results show that the system based on LoRa technology can achieve the intended purpose of system design and meet the basic requirements of system application.

IoT technologies are described in [87] including its relation to wireless sensor networks and its inter-operation with LPWAN networks technologies, mainly through LoRaWAN solution. The paper proposes a congestion classifier using logistic regression and modified adaptative data rate control. The proposed scheme controls the data rate according to the congestion estimation.

Narrowband Internet of Things (NB-IoT) is presented in [129] as a new radio access technology standardized by 3GPP for supporting IoT devices. It offers a range of flexible deployment options and provides improved coverage and support for a massive number of devices within a cell. The paper provides a detailed evaluation of the coverage performance of NB-IoT and shows that it achieves a coverage enhancement compared with other LTE technologies.

work in [154] presents a comparison of the expected lifetime for IoT devices operating in several wireless networks. IEEE 802.15.4, Bluetooth Low Energy (BLE), IEEE 802.11 power saving mode, IEEE 802.11ah, LoRaWAN, and Sigfox technologies were used. In order to compare all technologies on an equal basis, the authors developed an analyzer that computes the energy consumption for a given protocol based on the power required in a given state: sleep, idle, Tx and Rx. The comparison shows that BLE offers the best lifetime for all traffic intensities in its capacity range. LoRaWAN achieves long lifetimes behind 802.15.4 while Sigfox only matches LoRaWAN for very small data sizes. In [27], it is possible to find a description of the LoRa PHY layer and presents a methodology for detecting and decoding LoRa frames with the use of SDRs (USRP B210, HackRF and RTL-SDR). For transmissions, commercial platforms were used (RN2483, HopeRF RFM96 and Semtech SX1272).

System features are shown in [155] in a Raspberry Pi embedded system, a camera, and a motion sensor. The operation consists in the recording of frames captured by the camera in real time of activity that the motion sensor detects. Later, the information is processed in a Matlab and Simulink toolbox. The images are transmitted to another host computer using a Wi-Fi transmission that operates at a frequency of 2.4 GHz. When motion is detected, the image is captured with the camera and stored in the SD memory of a Raspberry Pi board, and then the data is sent via Wi-Fi using the FTP transfer protocol. To access the images, the host PC must be in the same IP protocol address range as the Raspberry Pi board i.e. the same local network. The data transfer is performed with a SAMBA server, which allows file sharing between Linux and Windows systems. This method uploads the images on this server and any device connected to this network can access the images captured by the prototype. MATLAB is used to view the information and process the image on the Host PC. With this system, images of 160x120 size are obtained at 3m distance without delay, while for a

distance of 6 m there is a delay of 5 s to reach an image of size 340x240 and for a 640x480 image at 8 m a delay of 39 seconds.

A wireless compressed image transmission system is shown in [156]. By performing image compression, it ensures that the processing, transmission, and storage system is efficient compared with the system that performs no image compression. The prototype hardware uses NI myRIO and the software for the system used is Labview 2017. The wireless image transmission system uses Wi-Fi and the image compression method is the discrete cosine transform implemented in an FPGA, managing to compress up to 44% and thus minimize data transmission time and energy consumption. With this system it is possible to obtain 160x120 resolution images with an original file size of 7.7 kb. When performing the compression algorithm, it is reduced to 4.47 kb. With the 320x240 resolution image, the original image size is 38.6 kb and the size after compressing the image is 20.8 kb. Finally, the 640x480 resolution image had an original size of 127 kb and when compressing the image, it shifts to a size of 69.2 kb. Authors in [157] provide a comprehensive survey on LoRa networks, including technical challenges such as link coordination, resource allocation, reliable transmission and security. The paper also includes recent solutions about these challenges. In [158], a remote image capture system was developed for an application in lettuce crops. The system consists of several capture nodes and a local processing base station, which includes image processing algorithms to obtain key features for decision-making in irrigation and harvesting strategies. Placing multiple image capture nodes allows obtaining different observation zones that are representative of the entire crop. The nodes were designed to have autonomous power supply and wireless connection with the base station. The wireless connection was made using the ZigBee communication architecture, supported by XBee hardware. The two main benefits of this choice are its low energy consumption and the long range of the connection.

In [159], two coding methods are compared and the image transmission efficiency is measured using the LoRa protocol. The prototype transmitter and receiver have Raspberry Pi 3B + cards equipped with Semtech sx1276 modules with a range of 1.5 km. Tests were carried out using an image with a resolution of 200x150 pixels, by applying the two compression methods that resulted in the jpg and webp + base64 formats. In the results, it is possible to observe that the LoRa image transmission with Webp plus Base64 encoding requires 25.7 s, which is acceptable for practical application. This method apparently improves the transmission time, therefore, it is feasible to develop a picture transfer using LoRa technology.

The work in [160] was performed in Colombia, where the transmission of wireless images in the municipality of Covarachía Colombia is proposed. The difficulties encountered in carrying out this transmission are distance and obstacles between the crop and the nearest town. A review of technologies is carried out to identify the most appropriate one in terms of cost, scope and ease of implementation, however, the authors only describe some steps of its simulation and not its implementation in a real scenario.

Other works show different features of LPWAN, for example [93] and [161] describe a survey and analyze LoRaWAN technology operation, focusing on performance evaluation of its channel access as the most crucial component for massive machine type communication. Some other works provide applications, evaluations and scenarios for the use for LPWAN and IoT technologies. The evaluations for LPWAN technologies are presented in [26]. Particular evaluations for each technology (LoRaWAN and Sigfox, mainly) are presented in [135,138,141], platforms over IPV6 in [139], applications of locations in [85], and networks planning services in [137]. In [162], a novel chaining encryption method is proposed that can be used in any narrowband and lossy network including LPWAN. The proposed method introduces a module named appropriate key [U+FB01]nder (AKF), which assigns a dedicated key to each message using hash functions, Finally, tests of interference measurements in 868 MHz band with LoRa and Sigfox platforms are developed in [88]

Some other works in the literature describe techniques, methodologies or communication systems in order to transport a high amount of information. It is possible to find optical communication systems such as [163–166], and deep learning techniques in order to do more efficient a communications networks [167, 168]. Moreover, there are documents that refer to spectral efficiency [169], multiple in multiple output MIMO [170], modulation

scheme systems [171], Orthogonal Frequency-Division Multiple Access-OFDM systems [172], Wireless sensor network WSN [173], Narrow Band IoT [174] and mechanisms to improve a high data rate [169, 175]. All of the above aim to enhance or increase the data rate in wireless systems, particularly some of them in applications with LPWAN communications systems such as LoRa technology. Now, the next lines present methodologies in order to transport images with the use of LPWAN networks.

3.4. Survey on LPWAN-based monitoring systems for images

Authors in [18] present a low-cost, low-power and long-range image sensor. The author uses Teensy 3.2 board as the host micro-controller to drive the CMOS uCamII camera capable of providing JPEG bit stream. The authors retrieve raw 128x128 (8 bits per pixel) grey scale images, then, image compression is operated on the board. The author uses an encoding scheme proposed in [16] with the following features: (i) image compression must be carried out by independent block coding in order to ensure that data packets correctly received at the sink are always decodable and (ii) de-correlation of neighboring blocks must be performed prior to packet transmission by appropriate interleaving methods in order to ensure that error concealment algorithms can be efficiently processed on the received data. The proposal presented in [16] uses Discrete Cosine Transform for image compression. The result of this compression scheme is a JPEG-like coder and operates on 8x8 pixel blocks with advanced optimizations on data computation to keep the computational overhead low. An optimized block interleaving method is presented in [15], which proposes a pixel interleaving scheme based on Torus Automorphisms. Data are transmitted in different packets and some of them can get lost, then, the interleaving scheme has a high probability of retrieving enough information to obtain an approximation of the original value without affecting the energy consumption, time of use or complexity of the process. It is worth mentioning that the reconstruction image quality is acceptable until 80%. For transport, the data connects with LoRa module (inAir9 from Modtronix) built upon Semtech's LoRa SX1276 chip. In the transmission test, an image needs between 8 and 10 packets. The system operates in a range of 1800 meters without packet loss. Data presented in the paper leave some considerations, at least 50% of the original information is necessary to recover the information without considerable losses, DCT transform gives entire, decimal and in some cases with negative values, in this way, the paper provides no scheme of code implemented for the information in LoRa symbols.

The results of images and voice transmission by LoRa are depicted in [11] through the use of image compression with JPEG/JPEG2000. For voice compression, the A-law method was used. In the setup configuration about transmission, it is possible to find around 700 packets in order to be sent per each image, which needs around 576 mS. In other words, one image needs around 6.72 minutes in order to be sent without duty cycle politics. A method is proposed in [23] for monitoring with the use of image sensor data over LoRa physical layer. The authors have proposed a scheme for overcoming the bandwidth limitation on LoRa. The images are encrypted as hexadecimal data and then split into packets to transfer. The transmission node consists of a LoRa Arduino shield that comprises of an RN2903 transceiver stacked on an Arduino mega microprocessor. An Adafruit TTL serial JPEG camera was used for capturing images connected to the Arduino board. The receiver node is similarl as it consists of a LoRa RN2903 module. The experimental setup is the following: the TTL camera captures a JPEG image, then, the Arduino MEGA microprocessor saves the data into the SD memory and converts these data into a hexadecimal format. The hexadecimal data are transfered to the receiver node via LoRa. The data are split into packets to enable transmission. Once all these packets are received, they are sent by the Arduino processor to a personal computer, where they are reassembled and displayed using Matlab code. Also the document describes LoRa physical layer settings and the metrics of evaluation such as PSNR. Within the results, it is possible to find the features with different SFs and at different distances. In summary, with SF=7 is possible to use a minor time in the processes of transmission and reception, thus the number of transmitted packets was 314 and the elapsed time was 67 seconds. On the other hand, the number of transmitted images was 21 out of which 12 were successful and 9 were unsuccessful. Nevertheless, the data presented leave some questions: Which was the images size? Was the duty cycle considered at the submitted shipping times? How was the convertion among hexadecimal values and SF values (7-12) to generate LoRa symbols ?

Authors in [19] present two control mechanisms to enable the deployment of image sensor devices through LoRa technology. In *i* mechanism, an adapted CSMA avoids costly packet collision and packet losses, while in *ii* an activity time sharing mitigates the issue of duty-cycle. In the document, a quality factor of 10 is used as it offers a high trade off between image size and visual quality. If it uses a quality factor of 10, an image size of 900-1200 bytes is obtained and can be packed in 5 LoRa packets. The application transmits images when significant changes occur in the image (event detection scenario). The data presented in the paper leave some considerations: CSMA avoids packet losses but it does not increase the capacity to transmit more data; activity time sharing allows transporting more information for relieving the effect of consequent regulations with duty cycle. Nevertheless it is a mechanism that needs the register of the other devices. Its implementation needs a scenario where the devices are deployed by a single organization, which increases in devices that entail high expenses in resources.

The work in [14] describes a proposal of low power wide area network protocol, which combines LoRa modulation technique with embedded microprocessor technology. The proposal network is composed of three LoRa modules that provide three physical channels. Camera node allows bidirectional communications. Each uplink transmission is followed by two short downlink receiving windows. When the camera node needs to upload the data, it randomly selects a channel to execute channel activity detection. If the channel is occupied, the node randomly withdraws and remains off for a period of time for the next data deliver. If the channel is not occupied, the node can transmit to the gateway by LoRa modulation. In conclusion, the proposal gives only a theoretical analysis for the wireless visual sensor with the use of Lora modulation technology but this was not tested in real implementation.

Authors in [176] propose a new reliable delivery protocol, Multi-Packet LoRa (MPLR), for transmission of large messages, such as images, in LoRa networks. The proposed protocol is implemented and evaluated using a LoRa testbed network. In point-to-point experiments with a single sender/receiver pair, MPLR reduced image transmission time by an average of 24% in scenarios with no packet loss, and by averages of 30%, 42%, and 49% in scenarios with 2%, 5%, and 10% loss rate, respectively. When multiple LoRa nodes send images to a single gateway, high channel utilization and an unacceptable collision probability can be experienced with the standard LoRa MAC ALOHA protocol. In experiments with between 5 and 20 nodes, MPLR in conjunction with a channel reservation protocol can successfully send more images and reduce the maximum successful image transmission time between 2 and 7 times, compared with stop-and-wait packet transmission with ALOHA.

A novel system is introduced in [177] to transmit continuous images taken from a camera on a static environment through LoRa. The key challenge is to reduce the amount of transmitted data, while preserving the image quality and the quality of service delivered to the application. We developed a technique that splits image into grid patches, and transmits only the modified area of an image based on their dissimilarity measure. We implemented and evaluated our scheme on a real LoRa device to show its performance and image quality. The node is implemented by connecting Raspberry Pi, data comprises a Pi Camera 2 and Arduino Uno with LoRa shield. The node captures an image, divides the image into patches, and then applies the change detection algorithm between the patches from the previously taken image. It detects the distinct patches and finally sends patches by using LoRa modulation.

In [159], a system of LoRa based time division multiplexing (TDM) was proposed for transmission images between sensor nodes and gateway. The LoRa image transmission system is divided into three parts: the three image capturing sensor nodes, gateway and server. The three image sensor nodes use the Raspberry Pi as the platform and are responsible for capturing images as well as transmitting the JPEG compression images to the gateway, which also used the Raspberry Pi as the platform to decode the image pixel data transmitted from the sensor nodes and combined the image pixel values to restore the image. Finally, the restored image was transmitted to the server by Internet. In addition, broadcasting the timing from gateway to the three sensor nodes achieves the synchronization mechanism of the time division multiplexing. The experimental results showed that the single image of 200×150 pixels can be transmitted by LoRa in about 1 minute for a distance

of 2 km. By the times of division multiplexing technology, we can simultaneously transmit three images and monitor three environmental states in the experiment. The transmitted image was divided into 85 packets. The experimental hardware uses Semtech sx1276 single channel chip as the transceiver module and a Raspberry Pi 3 as the processing platform for transmission and reception. In conclusion, the fastest transmitting time was 54 seconds (SF=7 and BW = 500kHz).

In [178] is presented a study on the potential use of the Lora Ra-02 Module for low-speed image transfer applications was conducted. Transfer Time for RGB Image 480 x 640. It can be concluded that the maximum range setting will result in the fastest transmission time of 858 minutes for one image. This time value is not appropriate for image submission except for special applications that only need to send one image per day. The implementation consists of a node and a gateway. The node consists of a camera, Raspberry Pi as a data processor, ATMEGA328 as power management and supervisory devices, LoRa Ra-02 as a wireless communication device and RTC as a determinant of data retrieval and delivery time according to schedule. The gateway consists of the LoRa Ra-02 module, raspberry pi as a data processor, and a display as a data viewer.

The work in [179] aims to review the available methods applied to transfer images via LoRa infrastructure, for the first time in the literature. The limitations of each method are pointed out and the challenges that need to be managed in the future are also defined toward establishing a reliable image transfer over a LoRa network. A review of the LoRa approaches towards transmitting visual data was presented. Some of them use new protocols in order to alleviate the low data rate that LoRa has, while others use the physical layer in order to overcome the packet collision problem and few methods deal with the compact image representation. In the Table 6 presents a summary of the methods in order to transport a high amount of information (mainly images) in LPWAN networks. .

Table 6. Image transmission with LPWAN networks

Reference	Method	Transmission time (one image) (min)	Packets number	Image Compression method
Pham, 2016	Image compression Discrete Cosine Transform	-	8-10	JPEG
Kirichek et al., 2017	Fragmentation data	6	700	JPEG/JPEG2000
Jebril et al. , 2018	Data encrypted hexadecimal	1.1	314	JPEG
Pham, 2018	CSMA (avoid collisions)	-	5	JPEG
Fan & Ding, 2018	Multiple out single in	-	-	-
Chen et al. , 2019	MPLR protocol Tx/Rx	0.3	-	-
Ji et al. , 2019	Image processing (Only transmits data with change)	-	-	-
Wei et al. , 2020	Time Division Multiplexing	1	85	JPEG
Juliando et al. , 2021		858		

4. Evaluation of Agricultural Monitoring System using Images through LPWAN network

To transport an image through LPWAN network, it is necessary to reduce the amount of information, and implement a classification method of the images to find abnormal samples. When an abnormal sample is presented, it is compressed and then, it is adapted for transmission. For the purpose of this work, the method aims to reduce the information not to transmit the normal samples, which allows reducing the amount of information in the wireless communication network. The compressed data are transformed into LoRa symbols, then, they are delivered to a SDR platform to transmit them. In the receiver, another SDR platform receives the signal and it is delivered to decode the LoRa symbols, to perform the process of reconstruction and display of the image.

4.1. Image processing and classification

It is important to remember that the use of images correspond to a controlled capture. The problems of capturing images directly from crop were incidences of the sun, the shadow, the angle of capture and more are consequent and inherent to image processing. Therefore, each leaf was captured with a white background with the aim to facilitate classification process.

In this subsection, processing and classification techniques were supported on this document. Features and attributes extraction process in images were performed with reviewed methods such as: vector extraction of RGB components, L-a-b, hue, brightness and intensity components. With these features, K-means clustering classification was built as shown in figure **4-1**. A neuronal network was implemented as shown in figure **4-2**. The results achieved were close to 75% with clustering K-means and Neuronal network tools. In appendix A is possible to find the codes of K-means and neuronal network tools that were used. Appendix A contains the codes of K-means and neuronal network tools that were used.

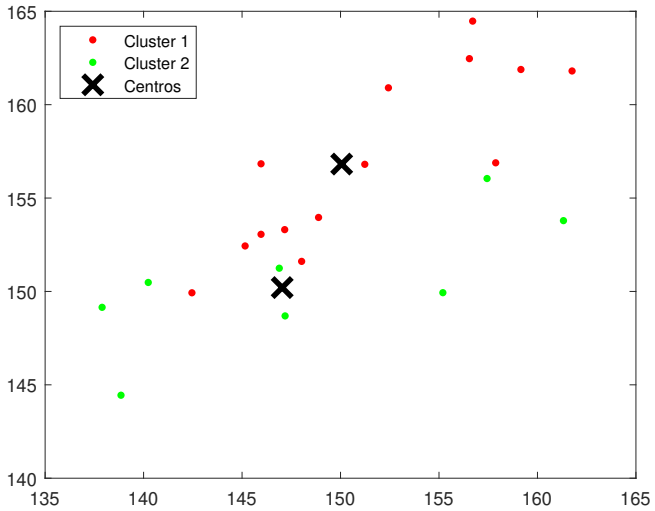

Figure **4-1**.: K-means grouping

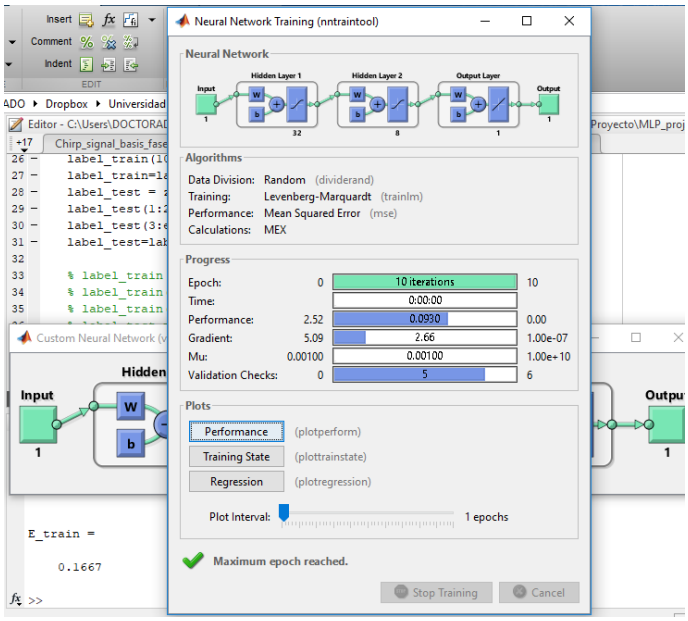

Figure **4-2**.: Neuronal network

On the other hand, Deep Learning was used to detect the samples. In the first moment, the samples were applied in already trained networks such as ResNet or GoogLeNet without obtaining good results in the classification process. In the second moment, the option of transferring learning to a previously trained network was explored, but the processing and the amount of information increased. Finally, a structure of a convolutional neural network without data was used, and the training was performed with normal and abnormal leaf samples, therefore, the samples were labeled in two classes:

1 = presence of abnormal sample (sick).

0 = presence of normal sample.

The methodology to solution is presented in the followed lines. First, the images were captured in a controlled environment. The samples are divided and a label is given to them with normal and abnormal features. Then, they are delivered through Matlab to train the convolutional neuronal network until reaching good values of training and validation. When acceptable values are reached in the training process, then, the trained network is saved. Second, it is done classification test with different samples with the goal to obtain an optimal classification. The evaluation of the performance of the trained network is evaluated by comparing the previous label of the samples and the labels delivered by the network. In the future, it is important to increase the number of the samples for training a network with a higher level of precision.

The framework of classification employed in this work is shown in **4-3**.
The information data of the training process can be observed in figure **4-4**
Deep Learning codes are presented in appendix A. The results show that the precision is near to 90%, however, it is necessary to increase the number of samples in order to improve the classification process.

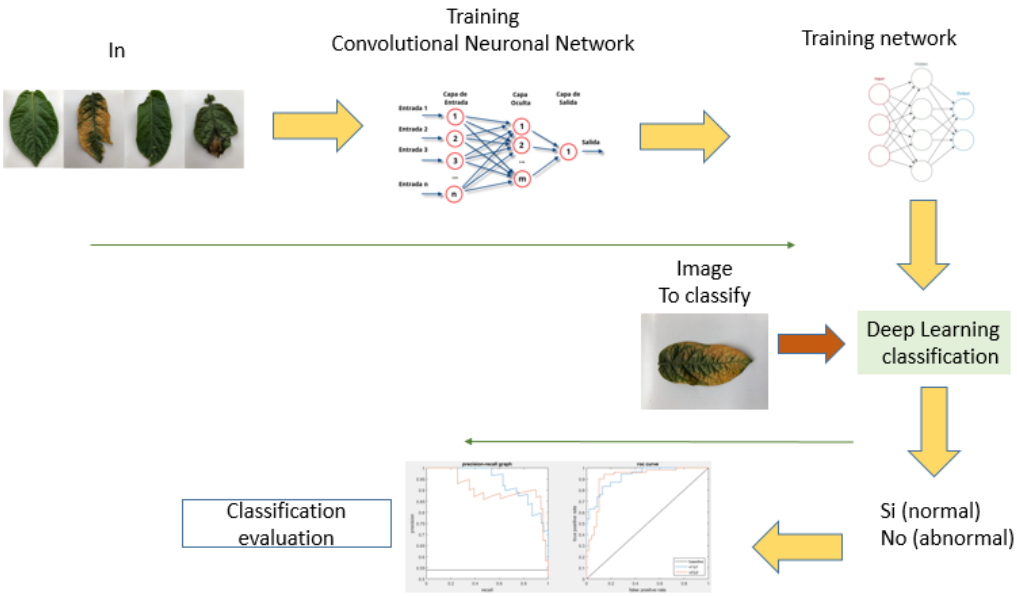

Figure **4-3**.: Framework of classification

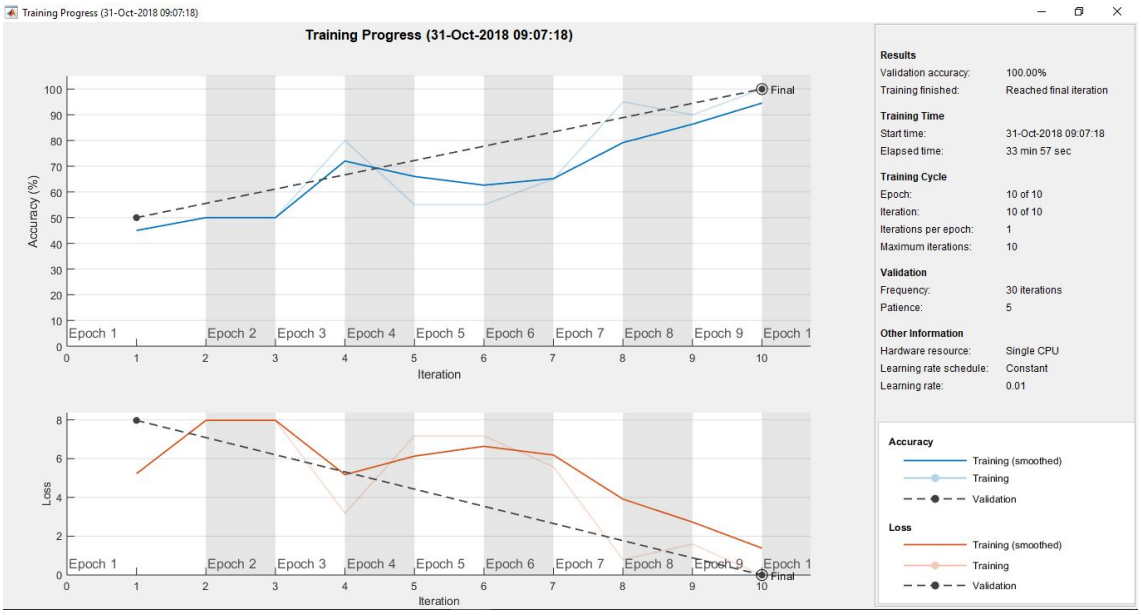

Figure **4-4**.: CNN training process

4.2. Compression technique and reconstruction algorithms

The present section describes the compression technique used.

An image in gray scale has the goal of achieve a high compression of its information. The model uses the information of a matrix $n \times n$ of the image, then, the matrix is converted in a vector of $N \times 1$; that allows adapting the information to exploit its features in compression and recovery of information.

The vector is processed until reaching a sparse signal, which represents a signal with components that has samples equals to zero. For example, when considering a signal that has n samples and m samples different from zero (where $m << n$), the signal is m-sparse and it is considered a signal with high sparsity because a high number of samples are zero.

The sparsity in images helps to reduce the amount of information to transport, its processing time, bandwidth uses, energy consumption and benefits the use of spectrum. If we have a signal with 2048 samples and 80 of them are different from zero, the signal is 80-sparse equal to a signal with high sparsity. If it is taken from 2048 original samples, only 512 through the use of compression technique, this represents a compression factor equal to 4. With this data, compression can recover the original data with low losses through recovery algorithms such as "IterativeHardThresholding (IHT), "OrthogonalMatchingPursuit" (OMP), "GradientProjectionforSparseReconstruction" (GPSR) or "Two − stepIterativeShrinkage/Thresholding" (Twist).

When more samples of the original data are used (a low compression), more precision and quality are reachable in the reconstruction process, however, more resources are necessary to processing. The goal was to design a system that can be adjusted for our needs and to possibility of transfer images through LPWAN network.

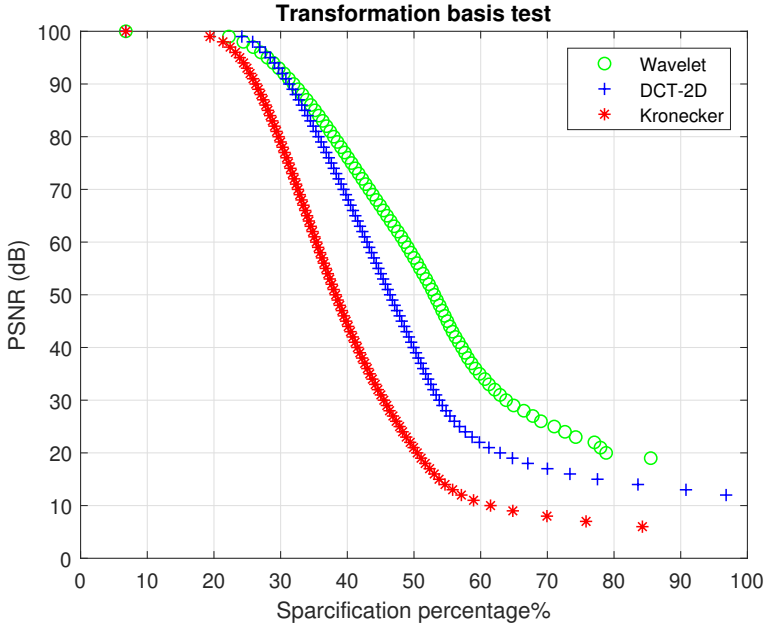

Figure **4-5**.: PSNR values vs sparsity percentage

In the processing of images, the sparsity was evaluated with the Wavelet, Kronecker and Discrete Cosine transforms with the aim to find a common base that allows improving the reduction of information. Figure **4-5** shows the Peak Signal-to-Noise Ratio (PSNR) values versus sparsity percentage. When the sparcification percentage increases, the wavelet transform achieves the best results of PSNR. Now, **4-6** shows the coefficients

of the transforms among DCT transform, Wavelet Transform and Kronecker Transform. Wavelet transform is the best because the values have a minimum variance, which entails that a high number of samples will be sparse and better results can be obtained in the compression technique.

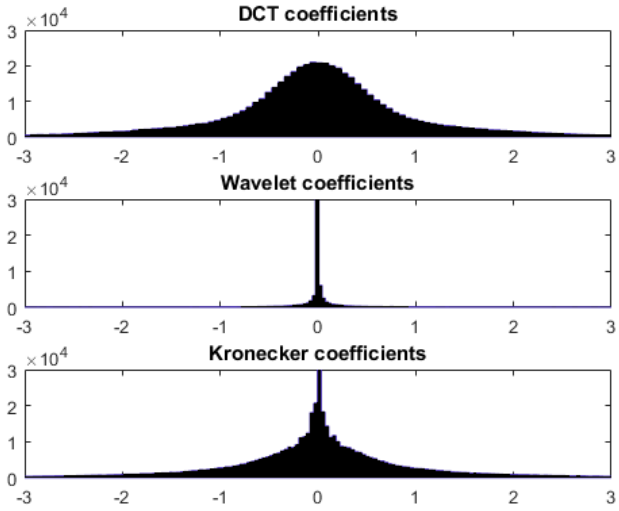

Figure **4-6**.: Coefficients distribution

4.2.1. Performance Comparison of Reconstruction Algorithms

This part of the document describes the reconstruction algorithms for sparse signals considered in the research. Reconstruction techniques are tools to build the signal with a few samples of its original signal. These few samples are at a resultant vector of the compression technique process. Reconstruction techniques are specialized mathematical algorithms. The tools considered were evaluated and compared to find the best solution in the data of images.

For the reconstruction process, each algorithm to be implemented was taken. The inputs were the sparse vector signals and the sample matrix. Other factors were implemented in particular for each algorithm. The outputs were a relation between the rebuilt signal and the original signal given by PSNR and the number of rebuilt samples (M). The outcome is depicted in the figure **4-7**. The outcome of the evaluation shows that the Twist algorithm reaches the best reconstruction index regarding M. The codes of this subsection are presented in appendix A.

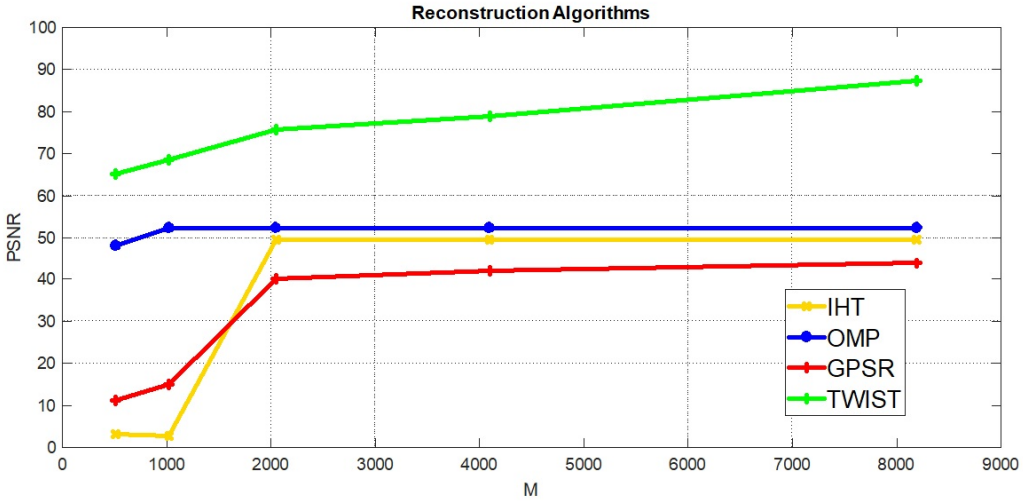

Figure **4-7**.: Reconstruction algorithms evaluation

4.3. LoRa modulation to transport data

The present section describes the method implemented to transport information between transmitter and receiver with the use of LoRa modulation and SDR cards.

4.3.1. LoRa symbols creation

Matlab software was used to make LoRa symbols. For this purpose, it is necessary to synchronize and know the beginning and end of the synchronization signal. For this reason, 10 symbols (up-chirps) of preamble were created and 2 of synchronization (down-chirps), here in after referred to as, start data symbols. It is important to remember that any symbol (preamble, synchronization or data) has the same symbol time consequent with the value of SF. Then, information data (preamble, synchronization or raw data) is converted to a LoRa symbol through a mathematical model.

To create a chirp with features of real data (SF, BW, symbol time, among others) in LoRa PHY modulation, it is necessary to setup real values. LoRa symbols of an up-chirp, a down-chirp and a data symbol are shown in figure **4-8** created with $SF = 8$ $BW = 500kHz$. Similarly, Tx spectrogram of a LoRa packet is shown in figure **4-9**, where 10 up-chirp symbols are used as the preamble packet, 2 down-chirps symbols are used for synchronization purposes and the last is a sample of data symbols.

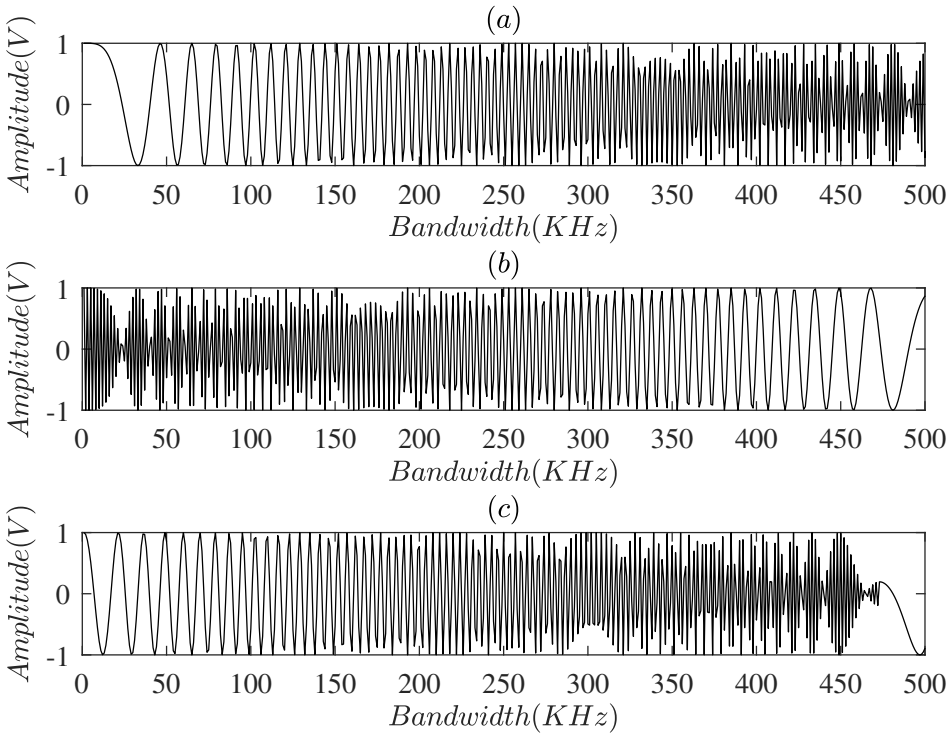

Figure **4-8**.: Transmitted signals: (a) up-chirp, (b) down-chirp and (c) data.

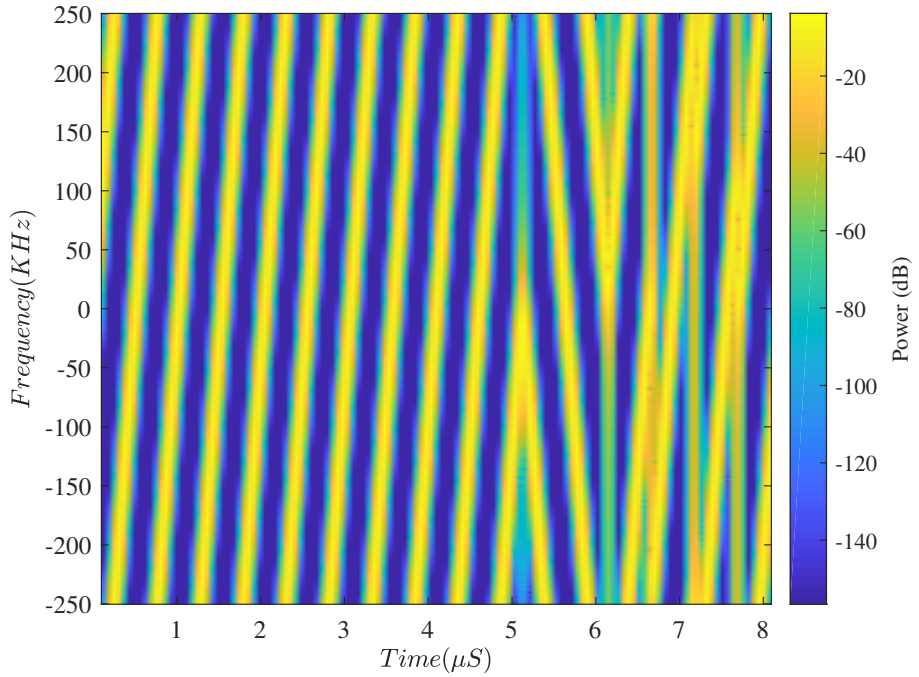

Figure **4-9**.: Tx spectogram

In the following lines, a pseudo code of LoRa symbols creation is explained.

Input: SDR connected, Matlab Software
Output: Data synchronization
Initialisation :
first statement
LOOP Process
if (synchronization) **then**
    To create LoRa symbols
else
    to check communication between SDR and laptop
end if
if (synchronization **then**
    Create 10 symbols of up-chirp and 2 symbols of down-chirp
    Set up comm.SDRuTransmitter and comm.SDRuReceiver objects from Matlab
    To setup SF, BW and T_s
end if
return

4.3.2. Transmission and Reception of LoRa symbols

For transmission and reception of LoRa signals, Matlab software was used and a USRP's - NI 2920. In the transmission process, a SDR was set up knowing the frequency and master clock rate of its operation. With this information, it is necessary to verify that the card is recognized by the software. For this reason, it is important to connect SDR with a laptop through fast Ethernet interface, then, it is configured with an IP address protocol.

IP Address = 192.168.10.10

Mask = 255.255.255.0

Gateway = 192.168.10.2

Afterward, it is verified in Matlab that SDR is recognized through $'findsdru'$ command. When the card is 'success' status, then, it is available to use.

Now, it is important to setup values such as Frequency, Bandwidth, Gain and interpolation factor, mainly to use the card through $'comm.SDRuTransmitter'$ object. In our case, we set values to transport data to $500kHz$ of bandwidth operation consequent with the value of master clock rate through feature of interpolation factor. To synchronize values of transmission and reception, it is necessary to perform several tests with the goal to find a synchronization time between SDRs. When features of communication are set between transmitter and receiver, it is possible to find two laptops independent of processing (figure **4-10**). These independent process needs to find a fixed time to know the moment when the transmission begins and the exact moment to begin the reception. In each implementation, the features of the devices must be known and the test must be performed with the goal to find time synchronization between devices.

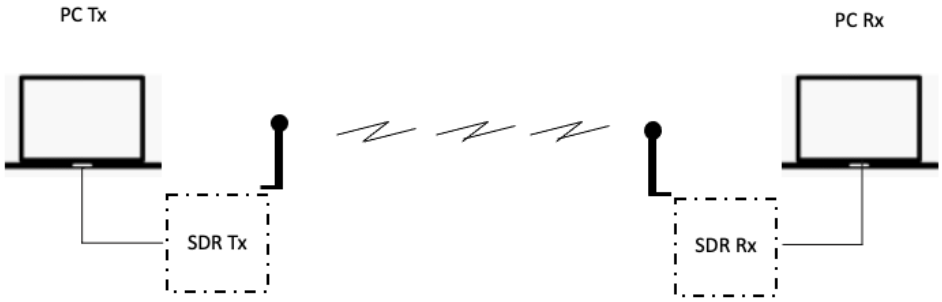

Figure **4-10**.: Network infrastructure

With the $'comm.SDRuTransmitter'$ object, it is possible to set a column vector or matrix input signal from MATLAB and transmit the signal and control data to a USRP board using the Universal Hardware Driver (UHD). In the receiver, it is necessary to find the SDR that it is connected to the receiver laptop. Figure **4-10**, shows the network infrastructure of the test-bed. To find the SDR in the receiver, it is necessary to follow the same process as in the transmitter (IP address 192.168.10.30 and $'findsdru'$ command). Then, in the receiver radio, it is necessary to adjust some specific features through Matlab interface, such as center frequency operation, gain, number of samples and decimation factor value. These values are necessary for the spectrum range to work. In our case, it was necessary to use a decimation factor that allows taking $2MHz$ of spectrum about central operation frequency with the aim to sweep the BW that was used in the transmitter ($500kHz$).

After setting up the values in the receiver, it is necessary to use *comm.SDRuReceiverobject* with the features described. This object receives signal and control data from a USRP board using UHD, and its outputs as a column vector or matrix signal of a fixed number of rows. The first call to this object might contain transient values, which can result in packets containing undefined data. The object allows using the *step* command to receive the signal. The received signal is stored with the goal to analyze it and decode it later. Then, it is necessary to restart the radio features with a *releasecommand* for future receptions. In the following lines, transmission and reception of LoRa symbols are explained.

Input: SDR connected, Matlab Software
Output: LoRa symbols Tx-Rx
initialization :
first statement
LOOP Process
if (Are Matlab and SDR connected ?) **then**
  Set up frequency and master clock rate consequent with BW to use
else
  Check connection between PC and SDR
end if
if Are Matlab and SDR connected ? **then**
  Set up Gain and interpolation factor features
  Set up synchronization time between SDR's of transmission and reception
  Set up comm.SDRuTransmitter and comm.SDRuReceiver objects from Matlab **Then**To restart the radio
end if
return

The received chirps are presented in figure **4-11** and the received spectrogram is presented in figure **4-12**.

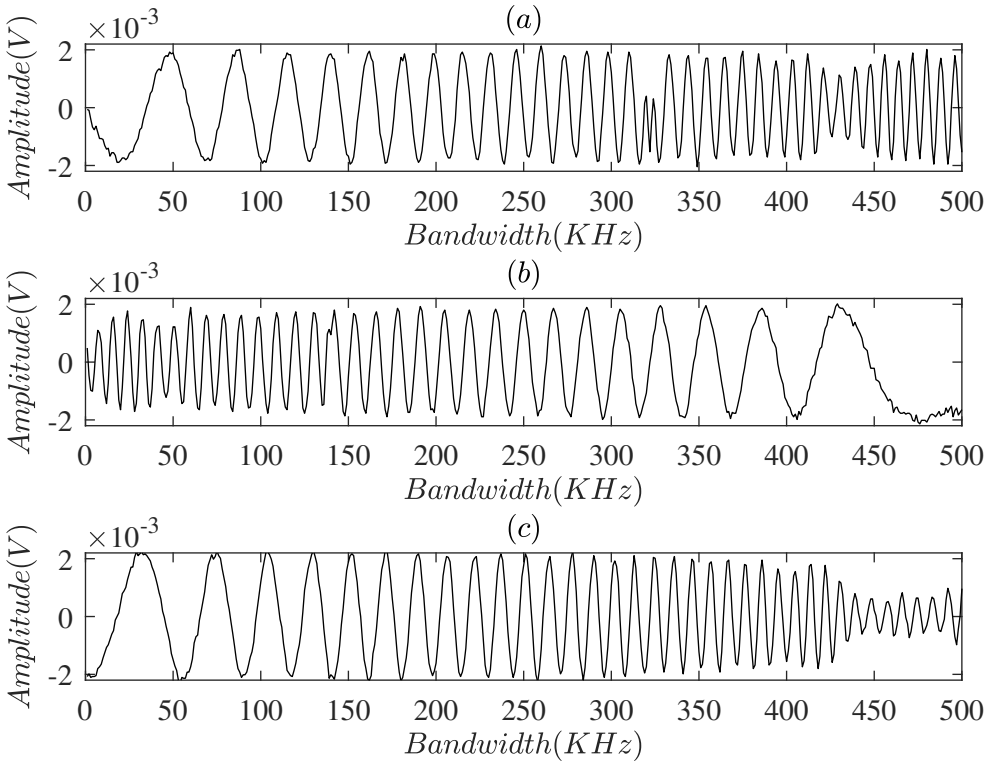

Figure **4-11**.: Received signal: (a) up-chirp, (b) down-chirp and (c) data.

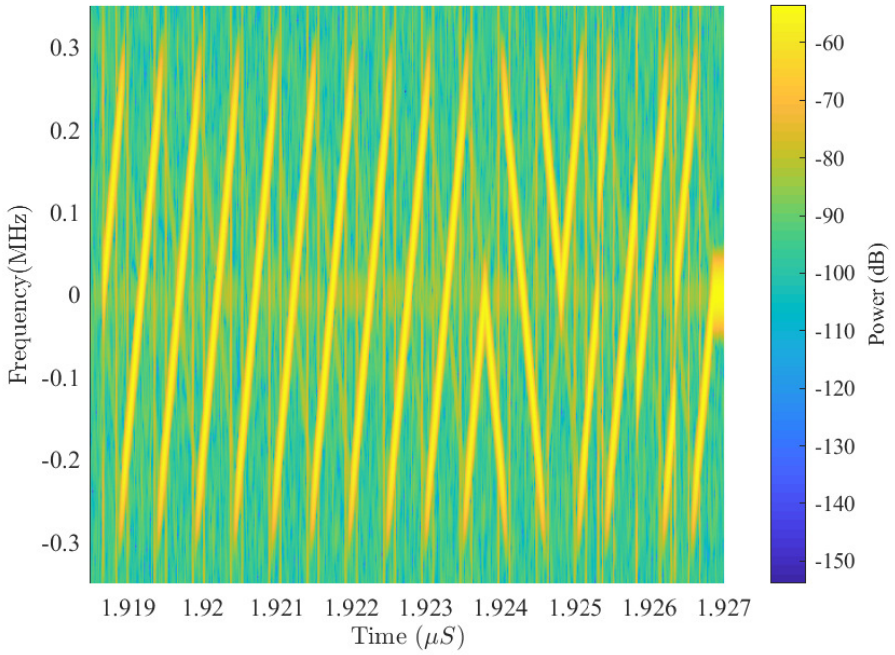

Figure **4-12**.: Spectrogram Rx

4.3.3. Signal processing and decoding

The aim is to show the methodological process to find the data in the stored vector that was received. In this case, it is worth considering that there is a ratio between sampling frequency in the receiver and in the LoRa bandwidth that was transmitted, which has a value of 4

$$\frac{2\ MHz}{500\ kHz} = 4$$

Therefore, a sweep is made from the beginning of the received vector until the end. Here, the first symbols are considered, i.e. 10 of preamble and 2 of synchronization. These first symbols are necessary to find the LoRa information in the signal that was received from the spectrum.

To decoding the data, it is necessary to create conjugate symbols in the receiver LoRa PHY with the same features as in the transmitter, therefore, the same values of SF and BW must be kept. Then, the received signal is multiplied with the conjugate symbols and the result is operated using FFT. The high peak in the signal must be found, thus next 2 LoRa symbols time of the high peak, the signal is multiplied with the reverse LoRa signal. In our case, the transmitter data signal was created with up-chirp LoRa PHY symbols, therefore, our reverse LoRa PHY signal in the receiver was a down-chirp LoRa symbol. the next step used FFT transform with the result $receivedLoRasymbols \times reversesignal$. Then, the high value peak in the FFT inside $1T_s$ can be found and corresponds to the data received. It is necessary to know how much data were transmitted, thus, the process is repeated the number of times needed. It is important to have in mind the number of Lora symbols with data, so that, the process is repeated only the necessary times.

Figure **4-13** shows a real component of signal with 10 preambles symbols, then, 2 synchronization symbols, and at the end, the first samples of the data. The high peak allows finding the end of the preamble and the beginning of the synchronization symbols. After 2 synchronization symbols ($2T_s$), it is possible to find the beginning of the data.

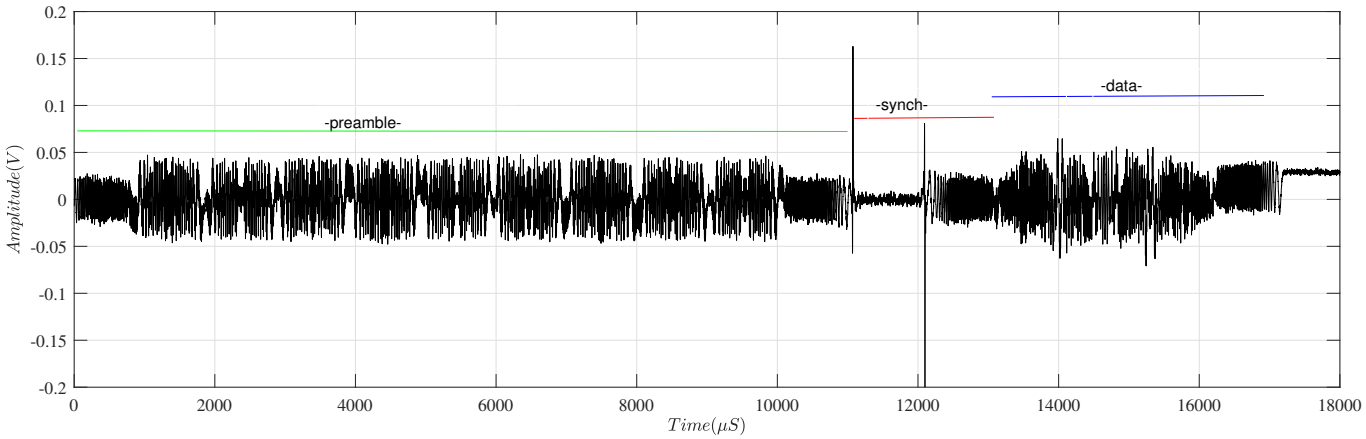

Figure **4-13**.: Real component of the received signal

4.3.4. Transmission and Reception of images through LoRa symbols

The first step is to follow the methodology that was proposed in this document, then, a classification process is performed with the aim to choose only the abnormal samples, which will be transmitted. Then, after

classification process and taking the images with abnormal samples, the images are compressed with the aim to reduce the amount of information and use it in the wireless LPWAN network.

With the results of the compression technique over information, it is possible to obtain a sparse vector with decimal and negative numbers. For the above, it is necessary to analyze and find a way to adapt the information because LoRa technology only allows transporting integer values within a range according to a spreading factor (SF). To use LoRa modulation technique, the sparse vector information must be converted to data supported in LoRa symbols. For this reason, the sparse vector is encoded. With the goal to find an easy way to encode the information, in this work an encoding and decoding process was implemented with a structure of 8 bits (1 byte) as a base.

To transmit and receive LoRa symbols, SDRs of National Instruments - reference 2920 was used through Matlab. The main technical features configured are: SF equal to 8, bandwith (BW) of 500 kHz and sampling frequency in the transmitter with interpolation factor value to reach BW and with decimation factor in the receiver to reach enough BW to sweep the value that was setup in the transmitter. Some features to consider:

To do LoRa symbols from the encoding of the data, Matlab software was used.

In the transmission process, a SDR was configured knowing the frequency and the value of the master clock rate of it operation.

Values of the SDR card are configured to be used with $'comm.SDRuTransmitter'$ object in Matlab through the Universal Hardware Driver (UHD).

In the receiver radio, some specific features have to be adjusted through Matlab interface, such as center frequency operation, gain, number of samples and decimation factor value. These value must be used with the spectrum range to work. In our case, a decimation factor was needed to allow taking 2 MHz of spectrum about central operation frequency with the aim to sweep the BW that was used in the transmitter (500 kHz). After to setting the values in the receiver, *comm.SDRuReceiver* object is used through Matlab and UHD. This object allows applying the *step* command to receive the signal. The received signal is stored with the goal to analyze it and decode it later, then, the radio features are restarted with *release* for future receptions.

To transport images through LoRa PHY modulation, the framework presented in figure **4-14** was implemented. It is important to remember that in order to process the image, first, its matrix is considered:

$$n_x n \quad [rows]x[columns]$$

and it s converted to a vector, which has a Nx1 size, where N is equal to $n_x n$.
To use the best solution of compression, Wavelet Transform is applied in the vector to have its samples in a common domain and reduce the deviation of the data values. A k-disperse signal $f \in R^N$ is sampled with compression to obtain a $g \in R^M$ signal, where $M << N$. The sampling can be represented in matrix form as $g = f \quad y \quad \in \quad R^{MxN}$, it is called system sampling matrix and, in this document, it was called sparse signal.

The values of the sparse signal have integer, decimal and some negative components. It is important to obtain the value of the position of these values with the objective of to transmit only those different to zero inside the sparse vector. The method implemented consisted in converting every component (integer, decimal, negative values and positions), to a byte representation, then, in the reception, decode every byte and rebuild the original data. Every byte representation created with an encode process has a size of 8 (bits). This value allows implementing a LoRa symbol with a spreading factor of the same length (SF=8).

In order to create a LoRa symbol, data was encoded into a structure of 8 bits (1 byte), which allows using LoRa modulation with SF=8. Each encode data has a value from 0 to 255 and these values represent the components

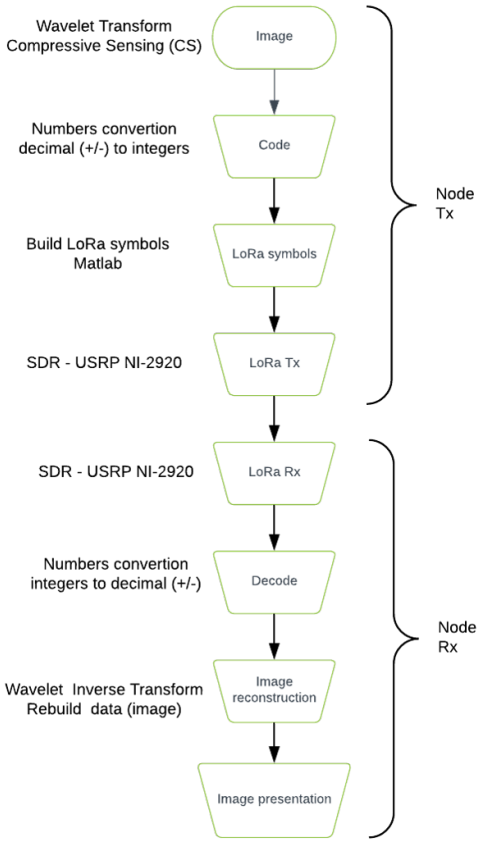

Figure **4-14**.: Framework implemented to transmit and receive LoRa symbols

of the integer, decimal and negative values of the sparse signal. Every symbol was created in Matlab through a mathematical model presented in [180] and in 4-1.

$$S_{css}(t) = e^{(j2\pi \ \frac{t^2}{2} \ \frac{BW}{T_s})} \tag{4-1}$$

To transmission and reception of LoRa symbols, the process described in **4.3.2** was followed.

Additionally, in order to decode the information and find its original values (Wavelet Transform representation), a program was created that converts the received data (LoRa symbols) to its base representation again.

Now, image recovery has to be made to rebuild it, therefore, data decoding allows finding a vector with a similar length to that of the transmitted data. These data contain information about values of output of Wavelet Transform, positions and negative values. Once rebuilt the vector with their features, the reconstruction algorithm is used with the sparse signal representation to recover the samples of the original signal and, with this output, Wavelet Inverse Transform is applied to recover the original vector of information. Now, it is necessary to adjust the original size of matrix $M \times N$ and screen the image. To test the original image transmitted with the one received, it is possible to use in Matlab the command $PSNR$, which calculates the peak signal to noise ratio for the image reconstructed and the image in array of reference (original image).

PSNR is usually expressed in logarithmic scale, thus the typical values of PSNR with non-significative loss are among 30 and 50 dB [181, 182] , where a high value is better. However, in wireless communication systems, the acceptable quality loss is considered from 20 to 25 dB [153, 183]. If the image under analysis is the same as the reference, the PSNR is infinite [43].

Inside results, the experiments were setup to find the difference among the change of the sparse signal. On the one hand, figure **4-15** shows a sample of the original and reconstructed images with a sparsity of 90%, where the PSNR value is 30.02 dB. On the other hand, figure **4-16** presents a sample of the original and reconstructed images with a sparsity of 95%, where the PSNR value is 26.81 dB.

(a)

(b)

Figure **4-15**.: (a) Original image, and (b) reconstructed image with 90% of sparsity

(a)

(b)

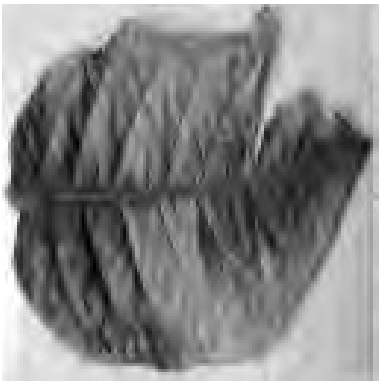

Figure **4-16**.: (a) Original image, and (b) reconstructed image with 95% of sparsity

The results proposes a potential solution to transmit images through LPWAN networks. Applications where the high quality of the reconstructed image is necessary can be easy and functionally adapted. For example, in our case, we applied the solution in a image that allows understanding if a leaf of potato has or not some disease or if it is attacked by any plague. This case is shown in figures **4-15** and **4-16** where a change in its representation is observed. This feature allows identifying the presence of a disease in the plant. The codes developed can be found in appendix A.

4.4. Study of Diversity in order to improve the data transmission in a LoRaWAN network

In order to observe the behavior between SISO or MIMO systems and to improve the data transmission, this work entails the follow considerations:

i. With the compression technique, it is possible to reduce an image in 4 packets: 3 of 1450 and 1 of 564, all of them in bytes (4914 bytes by one image).

ii. For one image and consequent with table 1.2, the best scenario in data transmission is when LoRa modulation system works with SF=7 and BW = 500 kHz, thus the bit rate is equal to 27.343 Kbit/s. Nevertheless, by coding process, it has worked with SF=8, then, the data rate is 15.625 Kbit/s, hence equation 3-12 expresses the symbol time equal to 512 μS. If it is necessary to transmit 4914 symbols per image with SF=8 and BW= 500 kHz, then, the data transmission time is 2.51 seconds. In this scenario, it is necessary to transmit 4 packets in the same SF=8.

iii. Now, in the second moment, the use of different SF value was calculated to work with SF equal to SF8, SF9, SF10 and SF11. As 4 packets were transported, it was necessary to analyze the behavior using 4 SF values in order to work with a diversity method, where a system was constructed with 4 transmitters and 4 receivers. Table 1.2 and equation 3-12 show that SF8 take 512μS by each packet, SF9 takes 1024μS, SF10 takes 2048μS, SF11 takes 4096μS. As in the data transmission packet, then, the image has 4 packets, 3 of 1450 and 1 of 564 bytes. This information is listed in Table **7**.

Table 7.

Spreading Factor (SF)	Symbol Time (Ts in μS)	Packets number	Total time (Seconds)
8	512	1450	0.7424
9	1024	1450	1.4848
10	2048	1450	2.9696
11	4096	564	2.31

Consequently, the packet with a high value in transmission time is the one in SF=10, as the transmission packets in SF8, SF9, SF10 and SF11 are transmitted at the same time. Then, the maximum time is when the last packet arrives to the receiver, and the image is transmitted in 2.96 seconds.

iv. If we analyze the last points (ii, iii), two scenarios can be compared:

First, 1 transmitter and 1 receiver use 4 packets in order to transmit 1 image inside a SF8 and take 2.51 seconds.

Second, 4 transmitters and 1 receiver transmit the same image inside SF8, SF9, SF10 and SF11 and take 2.96 seconds.

As a result, it is better to use the first scenario, because it takes less time (2.51 seconds vs. 2.96 seconds) and less resources use such as energy consumption, devices, cost, infrastructure, frequency use, among others.

On the other hand, it was necessary to analyze the potential interference when the same frequencies are used with different SFs in the same time, thus, in the literature the review of orthogonality in this case can be found in the literature [89, 118, 184–187]. After a literature review, we use "LoRa phy simulator"; which is a simulator tool for testing the performance of a LoRa link in case of collision within a LoRa packet modulated with different SFs. The output is the packet, symbol and bit error rate (PER, SER and BER, respectively). It also shows the interference of a particular SF with another possible SFs [184].

In **4-17** the values of the relation of $SF = 8$ can be identified with the others SFs(7,9,10,11,12). The bit error rate decreases when the SIR (Signal Interference Ratio)is near to 0 dB, while the other SFs is near to -15 dB, which shows a high relation value between a signal power with signal interference power. Nevertheless, for our purpose, to tune a particular SF between transmitter and receiver, the power signal of the others SFs is not relevant even when all of them use the same bandwith and the same frequencies range. All of the above is supported on the literature [89, 118, 184–187].

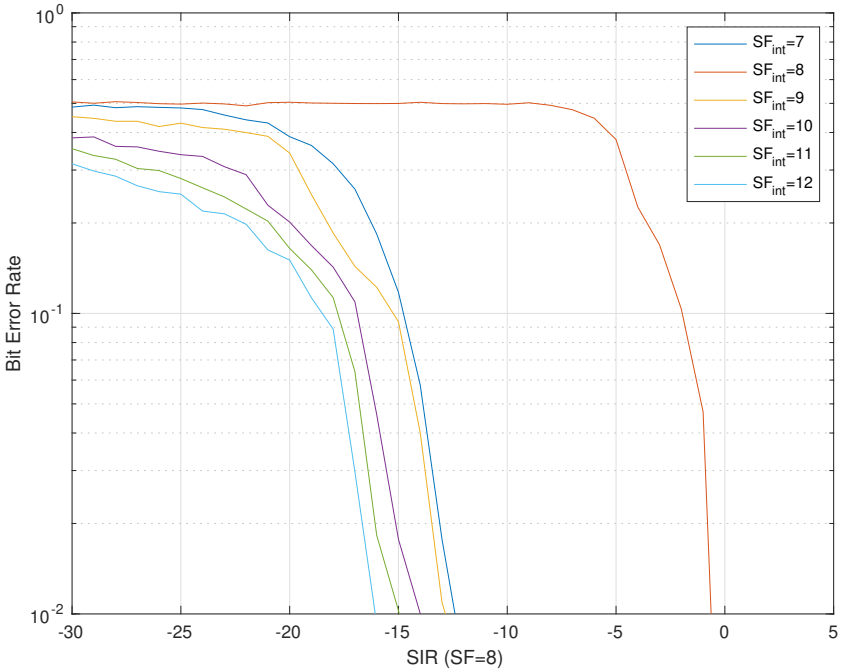

Figure **4-17**.: Interference on spreading factor equal to 8

In order to understand the relation between the signal interference ratio present in figure **4-17**, it is important to observe the relation between the signal of the particular SF and the interference of the other SFs. Therefore, in equation 4-2 expresses this relation.

$$SIR = 10log_{10}\frac{P_s}{(\sum_{n=1}^{N} P_i)} \tag{4-2}$$

where P_s is the signal power of the SF of our interest and P_i is the total interference of the other sources, in particular of the other signals with different SFs. Now, in general terms the relation among packet, symbol and bit error rate (PER, SER and BER, respectively), can be found in **4-18**.

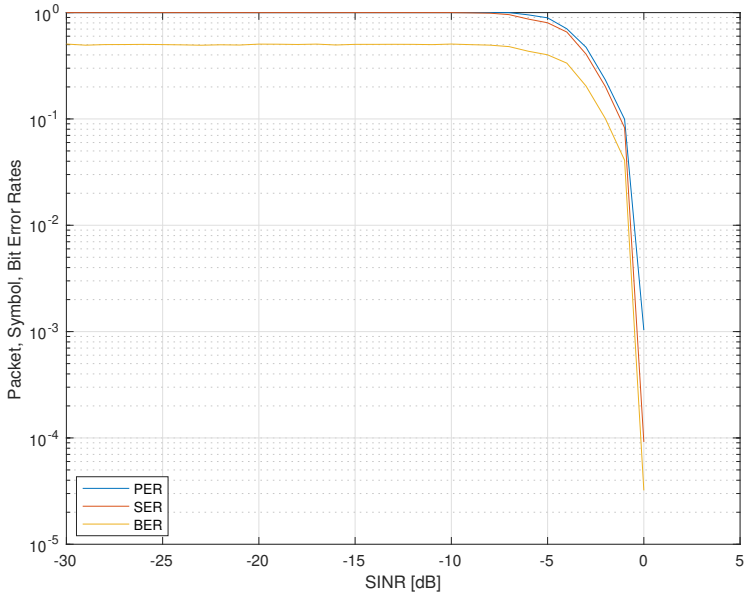

Figure **4-18**.: Relation among packet, symbol and bit error rate

The relation of packet, symbol and bit error rate in terms of interference is similar to the SIR. Nevertheless, for this relation, there is an additional feature, i.e. a noise feature. Therefore, a SINR factor can be found with relation to the Signal Interference Noise Ratio, where additional interference sources of the others signals can be found too. Equation 4-3 expresses this relation.

$$SINR = \frac{SignalPower}{Noise + InterferencePower} \tag{4-3}$$

In relation to the information present in **4-18**, when the signal power is high with respect to signal power interference, the values of Packet, Symbol and Bit error decrease considerably. It is important to design systems

with consideration of the lower interference and, in the case of LoRaWAN, there is a minimum probability of finding interference, when our designs have the different SFs in the same BW and in the same frequencies.

5. Conclusions

This final chapter presents the main conclusions of our work. Internet of things allows connecting physical devices with digital environments, and within IoT it is possible to find LPWAN networks that are used to send or receive short messages in short moments. Providers with licensed spectrum can allocate spectrum resources to IoT without restrictions. On the other hand, for LPWAN networks in unlicensed bands, the efficiency decreases and the noise floor increases, which can be mitigated by adding more gateways. Critical applications should not use unlicensed technologies, in fact the service should be provided by a network operator in licensed spectrum with the goal to reach trust in its operation. LPWAN networks in unlicensed spectrum frequency need to implement efficiency measures of use and interference reduction politicies. In this way, LPWAN networks have low power consumption, long-distance coverage and a low capacity to transport information, which is a problem when high amount of information needs to be transported. Hence, we addressed the proposal of a methodology to transport agricultural images under a LPWAN network, mainly through LoRa modulation technology. For this purpose, within the proposal methodology we present a framework with three main components. The first one is the classification of an image with the goal to separate normal or abnormal samples, thus, it is not necessary to transport all images, only, those with abnormal features that allow identifying that the plant has a high probability of having a disease. This allows optimizing the use of a communication channel through LPWAN network. The second component is compression of abnormal samples whose main goal is to reduce the amount of information, so that it is more efficient with the use of resources of channel, energy consumption and the time to transport a sample. The third one is the LPWAN network with the goal to know the technology and hence be able to replicate it in a SDRs that allow finding improvements and transporting images with it. We found in the state of the art some works that search how to transport real time data or high amounts of information through wireless sensor networks, then, some critical points should be considered such as restricted computational power, memory limitations, narrow bandwidth and energy consumption, mainly. Some works proposed image transmission over LPWAN networks, nevertheless, some of them only reach a theoretical analysis without implementation. In the other case, information is scarce about implementation process and to the best of our knowledge, there is no a study for testing the implementation of a LPWAN network through implementation of LoRa modulation technology with SDRs and Matlab in the transmitter and in the receiver.

We describe the contributions of the proposal method. We found in the state of the art some methods to transport images with LoRa modulation technology, nevertheless, information about this works is scarce and to the best of our knowledge there is no implementation of LoRa modulation technology with open platforms and Matlab in the transmitter and the receiver. We present a method to transport images with a LPWAN network, and an implementation in SDRs that allows considering and testing in the future improvements in the technology. Our principal contribution is the proposal of a framework, which creates a method to transport images through the use of a LPWAN network.

In summary, the main contributions are:

> A methodology to transmit images of agricultural crops showing disease features through LPWAN networks with the use of LoRa modulation technology. Only images with abnormal visual features will be transmitted, which entails an optimization process that allows reducing the amount of information to transport, because it is not necessary to load a limited resource through the transmission of normal samples where there are integrated features as energy consumption and use of spectrum, mainly.

Implementation of the LoRa modulation system in SDRs transmitter and receiver to know the features of the modulation technique and thus understand its potential for improvement, particularly in a method that allows increasing its capacity of data transport.

A method was evaluated to identify the considerations to use a method for evaluating a SISO or MIMO system to improve the time in transport images with LoRa modulation. In the test, it was possible to observe that one transmitter and with one receiver are enough to transport an image that was considered in this research.

This research has proposed a method to transport images through LPWAN networks using LoRa modulation. The proposal is composed of classification process, compressive sensing technique, LoRa symbols creation, transmission and reception of symbols through SDRs with Matlab and image reconstruction in the receiver. With the use of frequency hopping, the time necessary could reach 400ms to transmit an image of 128 x 128 size. Also, the implementation was possible through the use of SDRs in the receiver and the transmitter, which involves the creation of the LoRa symbols and setup the features to deliver it to the SDR.

5.1. Future work

In order to improve the method that was presented in this research, we recommended:

- Actually, in the literature there are many methods in order to classify samples and in particular with application in agricultural crops; therefore, it is necessary to evaluate more methods of classification of the samples. Particularly, with applications in capturing a sample or an image in the crop.

- To evaluate methods in order to improve the reduction of amount of information in an image and the consequent reconstruction process.

- To perform tests with implementation of LoRa modulation in order to know features that allow improving this modulation.

- To implement in free platforms, as SDRs and Matlab, the LoRaWAN technology. This work replicated the LoRa modulation. It is important to add features such as coding, duty cycle, among others.

- It is convenient to take into account various metrics in addition to PSNR when evaluating the reconstructed image, as this enables the integration of statistical findings in the proposal research.

Finally, it is necessary to integrate all stages that were presented in this research. Here a general framework and a methodology were presented, nevertheless, each stage was evaluated separately.

Bibliography

[1] S. d. M. y. E. G. de Boyacá, "Departamento de Boyacá," *1*, vol. 1, no. 1, p. 24, 2010. [Online]. Available: http://www.simco.gov.co/

[2] H. Al Hiary, S. Bani Ahmad, M. Reyalat, M. Braik, and Z. ALRahamneh, "Fast and Accurate Detection and Classification of Plant Diseases," *International Journal of Computer Applications*, vol. 17, no. 1, pp. 31–38, 2011. [Online]. Available: http://www.ijcaonline.org/volume17/number1/pxc3872754.pdf

[3] G. Athanikar and M. P. Badar, "Potato Leaf Diseases Detection and Classification System," vol. 5, no. 2, pp. 76–88, 2016.

[4] R. Hopkins, M. Rodrigues, and M. Rinaldi, "Trends and potencial uses of ICTs in Latin American and the Caribbean agriculture," *Information and communication technologies for agricultural development in Latin America: trends, barriers and policies*, pp. 77–156, 2013.

[5] X. Wang, M. Zhang, J. Zhu, and S. Geng, "Spectral prediction of Phytophthora infestans infection on tomatoes using artificial neural network (ANN)," *International Journal of Remote Sensing*, vol. 29, no. 6, pp. 1693–1706, 2008.

[6] A. Camargo and J. S. Smith, "An image-processing based algorithm to automatically identify plant disease visual symptoms," *Biosystems Engineering*, vol. 102, no. 1, pp. 9–21, 2009. [Online]. Available: http://dx.doi.org/10.1016/j.biosystemseng.2008.09.030

[7] A. T. Deever, "IMPROVED IMAGE CAPTURE USING LIVEVIEW IMAGES Aaron T . Deever Eastman Kodak Company Rochester , NY 14650," *2010 IEEE International Conference on Image Processing*, pp. 1681–1684, 2010.

[8] J. K. Sainis, R. Rastogi, and V. K. Chadda, "Applications of Image Processing in Biology and Agriculture," *DAE-BRNS Workshop on Applications in Image Processing in Plant Sciences and Agriculture (WIPSA)*, p. 8, 1998.

[9] A. Shirazinia, "Source and Channel Coding for Compressed Sensing and Control," Ph.D. dissertation, 2014. [Online]. Available: http://kth.diva-portal.org/smash/get/diva2:709596/FULLTEXT01.pdf

[10] M. Nasri, A. Helali, H. Sghaier, and H. Maaref, "Adaptive image transfer for wireless sensor networks (WSNs)," *5th Conference on Design and Technology of Integrated Systems in Nanoscale Era, DTIS 2010*, pp. 1–7, 2010.

[11] R. Kirichek, V. D. Pham, A. Kolechkin, M. Al-Bahri, and A. Paramonov, "Transfer of multimedia data via LoRa," *Lecture Notes in Computer Science (including subseries Lecture Notes in Artificial Intelligence and Lecture Notes in Bioinformatics)*, vol. 10531 LNCS, no. September, pp. 708–720, 2017.

[12] W.-c. Feng, B. Code, E. Kaiser, M. Shea, W.-c. Feng, and L. Bavoil, "Panoptes : Scalable Low-Power Video Sensor Networking Technologies Panoptes : Scalable Low-Power Video Sensor Networking Technologies," no. June 2014, 2005.

[13] S. Paniga, L. Borsani, A. Redondi, M. Tagliasacchi, M. Cesana, P. Milano, and P. Leonardo, "Experimental Evaluation of a Video Streaming System for Wireless Multimedia Sensor Networks," *2011 The 10th IFIP Annual Mediterranean Ad Hoc Networking Workshop*, pp. 165–170, 2011.

[14] C. Fan and Q. Ding, "A novel wireless visual sensor network protocol based on LoRa modulation," *International Journal of Distributed Sensor Networks*, vol. 14, no. 3, 2018.

[15] C. Duran-Faundez and V. Lecuire, "Error resilient image communication with chaotic pixel interleaving for wireless camera sensors," *REALWSN 2008 - Proceedings of the 2008 Workshop on Real-World Wireless Sensor Networks*, pp. 21–25, 2008.

[16] L. Makkaoui, V. Lecuire, and J. M. Moureaux, "Fast zonal DCT-based image compression for wireless camera sensor networks," *2010 2nd International Conference on Image Processing Theory, Tools and Applications, IPTA 2010*, no. Llm, pp. 126–129, 2010.

[17] L. Wang, L. Li, J. Li, J. Li, B. B. Gupta, and X. Liu, "Compressive sensing of medical images with confidentially homomorphic aggregations," *IEEE Internet of Things Journal*, vol. 6, no. 2, pp. 1402–1409, 2019.

[18] C. Pham, "Low-cost, low-power and long-range image sensor for visual surveillance," *Proceedings of the Annual International Conference on Mobile Computing and Networking, MOBICOM*, vol. 03-07-Octo, pp. 35–40, 2016.

[19] ——, "Enabling and deploying long-range IoT image sensors with LoRa technology," *2018 IEEE Middle East and North Africa Communications Conference, MENACOMM 2018*, pp. 1–6, 2018.

[20] R. Sanchez-Iborra and M. D. Cano, "State of the art in LP-WAN solutions for industrial IoT services," *Sensors (Switzerland)*, vol. 16, no. 5, 2016.

[21] C. Goursaud and J. M. Gorce, "Dedicated networks for IoT: PHY / MAC state of the art and challenges," *EAI Endorsed Transactions on Internet of Things*, vol. 1, no. 1, pp. 1–11, 2015. [Online]. Available: http://creativecommons.org/licenses/by/3.0/

[22] Agencia Nacional del Espectro-Colombia, "Resolución ANE 0711 de 2016 Bandas ICM Colombia," 2016. [Online]. Available: http://www.ane.gov.co/images/ArchivosDescargables/Normatividad/Planeacion{_}del{_}espectro/Resolucion711de2016.pdf

[23] A. H. Jebril, A. Sali, A. Ismail, and M. F. A. Rasid, "Overcoming limitations of LoRa physical layer in image transmission," *Sensors (Switzerland)*, vol. 18, no. 10, 2018.

[24] P. Pavan Kumar, "Implementation of software controlled radio for long range communication with high data rate and optimal capacity," *International Journal of Innovative Technology and Exploring Engineering*, vol. 8, no. 10, pp. 4150–4158, 2019.

[25] B. S. Matthew Knight, "Decoding LoRa: Realizing a Modern LPWAN with SDR," in *GNU Radio Conference 2016*, 2016, pp. 1–5.

[26] M. Aref and A. Sikora, "Free space range measurements with Semtech LoRa??? technology," *2014 2nd International Symposium on Wireless Systems within the Conferences on Intelligent Data Acquisition and Advanced Computing Systems, IDAACS-SWS 2014*, no. September, pp. 19–23, 2014.

[27] P. Robyns, P. Quax, W. Lamotte, and W. Thenaers, "A Multi-Channel Software Decoder for the LoRa Modulation Scheme," pp. 1–11, 2017.

[28] S. Theodoridis and K. Koutroumbas, *Pattern Recognition*, 2008.

[29] E. Alpaydin, *Introduction to Machine Learning. Second Edition*, 2010.

[30] K. Fukunaga, "Statistical Pattern Stas-tical Pattern Recognit ion," *Pattern Recognition*, vol. 22, no. 7, pp. 833–834, 1990. [Online]. Available: http://linkinghub.elsevier.com/retrieve/pii/0098300496000179

[31] O. I. Abiodun, A. Jantan, A. E. Omolara, K. V. Dada, N. A. E. Mohamed, and H. Arshad, "State-of-the-art in artificial neural network applications: A survey," *Heliyon*, vol. 4, no. 11, p. e00938, 2018. [Online]. Available: https://doi.org/10.1016/j.heliyon.2018.e00938

[32] L. Deng and D. Yu, "Deep Learning: Methods and Applications," *Foundations and Trends® in Signal Processing*, vol. 7, no. 3-4, pp. 197—-387, 2013.

[33] S. K. Pilli, B. Nallathambi, S. J. George, and V. Diwanji, "eAGROBOT- A Robot for Early Crop Disease Detection using Image Processing," no. Icecs, pp. 1–6, 2015.

[34] R. Laudien, G. Bareth, and R. Doluschitz, "Comparison of Remote Sensing Based Analysis of Crop Diseases By Using High Resolution Multispectral and Hyperspectral Data -Case Study: Rhizoctonia Solani in Sugar Beet," *Geoinformatics*, no. June, pp. 7–9, 2004. [Online]. Available: http://citeseerx.ist.psu.edu/viewdoc/download?doi=10.1.1.460.6544{&}rep=rep1{&}type=pdf

[35] S. Weizheng, W. Yachun, C. Zhanliang, and W. Hongda, "Grading Method of Leaf Spot Disease Based on Image Processing," *2008 International Conference on Computer Science and Software Engineering*, pp. 491–494, 2008. [Online]. Available: http://ieeexplore.ieee.org/document/4723305/

[36] M. S. P. Babu and B. S. Rao, "Leaves Recognition Using Back Propagation Neural Network-Advice for Pest & Disease Control on Crops . Leaves Recognition Using Back Propagation Neural Network-Advice for Pest & Disease Control on Crops . 3 . Requirement Specification 4 . Tools Techniques," 2007.

[37] S. P. Mohanty, D. P. Hughes, and M. Salathe, "Using Deep Learning for Image-Based Plant Disease Detection," *Frontiers in Plant Science*, vol. 7, p. 10, 2016.

[38] M. B. Dheeb Al Bashis and S. Bani, "Detection and Classification of Leaf Diseases using K-means-based Segmentation and Neuronal-networks-based Classification," *Information Technology Journal*, pp. 267–275, 2011.

[39] C. D. Sindhuja Sankaran, Ashish Mishra, Reza Ehsani, "A review of advanced techniques for detecting plant diseases," pp. 1–13, 2010.

[40] U. S. Rumpf, T., -K Mahlein, "Early Detection and classification of plant diseases with Support Vector Machines based on hyperspectral reflectance," pp. 91 – 99, 2010.

[41] L. P. Jan Behmann, Jorg Steinrucken, "Detection of early plant stress responses in hyperspectral images," pp. 98–111, 2014.

[42] A. S. Jagadeesh D. Pujari, Rajesh Yakkundimath, "Image processing based detection of fungal diseases in plants," pp. 1802–1808, 2015.

[43] D. Salomon, *Data Compression The Complete Reference FourthEdition*, 2007, vol. 53, no. 9.

[44] P. Qian, Y. Guo, N. Li, and B. Sun, "Multiple Target Localization and Power Estimation in Wireless Sensor Networks using Compressive Sensing," pp. 1–5, 2015.

[45] E. Candes and M. Wakin, "An Introduction To Compressive Sampling," *IEEE Signal Processing Magazine*, vol. 25, no. 2, pp. 21–30, 2008.

[46] C. Feng, S. Valaee, and Z. Tan, "Multiple Target Localization Using Compressive Sensing," 2009.

[47] J. a. Tropp and A. C. Gilbert, "Via Orthogonal Matching Pursuit," *IEEE Transactions on Information Theory*, vol. 53, no. 12, pp. 4655–4666, 2007.

[48] B. A. Jayawickrama, E. Dutkiewicz, I. Oppermann, G. Fang, and J. Ding, "Improved performance of spectrum cartography based on compressive sensing in cognitive radio networks," *2013 IEEE International Conference on Communications (ICC)*, pp. 5657–5661, 2013. [Online]. Available: http://ieeexplore.ieee.org/document/6655495/

[49] B. A. Jayawickrama, E. Dutkiewicz, G. Fang, and M. Mueck, "Downlink Power Allocation Algorithm for Licence-exempt LTE Systems Using Kriging and Compressive Sensing Based Spectrum Cartography," pp. 3766–3771, 2013.

[50] H. Jamali-rad, H. Ramezani, and G. Leus, "Sparse Multi-Target Localization Using Cooperative Access Points," pp. 353–356, 2012.

[51] B. S. Krishnan and R. Vaze, "On White-Space Detection , Localization and Coverage."

[52] S. K. Sharma, E. Lagunas, S. Chatzinotas, and B. Ottersten, "Application of Compressive Sensing in Cognitive Radio Communications: A Survey," *IEEE Communications Surveys & Tutorials*, vol. 18, no. 3, pp. 1838–1860, 2016. [Online]. Available: http://ieeexplore.ieee.org/document/7397824/

[53] S.-J. Kim, E. Dall'Anese, and G. B. Giannakis, "Cooperative Spectrum Sensing for Cognitive Radios Using Kriged Kalman Filtering," *IEEE Journal of Selected Topics in Signal Processing*, vol. 5, no. 1, pp. 24–36, 2011. [Online]. Available: http://ieeexplore.ieee.org/document/5484600/

[54] S.-j. Kim, E. D. Anese, S. Member, and G. B. Giannakis, "Cooperative Spectrum Sensing for Cognitive Radios Using Kriged Kalman Filtering," vol. 5, no. 1, pp. 24–36, 2011.

[55] J. Marin, L. Betancur, and H. Arguello, "Modelo de Muestreo Comprimido Multiespectral para Radio Cognitiva Compressed Sensing Multiespectral Model for Cognitive Radio Networks," no. 70.

[56] S. Feizi, M. Médard, and M. Effros, "Compressive sensing over networks," *2010 48th Annual Allerton Conference on Communication, Control, and Computing, Allerton 2010*, pp. 1129–1136, 2010.

[57] R. Baraniuk, "Compressive Sensing [Lecture Notes]," *IEEE Signal Processing Magazine*, vol. 24, no. July, pp. 118–121, 2007.

[58] N. Naghsh, A. Ghorbani, and H. Amindavar, "Compressive sensing for microwave breast cancer imaging," *IET Signal Processing*, vol. 12, no. 2, pp. 242–246, 2018.

[59] C. Ruland, "An Improved Authenticated Compressive Sensing Imaging," no. 1, 2018.

[60] L. Deng, Y. Zheng, P. Jia, S. Lu, and J. Yang, "Adaptively Group Based on the First Joint Sparsity Models Distributed Compressive Sensing of Hyperspectral Image," pp. 429–434, 2017.

[61] Z. Wei, L. Yang, Z. Wang, B. Zhang, Y. Lin, and Y. Wu, "Wide Angle SAR Subaperture Imaging Based on Modified Compressive Sensing," vol. 1748, no. c, pp. 1–6, 2018.

[62] D. L. Donoho, "Compressed sensing," *IEEE Transactions on Information Theory*, vol. 52, no. 4, pp. 1289–1306, 2006.

[63] T. Geng, G. Sun, Y. Xu, and B. Zheng, "Adaptive group sparse representation for image compressive sensing," *2017 IEEE 8th International Conference on Intelligent Computing and Information Systems, ICICIS 2017*, vol. 2018-Janua, no. 2015, pp. 52–57, 2018.

[64] M. K. B. Suhani Salan, "Image Reconstruction Based on Compressive Sensing," no. 2011, pp. 2123–2128, 2008.

[65] S. Ramdani, "Compressive Sensing Approach for Microwave Imaging Application," pp. 197–200, 2018.

[66] M. Figueiredo, R. Nowak, and S. J. Wright, "Gradient projection for sparse reconstruction: application to compressed sensing and other inverse problems, IEEE J," *Sel. Top. Signa*, vol. vol, no. 4, pp. 1pp586–597, 2007.

[67] J. N. Tehrani, C. Jin, A. McEwan, and A. Van Schaik, "A comparison between compressed sensing algorithms in Electrical Impedance Tomography," *2010 Annual International Conference of the IEEE Engineering in Medicine and Biology Society, EMBC'10*, no. 2, pp. 3109–3112, 2010.

[68] N. Koep and R. Mathar, "Binary Iterative Hard Thresholding for Frequency-Sparse Signal Recovery," *Wsa 2017*, pp. 258–264, 2017.

[69] X. Cai, Z. Zhou, Y. Yang, and Y. Wang, "Improved Sufficient Conditions for Support Recovery of Sparse Signals via Orthogonal Matching Pursuit," vol. 3536, no. c, pp. 1–6, 2018.

[70] ITU UITgital, "ITU-T," *ITU*, vol. 57, pp. 1–71, 2015.

[71] K. E. Nolan, W. Guibene, and M. Y. Kelly, "An evaluation of low power wide area network technologies for the Internet of Things," *2016 International Wireless Communications and Mobile Computing Conference (IWCMC)*, pp. 439–444, 2016. [Online]. Available: http://ieeexplore.ieee.org/document/7577098/

[72] M. Blackstock and R. Lea, "IoT interoperability: A hub-based approach," in *2014 International Conference on the Internet of Things, IOT 2014*. Cambridge, MA, USA: IEEE, 2014, pp. 79–84.

[73] M. Centenaro, L. Vangelista, A. Zanella, and M. Zorzi, "Long-Range Communications in Unlicensed Bands : the Rising Stars in the IoT and Smart City Scenarios," *IEEE WIRELESS COMMUNICATIONS LETTERS*, vol. 23, no. 5, pp. 1–8, 2016.

[74] D. Chaves-Diéguez, A. Pellitero-Rivero, D. García-Coego, F. J. González-Casta??o, P. S. Rodríguez-Hernández, Ó. Piñeiro-Gómez, F. Gil-Castiñeira, and E. Costa-Montenegro, "Providing iot services in smart cities through dynamic augmented reality markers," *Sensors (Switzerland)*, vol. 15, no. 7, pp. 16 083–16 104, 2015.

[75] G. Margelis, R. Piechocki, D. Kaleshi, and P. Thomas, "Low Throughput Networks for the IoT : Lessons Learned From Industrial Implementations," in *2015 IEEE 2nd World Forum on Internet of Things (WF-IoT)*, vol. 1. Milan, Italy: IEEE, 2015, pp. 181 – 186.

[76] R. U. Quinnell, "Low power wide-area networking alternatives for the IoT," *EDN Networks*, pp. 1–7, 2015. [Online]. Available: http://www.edn.com/design/systems-design/4440343/1/Low-power-wide-area-networking-alternatives-for-the-IoT

[77] L. Vangelista, A. Zanella, and M. Zorzi, "Long-range IoT technologies: The dawn of LoRa," in *1st EAI International Conference on Future access enablers of ubiquitous and intelligent infrastructures*, vol. 159. Ohrid, Republic of Macedonia: Springer Verlag, 2015, pp. 51–58.

[78] J. Butler, E. Pietrosemoli, M. Zennaro, C. Fonda, S. Okay, and C. Aichele, *Wireless Networking In The Developing World*, 3rd ed., 2013. [Online]. Available: http://wndw.net/

[79] L. Krupka, L. Vojtech, and M. Neruda, "The Issue of LPWAN Technology Coexistence in IoT Environment," in *Mechatronics - Mechatronika (ME), 2016 17th International Conference on Mechatronics - Mechatronika (ME)*, 2016, pp. 1 – 8. [Online]. Available: http://ieeexplore.ieee.org/abstract/document/7827866/

[80] L. D. Kyle Benson, Charles Fracchia, Guoxi Wang, Qiuxi Zhu, Serene Almomen, John Cohn, "SCALE: Safe Community Awareness and Alerting Leveraging the Internet of Things," *Ieee Wireless Communications*, no. December, pp. 2–10, 2015.

[81] D. R. David, A. Nait-Sidi-moh, D. Durand, and J. Fortin, "Using Internet of Things technologies for a collaborative supply chain: Application to tracking of pallets and containers," *Procedia Computer Science*, vol. 56, no. 1, pp. 550–557, 2015. [Online]. Available: http://dx.doi.org/10.1016/j.procs.2015.07.251

[82] A. Ali, G. A. Shah, and J. Arshad, "Energy efficient techniques for M2M communication: A survey," *Journal of Network and Computer Applications*, vol. 68, pp. 42–55, 2016.

[83] O. Vermesan and P. Friess, *Internet of Things Applications - From Research and Innovation to Market Deployment*, 2014. [Online]. Available: https://books.google.com.br/books?id=kw2doAEACAAJ

[84] X. Xiong, K. Zheng, R. Xu, W. Xiang, and P. Chatzimisios, "Low power wide area machine-to-machine networks: Key techniques and prototype," *IEEE Communications Magazine*, vol. 53, no. 9, pp. 64–71, 2015.

[85] J. Petajajarvi, K. Mikhaylov, M. Hamalainen, and J. Iinatti, "Evaluation of LoRa LPWAN technology for remote health and wellbeing monitoring," in *International Symposium on Medical Information and Communication Technology, ISMICT*, vol. 2016-June, 2016, p. 1/5.

[86] A. Zanella, N. Bui, A. Castellani, L. Vangelista, S. Member, and M. Zorzi, "Internet of Things for Smart Cities," *IEEE INTERNET OF THINGS JOURNAL*, vol. 1, no. 1, pp. 22–32, 2014.

[87] D. H. Kim, J. B. Park, J. H. Shin, and J. D. Kim, "Design and implementation of object tracking system based on LoRa," in *2017 International Conference on Information Networking (ICOIN)*. Da Nang, Vietnam: IEEE, 2017, pp. 463–467. [Online]. Available: http://ieeexplore.ieee.org/document/7899535/

[88] A. Al-Fuqaha, M. Guizani, M. Mohammadi, M. Aledhari, and M. Ayyash, "Internet of Things: A Survey on Enabling Technologies, Protocols, and Applications," *IEEE Communications Surveys and Tutorials*, vol. 17, no. 4, pp. 2347–2376, 2015.

[89] M. Bor, J. Vidler, and U. Roedig, "LoRa for the Internet of Things," in *Proceedings of the 2016 International Conference on Embedded Wireless Systems and Networks*, 2016, pp. 361–366.

[90] E. Borgia, "The Internet of Things vision: Key features, applications and open issues," *Computer Communications*, vol. 54, pp. 1–31, 2014. [Online]. Available: http://linkinghub.elsevier.com/retrieve/pii/S0140366414003168

[91] A. Ali, G. A. Shah, M. O. Farooq, and U. Ghani, "Technologies and challenges in developing Machine-to-Machine applications: a survey," *Journal of Network and Computer Applications*, vol. 83, no. February, pp. 124–139, 2017. [Online]. Available: http://linkinghub.elsevier.com/retrieve/pii/S1084804517300620

[92] Z. Zelenika and T. Pusnik, "Reinventing Telecom OSS Toolkit as an loT Platform," *58th International Symposium ELMAR-2016*, vol. 1, no. September, pp. 12–14, 2016.

[93] D. Bankov, E. Khorov, and A. Lyakhov, "On the Limits of LoRaWAN Channel Access," in *2016 International Conference on Engineering and Telecommunication*, 2016, pp. 10–14.

[94] Semtech, "LoRa Modulation Basics," pp. 1–26, 2015. [Online]. Available: http://www.semtech.com/images/datasheet/an1200.22.pdf

[95] V. C. Gungor, D. Sahin, T. Kocak, S. Erg??t, C. Buccella, C. Cecati, and G. P. Hancke, "Smart grid technologies: Communication technologies and standards," *IEEE Transactions on Industrial Informatics*, vol. 7, no. 4, pp. 529–539, 2011.

[96] M. Zennaro, *Wireless Sensor Networks for Development: Potentials and Open Issues*, 2010. [Online]. Available: http://www.diva-portal.org/smash/record.jsf?pid=diva2:375245

[97] D. Ismail, M. Rahman, and A. Saifullah, "Low-Power Wide-Area Networks: Opportunities, challenges, and directions," *ACM International Conference Proceeding Series*, no. January 2019, pp. 1–7, 2018.

[98] M. O. Ojo, D. Adami, and S. Giordano, "Experimental evaluation of a Lora wildlife monitoring network in a forest vegetation area," *Future Internet*, vol. 13, no. 5, pp. 1–22, 2021.

[99] B. S. Chaudhari, M. Zennaro, and S. Borkar, "LPWAN technologies: Emerging application characteristics, requirements, and design considerations," *Future Internet*, vol. 12, no. 3, 2020.

[100] M. A. Ertürk, M. A. Aydın, M. T. Büyükakkaşlar, and H. Evirgen, "A Survey on LoRaWAN Architecture, Protocol and Technologies," *Future Internet*, vol. 11, no. 10, p. 216, 2019.

[101] K. Mekki, E. Bajic, F. Chaxel, and F. Meyer, "A comparative study of LPWAN technologies for large-scale IoT deployment," *ICT Express*, vol. 5, no. 1, pp. 1–7, 2019. [Online]. Available: https://doi.org/10.1016/j.icte.2017.12.005

[102] R. S. Sinha, Y. Wei, and S.-H. Hwang, "A survey on LPWA technology: LoRa and NB-IoT," *ICT Express*, pp. 4–11, 2017. [Online]. Available: http://linkinghub.elsevier.com/retrieve/pii/S2405959517300061

[103] R. S. Sinha, Y. Wei, and S. H. Hwang, "A survey on LPWA technology: LoRa and NB-IoT," *ICT Express*, vol. 3, no. 1, pp. 14–21, 2017.

[104] ——, "A survey on LPWA technology: LoRa and NB-IoT," *ICT Express*, vol. 3, no. 1, pp. 14–21, 2017. [Online]. Available: http://dx.doi.org/10.1016/j.icte.2017.03.004

[105] J. Finnegan and S. Brown, "A Comparative Survey of LPWA Networking," pp. 1–10, 2018. [Online]. Available: http://arxiv.org/abs/1802.04222

[106] B. Buurman, J. Kamruzzaman, G. Karmakar, and S. Islam, "Low-Power Wide-Area Networks: Design Goals, Architecture, Suitability to Use Cases and Research Challenges," *IEEE Access*, vol. 8, pp. 17 179–17 220, 2020.

[107] Q. M. Qadir, T. A. Rashid, N. K. Al-Salihi, B. Ismael, A. A. Kist, and Z. Zhang, "Low power wide area networks: A survey of enabling technologies, applications and interoperability needs," *IEEE Access*, vol. 6, pp. 77 454–77 473, 2018.

[108] N. Poursafar, M. E. E. Alahi, and S. Mukhopadhyay, "Long-range wireless technologies for IoT applications: A review," *Proceedings of the International Conference on Sensing Technology, ICST*, vol. 2017-Decem, pp. 1–6, 2018.

[109] S. Al-sarawi, M. Anbar, K. Alieyan, and M. Alzubaidi, "Internet of Things (IoT) Communication Protocols :Review," *2017 8th International Conference on Information Technology (ICIT) Internet*, pp. 685–690, 2017.

[110] U. Raza, P. Kulkarni, and M. Sooriyabandara, "Low Power Wide Area Networks: An Overview," *IEEE Communications Surveys and Tutorials*, vol. 19, no. 2, pp. 855–873, 2017.

[111] K. A. Suharja, R. P. Astuti, L. Meylani, and A. Fahmi, "Enhancement of MC-CDMA Performance System using Rotated Modulation," pp. 14–17, 2016.

[112] V. N. Mikhailov, A. B. Khachaturian, and A. S. Mikheev, "CDMA Signatures Based on the Shortened Minimax Binary Sequences," pp. 704–705, 2017.

[113] H. G. Myung and D. J. Goodman, "Peak-To-Average Power Ratio of Single Carrier Fdma Signals With Pulse Shaping," pp. 3–7, 2006.

[114] P. Jung, P. W. Baier, and A. Steil, "Advantages of CDMA and Spread Spectrum Techniques over FDMA and TDMA in Cellular Mobile Radio Applications," *IEEE Transactions on Vehicular Technology*, vol. 42, no. 3, pp. 357–364, 1993.

[115] A. M. Abdelhady, O. Amin, A. Chaaban, and M.-s. Alouini, "Downlink Resource Allocation for Multi-channel TDMA Visible Light Communications," *GlobalSIP 2016*, pp. 1–5, 2016.

[116] E. Engineering, T. Dhaka, I. I. Alam, and F. Hossain, "A TDMA based EM Controlled Multi-Channel MAC Protocol for Underwater Sensor Networks," pp. 279–284, 2017.

[117] S. Hossen, A. F. M. S. Kabir, R. H. Khan, and A. Azfar, "Interconnection between 802 . 15 . 4 Devices and IPv6 : Implications and Existing Approaches," *Journal of Computer Science*, vol. 7, no. 1, pp. 19–31, 2010. [Online]. Available: http://arxiv.org/abs/1002.1146

[118] B. Reynders, W. Meert, and S. Pollin, "Range and coexistence analysis of long range unlicensed communication," in *2016 23rd International Conference on Telecommunications, ICT 2016*, no. c, 2016.

[119] L. A. N. Man, S. Committee, and I. Computer, *Part 15 . 4 : Low-Rate Wireless Personal Area Networks (LR-WPANs)*, 2012, vol. 2012, no. April.

[120] M. Kirsche and M. Schnurbusch, "A New IEEE 802 . 15 . 4 Simulation Model for OMNeT ++ / INET," vol. 4, pp. 15–16, 2015.

[121] C. Kone, a. Hafid, and M. Boushaba, "Performance management of IEEE 802.15.4 wireless sensor network for precision agriculture," *Sensors Journal, IEEE*, vol. PP, no. 99, p. 1, 2015.

[122] N. Sornin, M. Luis, T. Eirich, T. Kramp, and O. Hersent, *LoRaWAN Specification*. LoRa Alliance, 2015. [Online]. Available: https://www.lora-alliance.org/portals/0/specs/LoRaWANSpecification1R0.pdf

[123] G. R. A. Stan Valentin Alexandru, Timnea Radu Serban and Ndrei, "Overview of high reliable radio data infrastructures for public automation applications," in *ECAI 2016 - International Conference – 8th Edition Electronics, Computers and Artificial Intelligence*, Ploiesti, ROMÂNIA, 2016, pp. 978–981.

[124] D. J. Ramírez and D. Ph, "Redes celulares : Acceso múltiple e interferencia (3G) Comunicaciones Inalámbricas."

[125] A. Laya, L. Alonso, and J. Alonso-Zarate, "Efficient contention resolution in highly dense LTE networks for machine type communications," in *2015 IEEE Global Communications Conference, GLOBECOM 2015*, 2015.

[126] ——, "Contention resolution queues for massive machine type communications in LTE," in *IEEE International Symposium on Personal, Indoor and Mobile Radio Communications, PIMRC*, vol. 2015-Decem, 2015, pp. 2314–2318.

[127] A. Laya, L. Alonso, and J. Alonso-zarate, "The Limits of the Random Access Channel of LTE for Machine-to-Machine Communications : an Energy Perspective," no. Scpa, pp. 1–14, 2015.

[128] A. Laya, K. Wang, L. Alonso, and J. Alonso-Zarate, "Multi-radio cooperative retransmission scheme for reliable machine-to-machine multicast services," in *IEEE International Symposium on Personal, Indoor and Mobile Radio Communications, PIMRC*, 2012, pp. 1–6.

[129] A. Adhikary, X. Lin, and Y. P. Eric Wang, "Performance evaluation of NB-IoT coverage," *IEEE Vehicular Technology Conference*, 2017.

[130] M. Lauridsen and B. Vejlgaard, "Interference Measurements in the European 868 MHz ISM Band with Focus on LoRa and SigFox," 2017.

[131] M. Lauridsen, I. Z. Kovács, P. Mogensen, M. Sørensen, and S. Holst, "Coverage and capacity analysis of LTE-M and NB-IoT in a rural area," *IEEE Vehicular Technology Conference*, vol. 20, pp. 2–6, 2017.

[132] N. Mangalvedhe, R. Ratasuk, and A. Ghosh, "NB-IoT deployment study for low power wide area cellular IoT," *IEEE International Symposium on Personal, Indoor and Mobile Radio Communications, PIMRC*, no. 1, 2016.

[133] C. Yu, L. Yu, Y. Wu, Y. He, and Q. Lu, "Uplink scheduling and link adaptation for narrowband internet of things systems," *IEEE Access*, vol. 5, pp. 1724–1734, 2017.

[134] D. Troha, D. Troha, and P. Krasowski, "Wireless system design NB-IoT downlink simulator Wireless system design : NB-IoT downlink simulator," 2017.

[135] D. Lachartre, F. Dehmas, C. Bernier, C. Fourtet, L. Ouvry, F. Lepin, E. Mercier, S. Hamard, L. Zirphile, S. Thuries, and F. Chaix, "7.5 A TCXO-less 100Hz-minimum-bandwidth transceiver for ultra-narrow-band sub-GHz IoT cellular networks," *2017 IEEE International Solid-State Circuits Conference (ISSCC)*, pp. 134–135, 2017. [Online]. Available: http://ieeexplore.ieee.org/document/7870297/

[136] J. P. Bardyn, T. Melly, O. Seller, and N. Sornin, "IoT: The era of LPWAN is starting now," *European Solid-State Circuits Conference*, vol. 2016-Octob, pp. 25–30, 2016.

[137] S. L. City, P. P. Data, and A. O. Extraction, "(12) Ulllted States Patent (10) Patent N0 .:," vol. 2, no. 12, 2013.

[138] T. Wendt, F. Volk, and E. Mackensen, "A benchmark survey of Long Range (LoRa TM) Spread-Spectrum-Communication at 2.45 GHz for safety applications," *Wireless and Microwave Technology Conference (WAMICON), 2015 IEEE 16th Annual*, pp. 1–4, 2015.

[139] K. Mikhaylov, J. Petäjäjärvi, and T. Hänninen, "Analysis of Capacity and Scalability of the LoRa Low Power Wide Area Network Technology," pp. 119–124, 2016.

[140] J. Petäjäjärvi, K. Mikhaylov, A. Roivainen, T. Hänninen, and M. Pettissalo, "On the coverage of LP-WANs: Range evaluation and channel attenuation model for LoRa technology," in *2015 14th International Conference on ITS Telecommunications, ITST 2015*. Copenhagen, Denmark: IEEE, 2016, pp. 55–59.

[141] F. Adelantado, X. Vilajosana, P. Tuset-Peiro, B. Martinez, and J. Melia, "Understanding the limits of LoRaWAN," *IEEE Communications Magazine*, vol. 55, no. January, pp. 8–12, 2017.

[142] A. Rahmadhani and F. Kuipers, "Understanding collisions in a LoRaWAN," 2017. [Online]. Available: https://wiki.surfnet.nl/download/attachments/11211020/TUD-LoRaWAN-RoN-2017.pdf

[143] M. C. Bor, U. Roedig, T. Voigt, and J. M. Alonso, "Do LoRa Low-Power Wide-Area Networks Scale?" *Proceedings of the 19th ACM International Conference on Modeling, Analysis and Simulation of Wireless and Mobile Systems*, no. November, pp. 59–67, 2016. [Online]. Available: http://doi.acm.org/10.1145/2988287.2989163

[144] Dialogic, "The wireless Internet of Things : Spectrum utilisation and monitoring," no. October, 2016.

[145] H. Hourani, "An Overview of Diversity Techniques in Wireless Communication Systems," pp. 1–5, 2005.

[146] D. J. Ramírez and D. Ph, "Comunicaciones Inalámbricas Daniel Jaramillo Ramírez, Ph.D."

[147] Y. Zou, J. Zhu, X. Wang, and V. C. M. Leung, "Improving physical-layer security in wireless communications using diversity techniques," *IEEE Network*, vol. 29, no. February, pp. 42–48, 2015.

[148] F. Yang, G. S. Ramachandran, P. Lawrence, S. Michiels, W. Joosen, and D. Hughes, "PnP-WAN: Wide Area Plug and Play Sensing and Actuation with LoRa," *IEEE*, pp. 229–230, 2016.

[149] P. Kulkarni, Q. O. A. Hakim, and A. Lakas, "Experimental Evaluation of a Campus-Deployed IoT Network Using LoRa," *IEEE Sensors Journal*, vol. 20, no. 5, pp. 2803–2811, 2020.

[150] I. Allai, S.-M. Senouci, J. Penhoat, and Y. Gourhant, "A new sustainable mechanism to wake-up bast stations in mobile networks," *2016 Global Information Infrastructure and Networking Symposium (GIIS)*, pp. 1–6, 2016. [Online]. Available: http://ieeexplore.ieee.org/document/7814933/

[151] J. Gao and Z. Wang, "The Key Technology of Image Transmission Based on ZigBee," no. January, pp. 1–6, 2016.

[152] A. Augustin, J. Yi, T. Clausen, and W. Townsley, "A Study of LoRa: Long Range & Low Power Networks for the Internet of Things," *Sensors*, vol. 16, no. 9, p. 1466, 2016. [Online]. Available: http://www.mdpi.com/1424-8220/16/9/1466

[153] L. Li, J. Ren, and Q. Zhu, "On the Application of LoRa LPWAN Technology in Sailing Monitoring System," *2017.wons-conference.org*, pp. 77–80, 2017. [Online]. Available: http://2017.wons-conference.org/Papers/1570315122.pdf

[154] E. MORIN, M. Maman, R. GUIZZETTI, and A. DUDA, "Comparison of the Device Lifetime in Wireless Networks for the Internet of Things," *IEEE Access*, vol. 3536, no. c, pp. 1–1, 2017. [Online]. Available: http://ieeexplore.ieee.org/document/7894201/

[155] A. Ahmad, M. M. Mohd Nadzri, I. M. Rosli, and A. Amira, "Rapid prototyping of wireless image transmission for wildlife (tiger) monitoring system - A preliminary study," *Journal of Telecommunication, Electronic and Computer Engineering*, vol. 10, no. 2-5, pp. 75–79, 2018.

[156] M. M. Mohd Nadzri, A. Ahmad, and A. Amira, "Exploiting LabVIEW FPGA in Implementation of DCT-based Wireless Image Transmission for Wildlife Surveillance System," *2018 IEEE 16th Student Conference on Research and Development, SCOReD 2018*, pp. 2–6, 2018.

[157] J. P. S. Sundaram, W. Du, and Z. Zhao, "A Survey on LoRa Networking: Research Problems, Current Solutions and Open Issues," no. i, pp. 2–18, 2019. [Online]. Available: http://arxiv.org/abs/1908.10195

[158] A. Mateo-Aroca, G. García-Mateos, A. Ruiz-Canales, J. M. Molina-García-Pardo, and J. M. Molina-Martínez, "Remote image capture system to improve aerial supervision for precision irrigation in agriculture," *Water (Switzerland)*, vol. 11, no. 2, pp. 1–21, 2019.

[159] C. C. Wei, J. K. Huang, C. C. Chang, and K. C. Chang, "The development of LOra image transmission based on time division multiplexing," *Proceedings - 2020 International Symposium on Computer, Consumer and Control, IS3C 2020*, no. ii, pp. 323–326, 2020.

[160] M. Villareal, J. Cuaran, J. Leon, A. Chica, V. Prada, and M. Hurtado, "Wireless Image Transmission Technologies," pp. 1–6, 2020.

[161] A. Lavric and V. Popa, "Internet of Things and LoRa™ Low-Power Wide-Area Networks: A survey," *ISSCS 2017 - International Symposium on Signals, Circuits and Systems*, pp. 1–5, 2017.

[162] A. J. Bidgoly and H. J. Bidgoly, "A Novel Chaining Encryption Algorithm for LPWAN IoT Network," *IEEE Sensors Journal*, vol. 19, no. 16, pp. 7027–7034, 2019.

[163] A. I. N. I. Mir, M (IMDEA NEtwork Institute), Guzman, B (IMDEA NEtwork Institute), Galisteo and D. I. N. I. Giustiniano, "Mir,2020.pdf," Mir,2020, pp. 1–6, 2020.

[164] F. Seguel, C. Azurdia-Meza, N. Krommenacker, P. Charpentier, V. Bombardier, and C. Carreno, "Miner Video Tracking and Identification Using Optical Camera Communications in a Wireless Multimedia Sensor Network," *2020 12th International Symposium on Communication Systems, Networks and Digital Signal Processing, CSNDSP 2020*, 2020.

[165] O. Z. Alsulami, M. T. Alresheedi, and J. M. Elmirghani, "Optical Wireless Cabin Communication System," *2019 IEEE Conference on Standards for Communications and Networking, CSCN 2019*, pp. 2019–2022, 2019.

[166] R. Alghamdi, N. Saeed, H. Dahrouj, M. S. Alouini, and T. Y. Al-Naffouri, "Towards ultra-reliable low-latency underwater optical wireless communications," *IEEE Vehicular Technology Conference*, vol. 2019-September, 2019.

[167] H. Guo, S. Wu, H. Wang, and M. Daneshmand, "DSIC: Deep learning based self-interference cancellation for in-band full duplex wireless," *2019 IEEE Global Communications Conference, GLOBECOM 2019 - Proceedings*, 2019.

[168] T. H. Li, M. R. Khandaker, F. Tariq, K. K. Wong, and R. T. Khan, "Learning the wireless V2I channels using deep neural networks," *IEEE Vehicular Technology Conference*, vol. 2019-September, 2019.

[169] K. Y. Kim and Y. Shin, "Inter-relay interference mitigation for chirp-based two-path successive relaying protocol," *Sensors (Switzerland)*, vol. 19, no. 15, 2019.

[170] S. Chen, J. Zhang, E. Bjornson, J. Zhang, and B. Ai, "Structured Massive Access for Scalable Cell-Free Massive MIMO Systems," *IEEE Journal on Selected Areas in Communications*, vol. 39, no. 4, pp. 1086–1100, 2021.

[171] Z. Ahmad, S. J. Hashim, F. Z. Rokhani, S. A. R. Al-Haddad, A. Sali, and K. Takei, "Quaternion model of higher-order rotating polarization wave modulation for high data rate M2M lpwan communication," *Sensors (Switzerland)*, vol. 21, no. 2, pp. 1–18, 2021.

[172] A. Kumar, S. K. Kaushik, R. Sharma, and P. Raj, "Simulators for Wireless Networks: A Comparative Study," in *2012 International Conference on Computing Sciences*, 2012, pp. 338–342. [Online]. Available: http://ieeexplore.ieee.org/document/6391700/

[173] M. Ayedi, E. Eldesouky, and J. Nazeer, "Energy-Spectral Efficiency Optimization in Wireless Underground Sensor Networks Using Salp Swarm Algorithm," *Journal of Sensors*, vol. 2021, 2021.

[174] S. S. Basu, J. Haxhibeqiri, M. Baert, B. Moons, A. Karaagac, P. Crombez, P. Camerlynck, and J. Hoebeke, "An end-to-end lwm2m-based communication architecture for multimodal NB-IoT/BLE devices," *Sensors (Switzerland)*, vol. 20, no. 8, pp. 1–17, 2020.

[175] S. Kim, H. Lee, and S. Jeon, "An adaptive spreading factor selection scheme for a single channel lora modem," *Sensors (Switzerland)*, vol. 20, no. 4, 2020.

[176] T. Chen, D. Eager, and D. Makaroff, "Efficient image transmission using lora technology in agricultural monitoring iot systems," *Proceedings - 2019 IEEE International Congress on Cybermatics: 12th IEEE International Conference on Internet of Things, 15th IEEE International Conference on Green Computing and Communications, 12th IEEE International Conference on Cyber, Physical and So*, pp. 937–944, 2019.

[177] M. Ji, J. Yoon, J. Choo, M. Jang, and A. Smith, "LoRa-based Visual Monitoring Scheme for Agriculture IoT," *SAS 2019 - 2019 IEEE Sensors Applications Symposium, Conference Proceedings*, pp. 1–6, 2019.

[178] D. E. Juliando, R. G. Putra, D. A. Sartika, and R. G. Yudha, "Study of Lora Module Ra-02 for Long Range, Low Power, Low Rate Picture Transfer Applications," *Journal of Physics: Conference Series*, vol. 1845, no. 1, pp. 1–9, 2021.

[179] A. Staikopoulos, V. Kanakaris, and G. A. Papakostas, "Image Transmission via LoRa Networks - A Survey," *2020 IEEE 5th International Conference on Image, Vision and Computing, ICIVC 2020*, pp. 150–154, 2020.

[180] T. Elshabrawy and J. Robert, "Interleaved chirp spreading LoRa-based modulation," *IEEE Internet of Things Journal*, vol. 6, no. 2, pp. 3855–3863, 2019.

[181] D. Walter, "Fractal and Wavelet Image Compression of Astronomical Images," no. May 2019, 2003.

[182] D. Saupe, R. Hamzaoui, and H. Hartenstein, "Fractal Image Compression An Introductory Overview," p. 66, 2006. [Online]. Available: https://karczmarczuk.users.greyc.fr/matrs/Dess/RADI/Refs/SaHaHa96a.pdf

[183] N. Thomos, N. V. Boulgouris, and M. G. Strintzis, "Optimized transmission of JPEG2000 streams over wireless channels," *IEEE Transactions on Image Processing*, vol. 15, no. 1, pp. 54–67, 2006.

[184] D. Croce, M. Gucciardo, S. Mangione, G. Santaromita, and I. Tinnirello, "Impact of LoRa Imperfect Orthogonality : Analysis of Link-Level Performance," *IEEE Communications Letters*, vol. 22, no. 4, pp. 796–799, 2018.

[185] M. C. Bor, "Towards the efficient use of LoRa for Wireless Sensor Networks," p. 202, 2020.

[186] R. Marini, K. Mikhaylov, G. Pasolini, and C. Buratti, "Lorawansim: A flexible simulator for lorawan networks," *Sensors (Switzerland)*, vol. 21, no. 3, pp. 1–19, 2021.

[187] T. Voigt, M. Bor, U. Roedig, and J. Alonso, "Mitigating Inter-network Interference in LoRa Networks," 2016. [Online]. Available: http://arxiv.org/abs/1611.00688

A. Appendix A

Clustering K-means classification

```
clear all; close all; clc;

cd ('C:JAverianaIV - 2018-1de Patrones');

X=project_data';
cluster = 2;

opts = statset('Display','final');
idx,C
= kmeans(X,cluster,'Distance','cityblock',... 'Replicates',10,'Options',opts);

figure;
plot(X(idx==1,1),X(idx==1,2),'r.','MarkerSize',12)
hold on
plot(X(idx==2,1),X(idx==2,2),'g.','MarkerSize',12)
plot(C(:,1),C(:,2),'kx',... 'MarkerSize',15,'LineWidth',3)
legend('Cluster 1','Cluster 2','Centros',... 'Location','NW')
hold off
```

Neuronal network classification

```
clear all; close all; clc;
data_normal = xlsread('leaf',' leafok2');
Imgs_no = data_normal;

data_sick = xlsread('leaf',' leafsick2');
Imgs_si = data_sick;
index_si = randperm(11, 11);
index_no = randperm(11, 11);
Ntrain = 9;
Ntest = 11 − Ntrain;
Imgs_sitrain = Imgs_si(:, index_si(1 : Ntrain));
Imgs_sitest = Imgs_si(:, index_si(Ntrain + 1 : end));
Imgs_notrain = Imgs_no(:, index_no(1 : Ntrain));
Imgs_notest = Imgs_no(:, index_no(Ntrain + 1 : end));
Imgs_train = mean([Imgs_sitrainImgs_notrain]);
Imgs_test = mean([Imgs_sitestImgs_notest]);

label_train = zeros(18, 1);
label_train(1 : 9, 1) = 1;
label_train(10 : end, 1) = −1;
label_train = label_train';
```

$label_test = zeros(4, 1);$
$label_test(1 : 2, 1) = 1;$
$label_test(3 : end, 1) = -1;$
$label_test = label_test';$

net = newff(Imgs$_t$$rain, label_train, [328]);
$view(net);$
$net.trainParam.epochs = 10;$
$net = train(net, Imgs_train, label_train);$

output$_t$$est = net(Imgs_test);$
$output_train = net(Imgs_train);$

E$_t$$est = sum(double(sign(output_test) = label_test))/4$
$E_train = sum(double(sign(output_train) = label_train))/18$

Deep Learning train code

clear all; clc; close all;

digitDatasetPath=('imágenes$'_1)imds = imageDatastore(digitDatasetPath, ...'IncludeSubfolders', true,' LabelSource',' .$

figure;
perm = randperm(22,6);
for i = 1:6
subplot(4,5,i);
imshow(imds.Filesperm(i));
end

labelCount = countEachLabel(imds)

img = readimage(imds,22);
size(img)

numTrainFiles = 9;
imdsTrain,imdsValidation
= splitEachLabel(imds,numTrainFiles,'randomize');

layers = [imageInputLayer([1512 2016 3])

convolution2dLayer(3,8,'Padding','same')
batchNormalizationLayer
reluLayer

maxPooling2dLayer(2,'Stride',2)

convolution2dLayer(3,16,'Padding','same')
batchNormalizationLayer
reluLayer

maxPooling2dLayer(2,'Stride',2)

A Appendix A

```
convolution2dLayer(3,32,'Padding','same')
batchNormalizationLayer
reluLayer

fullyConnectedLayer(2)
softmaxLayer
classificationLayer];

options = trainingOptions('sgdm', ...
'InitialLearnRate',0.01, ...
'MaxEpochs',10, ...
'Shuffle','every-epoch', ...
'ValidationData',imdsValidation, ...
'ValidationFrequency',30, ...
'Verbose',false, ...
'Plots','training-progress');

net = trainNetwork(imdsTrain,layers,options);

YPred = classify(net,imdsValidation);
YValidation = imdsValidation.Labels;

accuracy = sum(YPred == YValidation)/numel(YValidation)
```

Leaves classify network

```
clear all; clc; close all;

net=load ('net_project_2.mat');
digitDatasetPath = ('C : JAverianaV − 2018 − 2DEIMÁGENESYVIDEOánChaparroBecerraentregaánChaparroBecerra'
imds = imageDatastore(digitDatasetPath, ...'IncludeSubfolders', true,' LabelSource',' foldernames');

labelCount = countEachLabel(imds)

img = readimage(imds,11);
size(img)

YPred = classify(net.net,imds);
YPrednum=double(YPred);
```

Compression technique - sparse signal and coefficients values

```
close all
clear all
clc

Load_matrix = input('Carguelamatrizaevaluar');
M,N,L
= size(spectralimage);
longitud_vector = size(spectralimage);
size_matrix = longitud_vector(1) ∗ longitud_vector(2) ∗ longitud_vector(3);

for j=1:1:L
dct(:,:,j)=zeros(M);
```

if j ¡= L
dct(:,:,j) =
dct2(spectralimage(:,:,j));
else
end
end

for m=1:1:L;
lineal$_m atrix_d ct = zeros(size_m atrix, 1)$;
$if m <= L$;
$lineal_m atrix_d ct = reshape(dct, [size_m atrix, 1])$;
else
end
end

coef$_d ct = sort(lineal_m atrix_d ct)$;

negative$_v alues = zeros(size_m atrix, 1)$;
$for i = 1 : size(lineal_m atrix_d ct, 1)$;
$if lineal_m atrix_d ct(i) < 0$;
$negative_v alues(i) = -1$;
end
$if lineal_m atrix_d ct(i) >= 0$;
$negative_v alues(i) = 1$;
end
end

absolut$_v alue_d ct = abs(lineal_m atrix_d ct)$;

PSNR$_d ct = zeros(100, 1)$;
$for i = [1 : 1 : 100]$;
$porcentajes = i$;

datos$_{ac} ero = size_m atrix * porcentajes$;

ind =porcentaje(absolut$_v alue_d ct, porcentajes)$;
$b = porcentaje([absolut_v alue_d ct], porcentajes)$;
$absolut_v alue_d ct(b) = 0$;
$disp(absolut_v alue_d ct)$;

negative=(-1);
lineal$_m atrix = zeros(size_m atrix, 1)$;

for j=1:size(negative$_v alues, 1)$;
$if negative_v alues(j) == 1$;
$lineal_m atrix(j) = absolut_v alue_d ct(j)$;
else
$lineal_m atrix(j) = absolut_v alue_d ct(j) * negative$;
end
end

MxN$_m atrix = reshape(lineal_m atrix, [longitud_v ector(1), longitud_v ector(2), longitud_v ector(3)])$;

for j=1:1:L;
idct(:,:,j)=zeros(M);
if j ¡= L
idct(:,:,j) = idct2(MxN$_m atrix(:,:,j)$);
$else$
end
end

PSNR$_d ct(i) = psnr(idct, spectralimage)$;
end

Lo=1;
qmf = MakeONFilter('Symmlet',8);

for j=1:1:L;
fwav(:,:,j)=zeros(M);
if j ¡= L
fwav(:,:,j) = FWT2$_P O(spectralimage(:,:,j), Lo, qmf)$;
$else$
end
end

for m=1:1:L;
lineal$_m atrix_w av = zeros(size_m atrix, 1)$;
$if m <= L$;
$lineal_m atrix_w av = reshape(fwav, [size_m atrix, 1])$;
$else$
end
end

coef$_w av = sort(lineal_m atrix_w av)$;

negative$_v alues_w av = zeros(size_m atrix, 1)$;
$fori = 1 : size(lineal_m atrix_w av, 1)$;
$iflineal_m atrix_w av(i) < 0$;
$negative_v alues_w av(i) = -1$;
$endiflineal_m atrix_w av(i) >= 0$;
$negative_v alues_w av(i) = 1$;
$endend$
absolut$_v alue_w av = abs(lineal_m atrix_w av)$;

PSNR$_w av = zeros(1, 1)$;
$fori = [1 : 1 : 100]$;
$porcentajes = i$;

datos$_a cero_w av = (size_m atrix * porcentajes)$;

ind$_w av$
$= porcentaje_w av(absolut_v alue_w av, porcentajes)$;
$b = porcentaje_w av([absolut_v alue_w av], porcentajes)$;
$absolut_v alue_w av(b) = 0$;

$disp(absolut_value_wav)$;

negative=(1);
$\text{lineal}_matrix_wav = zeros(size_matrix, 1)$;

for j=1:size($\text{negative}_values_wav$, 1);
if
$negative_values_wav(j) == 1$;
$lineal_matrix_wav(j) = absolut_value_wav(j)$;
$else$
$lineal_matrix_wav(j) = absolut_value_wav(j) * negative$;
end
end

$\text{MxN}_matrix_wav = reshape(lineal_matrix_wav, [longitud_vector(1), longitud_vector(2), longitud_vector(3)])$;

for j=1:1:L;
fwavi(:,:,j)=zeros(M);
if j ¡= L
fwavi(:,:,j) = $\text{IWT2}_PO(MxN_matrix_wav(:, :, j), Lo, qmf)$;
$else$
end
end

$\text{PSNR}_wav(i) = psnr(fwavi, spectralimage)$;
end

Lo=1;
qmf = MakeONFilter('Symmlet',8);

for j=1:1:L;
fwavk(:,:,j)=zeros(M);
if j ¡= L
fwavk(:,:,j) = KronerDCTdirect(spectralimage(:,:,j),qmf, M, N, Lo);
else
end
end

for m=1:1:L;
$\text{lineal}_matrix_kron = zeros(size_matrix, -1); ifm <= L$;
$lineal_matrix_kron = reshape(fwavk, [size_matrix, 1])$;
$else$
end
end

$\text{coef}_kron = sort(lineal_matrix_kron)$;

$\text{negative}_values_kron = zeros(size_matrix, 1)$;
$fori = 1 : size(lineal_matrix_kron, 1)$;
$iflineal_matrix_kron(i) < 0$;
$negative_values_kron(i) = -1$;
end

A Appendix A

$if lineal_matrix_kron(i) >= 0;$
$negative_values_kron(i) = 1;$
end
end

$\text{absolut}_value_kron = abs(lineal_matrix_kron);$

$\text{PSNR}_kron = zeros(100, 1);$
$fori = [1 : 1 : 100];$
$porcentajes = i;$

$\text{datos}_acero_kron = size_matrix * porcentajes;$

$\text{ind}_kron = porcentaje_kron(absolut_value_kron, porcentajes);$
$b = porcentaje_kron([absolut_value_kron], porcentajes);$
$absolut_value_kron(b) = 0;$
$disp(absolut_value_kron);$

negative=(1);
$\text{lineal}_matrix_kron = zeros(size_matrix, 1);$

for j=1:size($\text{negative}_values_kron, 1$);
$if negative_values_kron(j) == 1;$
$lineal_matrix_kron(j) = absolut_value_kron(j);$
$else$
$lineal_matrix_kron(j) = absolut_value_kron(j) * negative;$
end
end

$\text{MxN}_matrix_kron = reshape(lineal_matrix_kron, [longitud_vector(1), longitud_vector(2), longitud_vector(3)]);$

for j=1:1:L;
Ifwavk(:,:,j)=zeros(M);
if j ¡= L
Ifwavk(:,:,j) = KronerDCTinverse($\text{MxN}_matrix_kron(:, :, j), qmf, M, N, Lo$);
$else$
end
end

$\text{PSNR}_kron(i) = psnr(Ifwavk, spectralimage);$
end

i=[1:1:100]';
plot($\text{PSNR}_wav, i,' gx', PSNR_dct, i,' bo', PSNR_kron, i,' r+'$);
$title('Wavelet, DCT - 2D and Kronecker Transforms')$;
$legend('Wavelet',' DCT - 2D',' Kronecker')$;
$xlabel('Percentaje - ylabel('Spreading - PSNR')$
$gridon$
$axis([0100 - 0100])$;

hold on
figure

$\text{original}_i mage = subplot(3,1,1);$
$hist(coef_d ct, size_m atrix);$
$title(original_i mage,' DCTcoefficients')$
$axis([-33-5030e3]);$
$Red_c omponent = subplot(3,1,2);$
$hist(coef_w av, size_m atrix);$
$title(Red_c omponent,' Waveletcoefficients')$
$axis([-33-5030e3]);$
$Green_c omponent = subplot(3,1,3);$
$hist(coef_k ron, size_m atrix);$
$title(Green_c omponent,' Kroneckercoefficients')$
$axis([-33-5030e3]);$

Wavelet Transform

close all; clear all; clc

image=imread;
('C:7.jpg');
$\text{image}_= rgb2gray(image);$
$image = imresize(image_,[128,128]);$
$figure$
$subplot(2,1,1)$
$imshow(image)$
$title('(a)',...'FontUnits','points',...'Interpreter','latex',...'FontSize',11,...'FontName','Times')$
$holdon$

Iw=double(image);
L=1;
qmf = MakeONFilter('Symmlet',8);
fwav = $\text{FWT2}_P O(Iw, L, qmf);$
$longitud_v ector_w av = size(Iw);$
$size_m atrix_w av = longitud_v ector_w av(1) * longitud_v ector_w av(2)$
$lineal_m atrix_w av = reshape(fwav,[size_m atrix_w av,1]);$
$negative_v alues_w av = zeros(size_m atrix_w av,1);$
$fori = 1 : size(lineal_m atrix_w av,1);$
$iflineal_m atrix_w av(i) < 0;$
$negative_v alues_w av(i) = -1;$
end
$iflineal_m atrix_w av(i) >= 0$
$negative_v alues_w av(i) = 1;$
end
end

$\text{absolut}_v alue_w av = abs(lineal_m atrix_w av);$

$\text{PSNR}_w av = zeros(100,1);$
$i = 95;$
$porcentajes = i;$
$datos_a cero_w av = size_m atrix_w av * porcentajes;$

$\text{ind}_w av$
$= porcentaje_w av(absolut_v alue_w av, porcentajes);$

A Appendix A

$b = porcentaje_wav([absolut_value_wav], porcentajes);$
$absolut_value_wav(b) = 0;$
$disp(absolut_value_wav);$

negative=(-1);
$\text{lineal}_matrix_wav = zeros(size_matrix_wav, 1);$

for j=1:size($\text{negative}_values_wav, 1$);
if
$negative_values_wav(j) == 1;$
$lineal_matrix_wav(j) = absolut_value_wav(j);$
$else$
$lineal_matrix_wav(j) = absolut_value_wav(j) * negative;$
end
end

$\text{negative}_values = zeros(size_matrix_wav, 1);$
$fori = 1 : size(lineal_matrix_wav, 1);$
$iflineal_matrix_wav(i) < 0;$
$negative_values(i) = -1;$
end
$iflineal_matrix_wav(i) >= 0;$
$negative_values(i) = 0;$
end
end
$negative_values_=negative_values * (-1);$
$MxN_matrix_wav = reshape(lineal_matrix_wav, [longitud_vector_wav(1), longitud_vector_wav(2)]);$
$fwavi = uint8(IWT2_PO(MxN_matrix_wav, L, qmf));$
$PSNR_wav(i) = psnr(fwavi, image)$
$subplot(2, 1, 2)$
$imshow(fwavi)$
$title('(b)', ...'FontUnits', 'points', ...'Interpreter', 'latex', ...'FontSize', 11, ...'FontName', 'Times')filename =$
$['C : JAverianaísículosresultadosículo_2processing_95.eps']; print(filename, '-depsc2');$

Encode of information
function [B1,B2,B3,B4]= $\text{pack}_byte(dat)$

temp=dat;
$\text{int}_part = cast(floor(dat), 'uint16');$
$mask = cast(hex2dec('FF00'), 'uint16');$
$B1 = cast(bitshift(bitand(mask, int_part), -8), 'uint8');$
$mask = cast(hex2dec('00FF'), 'uint16');$
$B2 = cast(bitand(mask, int_part), 'uint8');$
$dec_part = cast(10000 * (dat - floor(dat)), 'uint16');$
$mask = cast(hex2dec('FF00'), 'uint16');$
$B3 = cast(bitshift(bitand(mask, dec_part), -8), 'uint8');$
$mask = cast(hex2dec('00FF'), 'uint16');$
$B4 = cast(bitand(mask, dec_part), 'uint8');$
end

Decode of information
function [tot]= $\text{unpack}_byte(B1, B2, B3, B4)$

$\text{int}_part = cast(B1,' uint16');$
$int_part = bitshift(int_part, 8);$
$B2 = cast(B2,' uint16');$
$int_part = int_part + B2;$
$int_part = cast(int_part,' double');$

$\text{dec}_part = cast(B3,' uint16');$
$dec_part = bitshift(dec_part, 8);$
$B4 = cast(B4,' uint16');$
$dec_part = dec_part + B4;$
$dec = cast(dec_part,' double');$
$tot = single(int_part + dec/10000);$
end

LoRa symbols creation
clear all; close all; clc;

SF = 8;
BW = 500000;
Fs = 500000;
$\text{preamble}_len = 10;$
$sync_len = 2;$
$total_sym = 4;$
$num_samples = Fs * (2^SF)/BW;$
$symbols = [50, 100, 255, 1];$

$\text{lora}_total_sym = preamble_len + sync_len + total_sym;$

outp = [];
inverse = 0;
for i = 1:$\text{preamble}_len[out_preamble] = LoRa_Modulation(SF, BW, Fs, num_samples, 0, inverse);$
$outp((i-1) * num_samples + 1 : i * num_samples) = out_preamble;$
end
inverse = 1;
for i = 1:$\text{sync}_len[out_sync] = LoRa_Modulation(SF, BW, Fs, num_samples, 32, inverse);$
$outp = [outpout_sync];$
end

inverse = 0;
for i = 1:$\text{total}_sym[out_sym] = LoRa_Modulation(SF, BW, Fs, num_samples, symbols(i), inverse);$
$outp = [outpout_sym];$
end

inverse = 1;

$[\text{out}_reverse] = LoRa_Modulation(SF, BW, Fs, num_samples, 0, inverse);$

for n = 1:1:$\text{lora}_total_symdecoded_out((n-1)*num_samples+1 : n*num_samples) = (outp((n-1)*num_samples+1 : n * num_samples). * out_reverse);$
$endXt_synch = zeros(1, length(decoded_out - 1024));$
$for n = 1 : length(decoded_out) - 1024Xt_synch(n) = sum(decoded_out(n : n + 1024 - 1));$
end;

A Appendix A

$form = 1:1:lora_total_symFFT_out(m,:) = abs((fft(decoded_out((m-1)*num_samples+1:$
$m*num_samples), 2^SF)));$
$endnum_samples = 2^SF;$
$k = 1;$
$form = preamble_len + sync_len + 1:1:lora_total_sym[r,c] = max(FFT_out(m,:));$
$data_received(k) = c-1;$
$k = k+1;$
end

figure(1);
samples = num$_samples$/4;
$title('DecodedLoRasymbols');$
$spectrogram(decoded_out, samples, samples-1, samples, Fs,'yaxis');$

figure;
samp$_time = 0:1:num_samples-1;$
$title('FFTofreceivedLoRasymbols');$
$form = 1:1:lora_totalsymplot(samp_time, FFT_out(m,:)); holdon;$
end
gridon;
$Prob_errs = length(find(data_received == symbols))/length(symbols)$
LoRa modulation function
function out$_preamble = LoRa_Modulation_new(SF, BW, Fs, symbol, inverse)$
$T = (2^SF)/BW;$
$num_samples = 2^SF*(Fs/BW);$
$ts = 0:1/Fs:num_samples/Fs-1/Fs;$
$phases = zeros(1, num_samples);$
$ifsymbol == 0phases = 2*pi*(ts*BW).^2/(2^(SF+1));$
$ifinverse == 1$
$phases = 2*pi*BW*ts-phases;$
end;
else
$fi = symbol*BW/(2^SF);$
$indx = find(ts <= T-symbol/BW);$
$phases(indx) = 2*pi*(fi*ts(indx)+(ts(indx)*BW).^2/(2^(SF+1)));$
$indx = find(ts > T-symbol/BW);$
$phases(indx) = 2*pi*(fi*ts(indx)+(ts(indx)*BW).^2/(2^(SF+1))-BW*ts(indx));$
$ifinverse == 1$
$phases = 2*pi*BW*ts-phases;$
end;
end;
$out_preamble = exp(1i*phases);$
end

LoRa Transmissor
clear all; close all; clc;

connectedRadios = findsdru;
if strncmp(connectedRadios(1).Status, 'Success', 7) radioFound = true;
platform = connectedRadios(1).Platform;
switch connectedRadios(1).Platform case 'B200','B210' address = connectedRadios(1).SerialNum;
case 'N200/N210/USRP2','X300','X310' address = connectedRadios(1).IPAddress;

end
else
radioFound = false;
address = '192.168.10.2';
platform = 'N200/N210/USRP2';
end

load('Data$_t est_S F_5'$);

data$_1$ = [$outp'$; $zeros(1536, 1)$]

tx$_1$ = $comm.SDRuTransmitter(...'Platform',' B200',...'SerialNum',' 30BA179',...'CenterFrequency', 920e6,...'Interp$
$release(tx_1)$
toc

LoRa Receiver
clear all; clc; close all

connectedRadios = findsdru;
if strncmp(connectedRadios(1).Status, 'Success', 7) radioFound = true;
platform = connectedRadios(1).Platform;
switch
connectedRadios(1).Platform case 'B200','B210'
address = connectedRadios(1).SerialNum;
case
'N200/N210/USRP2','X300','X310'
address = connectedRadios(1).IPAddress;
end
else
radioFound = false;
address = '192.168.10.2';
platform = 'N200/N210/USRP2';
end

fmRxParams = getParamsSdruFMExamples(platform);

switch platform
case 'B200','B210'
radio = comm.SDRuReceiver(... 'Platform', platform, ... 'SerialNum', address, ... 'MasterClockRate', fmRx-
Params.RadioMasterClockRate);
case 'X300','X310'
radio = comm.SDRuReceiver(... 'Platform', platform, ... 'IPAddress', address, ... 'MasterClockRate', fmRx-
Params.RadioMasterClockRate);
case 'N200/N210/USRP2'
radio = comm.SDRuReceiver(... 'Platform', platform, ... 'IPAddress', address);
end

radio.CenterFrequency = 868e6
radio.Gain = 35;
radio.DecimationFactor = 50;
radio.SamplesPerFrame = fmRxParams.RadioFrameLength;
radio.OutputDataType = 'single'

fmRxParams = getParamsSdruFMExamples(platform)
AudioFrameTime = fmRxParams.AudioFrameTime/10;

hwInfo = info(radio)

fmBroadcastDemod = comm.FMBroadcastDemodulator(... 'SampleRate', fmRxParams.RadioSampleRate, ... 'FrequencyDeviation', fmRxParams.FrequencyDeviation, ... 'FilterTimeConstant', fmRxParams.FilterTimeConstant, ... 'AudioSampleRate', fmRxParams.AudioSampleRate, ... 'PlaySound', true, ... 'BufferSize', fmRxParams.BufferSize, ... 'Stereo', true);

$freqs_ax = -2000000/2 : 2000000/4000 : 2000000/2 - 2000000/4000;$
$axis([freqs_ax(1) freqs_ax(2) 0 0.1]);$
$ticifradioFound$
$timeCounter = 0;$
$Xt = NaN(4000, 5000);$
$c = 1;$

[x, len] = step(radio);
tic;
while timeCounter ¡ fmRxParams.StopTime
x, len
= step(radio);
timeCounter = timeCounter + AudioFrameTime;

Xt(1:4000,c)=x(1:4000);
c=c+1;
end
else
warning(message('sdru:sysobjdemos:MainLoop'))
end
toc
release(fmBroadcastDemod)
release(radio)

Wavelet Inverse Transform
close all; clear all; clc

input('Cargar los datos para realizar la transformada inversa wavelet...') L=1;
qmf = MakeONFilter('Symmlet',8);

load ('DATA$_fwavi'$);
$lineal_matrix_wav = data$
$longitud_vector = 128;$
$MxN_matrix_wav = reshape(lineal_matrix_wav, [longitud_vector, longitud_vector]);$

fwavi=uint8(IWT2$_PO(MxN_matrix_wav, L, qmf)$);
$fwavi = imresize(fwavi, [73138])$
$imshow(fwavi)$

1